Spring 2007

An improved power threshold method for estimating tool wear during milling

Bennett Desfosses
University of New Hampshire, Durham

AN IMPROVED POWER THRESHOLD METHOD

FOR ESTIMATING TOOL WEAR DURING MILLING

BY

BENNETT DESFOSSES

B.S., University of New Hampshire, 2005

THESIS

Submitted to the University of New Hampshire

in Partial Fulfillment of

the Requirements for the Degree of

Master of Science

in

Mechanical Engineering

May, 2007

This dissertation has been examined and approved.

Thesis Director, Dr. Robert B. Jerard
Professor of Mechanical Engineering

Thesis Co-Director, Dr. Barry K. Fussell
Professor of Mechanical Engineering

Dr. Brad L. Kinsey
Assistant Professor of Mechanical Engineering

May 10, 2007
Date

DEDICATION

I dedicate this thesis to my wife Cassandra for her patience, love, and support that made this possible.

As well as all the Desfosses named machinists that came before me:

Leo Desfosses

Gerry Desfosses

Mike Desfosses

Matt Desfosses

ACKNOWLEDGEMENTS

I would like to thank Dr. Jerard and Dr. Fussell for their encouragement and continued guidance that allowed me to complete my graduate studies. In addition I would like to thank Dr. Jerard for the extra hours he put in helping me improve the writing of my thesis. I would like to thank Dr. Kinsey for finding time to be on my committee and review my thesis on such short notice. I would also like to thank Donald Esterling for his time and input.

I greatly appreciate all of my lab partners for their support and friendship. Min, Chad, Cuneyt, Doug, and Toby have been great coworkers who became great friends. Thank you to Min Xu, for his programs which saved me countless hours of data processing time. Without his work, I would not have been able to finish my research.

I would also like to thank my parents who have supported me in everything I do. Their support helped me greatly in my college years and I would not have made it through without them.

TABLE OF CONTENTS

LIST OF FIGURES

LIST OF TABLES

LIST OF SYMBOLS

a	----	axial depth, (in)
b	----	radial depth, (in)
Φ	----	angular position of tooth (rad)
Φ_{eng}	----	Swept angle that the cutting tool is engaged per revolution (rad)
V	----	Cutting speed (ft/min)
f	----	Feed rate (in/min)
f	----	feed per tooth (in)
r	----	radius of tool (in)
ω	----	spindle speed (rpm)
$h(\Phi)$	----	chip thickness at Φ (in)
h_{avg}	----	average chip thickness (in)
F_t	----	tangential cutting force (lbf)
F_r	----	tangential cutting force (lbf)
K_{tc}	----	model parameter for tangential shearing force component (lbf/in^2)
K_{te}	----	model parameter for tangential rubbing force component (lbf/in)
K_{rc}	----	model parameter for radial shearing force component (lbf/in^2)
K_{re}	----	model parameter for radial rubbing force component (lbf/in)
P	----	average cutting power (in-lbf/sec)
$\dot{Q}$	----	average material removal rate (in^3/sec)
$\dot{A}_c$	----	contact area rate (in^2/sec)

VB ---- flank wear land width (in)

R^2 ---- Coefficient of Determination

ABSTRACT

AN IMPROVED POWER THRESHOLD METHOD FOR ESTIMATING TOOL WEAR DURING MILLING

By:

Bennett Desfosses

University of New Hampshire, May, 2007

It is well known that cutting forces increase as a cutting tool wears out. Current commercially available Tool Condition Monitoring (TCM) systems use this fact to set a threshold for the allowable percent power increase corresponding to a worn out tool. Typically, a training process is required whereby the first few parts cut with a sharp tool provide a baseline for comparison. This method works well when making large numbers of the same part with a single tool but is not as useful when making a single part or when the tool life is shorter than the time required to make a single part.

The goal of this research is to develop a TCM system that can estimate tool wear without the necessity of a training process and in the presence of different modes of tool wear. Our hypothesis is that tool wear can be accurately correlated with the coefficients of a tangential cutting force model. The model coefficients are estimated by online measurement of spindle motor power. One of the model coefficients (K_{tc}) relates cutting forces to chip thickness. The other coefficient (K_{te}) relates to rubbing or

edge forces. Research results indicate that K_{te} correlates well with flank wear while K_{tc} is a good indicator of edge chipping.

A number of experiments are performed with helical flat end mills made of High Speed Steel (HSS) and carbide tools cutting 1018 steel. Spindle motor power is used to calibrate the model coefficients at periodic intervals. Generally, the percent power increase at tool failure is much higher when flank wear is the dominant mode. Tool wear is estimated based on a weighted combination of the two model coefficients thereby establishing a threshold that is independent of the combination of chipping and flank wear.

Preliminary research was also performed to explore the potential of using a contact microphone mounted to the spindle for TCM. A contact microphone can provide frequency information based on the vibrations as well as relate the RMS value to cutting power.

CHAPTER 1.

INTRODUCTION

In milling, tool wear is an important variable that affects both the cost and quality of the finished part. The cutting conditions should produce a predictable mode of wear that can be monitored. If a tool wears out too fast the tooling cost can be excessive. If the tool fails abruptly or wears out before it is changed, it can cause unacceptable surface finish, tolerances, and even damage to the part.

> *Considerable research has been done in the area of tool monitoring due to the fact that tool failure represents about 20% of machine tool down time and that tool wear negatively impacts the work quality in the context of dimensions, finish and surface integrity. [16]*

> *It has been predicted that an accurate and reliable tool condition monitoring system (TCM) could result in cutting speed increases of 10-50%, a reduction in downtime by allowing it to be scheduled in advance, and an overall increase in savings of between 10% and 40%! [7]*

An experienced machinist can determine the best cutting conditions and also monitor the cutting process using visual and auditory clues to estimate the level of wear. But as modern metal cutting continues to be more automated with unattended machining, there is a need for improved computer-based methods for wear estimation. A robust/reliable Tool Condition Monitoring (TCM) system would improve the efficiency of unattended machining. Therefore, there has been considerable research on methods for automated TCM [6].

Currently used methods for TCM consist of setting power threshold limits based on a training process using the power recorded while cutting the first few parts with a sharp tool. These methods are useful when making multiple parts, but do not work well on parts like a stamping die or a large injection mold where you are only making one or two parts, or when the tool may wear out part way through the job. A mistake on these types of parts can be very costly and the ability to monitor the first part would be beneficial.

In this research we use a cutting force model that can be calibrated by measuring spindle motor power. The force model calibration coefficients provide an estimate of tool wear and also can be correlated with the type of wear. The model coefficients can be updated by measuring power while cutting the part, provided that there is sufficient variation in chip-thickness. Alternatively, it can also be calibrated offline with a periodic standard calibration routine.

A number of experiments are performed with helical flat end mills made of High Speed Steel (HSS) and carbide tools cutting 1018 steel. Spindle motor power is used to calibrate the model coefficients at periodic intervals. Generally, the percent power increase at tool failure is much higher when flank wear is the dominant mode. Tool wear is estimated based on a weighted combination of the two model coefficients thereby establishing a threshold that is independent of the combination of chipping and flank wear.

1.1. Tool Wear

Current TCM systems are based on the assumption that the final percent power increase is known and repeatable. To improve on current TCM systems the ability to identify chipping in addition to flank wear and to react to unexpected problems should be added. The physical interactions that cause tool wear are [15]:

1. Abrasion
2. Adhesion
3. Diffusion
4. Oxidation
5. Fatigue

Abrasion is the process whereby inclusions in the work-piece that are harder than the tool scratch the tool and abrasively wear away the cutting edge [2]. As the flank face of the tool heats up it becomes easier to scratch resulting in more abrasion [2]. Scratches can also come from tool material getting trapped between the tool and work piece [1]. Hard cutting tools like carbide are better at resisting abrasion but may not be as able to resist other load factors during machining [15]. **Adhesion** occurs when fragments of the work piece are welded to the tool edge, known as a "built up edge", and then sheared off tearing some of the tool material with it [1]. **Diffusion** is present when heat causes the atoms of the tool to migrate into the work piece and atoms from the work piece replace

them. Progressive diffusion leads to weakening of the cutting edge [1]. Molecules attaching to the cutting tool where it is exposed to air causes **oxidation**. Depending on the location of oxidation it can accelerate different modes of wear. **Fatigue** is cased by thermal cycling and the loading and unloading of the tool [15]. This leads to chipping, cracking, breaking, and plastic deformation of the cutting edge [15]. These mechanisms contribute to a few different modes of tool wear. The common modes for helical end mill cutters are:

1. Flank wear
2. Chipping
3. Notch wear

Flank wear is the most desirable and measurable mode of wear. Flank wear is caused by the friction between the flank face of the tool and the work-piece, causes abrasion and adhesion with some diffusion [1]. Flank wear can be measured under a microscope, where the length of the wear land is known as VB (**Fig 1-1**). The intermittent nature of cutting during milling causes loading and unloading of the cutting edge that results in **chipping** [15]. It has been shown that chipping can be minimized by choosing cutting conditions with a small exit angle [2]. This makes down milling and slotting a good strategy, as the exit angles are zero.

Notch wear can be caused by adhesion or oxidation. The notch is located at the top of the cut where the tool is exposed to air while in the cut. The top of the cut is a common place for adhesion to occur [15].

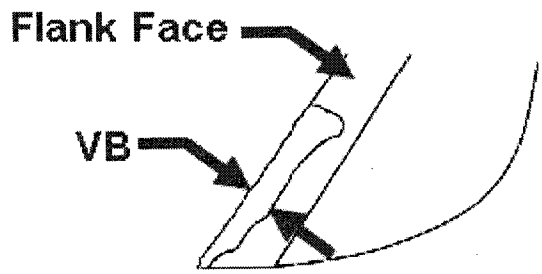

Figure 1-1 Flank Wear (VB)

Flank, chipping and notch wear are the most typical wear modes. Uniform flank wear is the most desirable mode of wear but chipping and notch wear can be unavoidable in some cases. Therefore, it is important for a TCM system to distinguish between these modes of wear. Heat is a factor in determining which mode of wear will occur, and at low temperatures adhesion and abrasion are dominant which are the dominant mechanisms of flank wear. Figure 1-2 shows that a typical temperature (Tc) for carbide cutters results in all four mechanisms of tool wear: adhesion, oxidation, abrasion and diffusion. Using this information we can design experiments that will allow us to investigate the desired modes of wear.

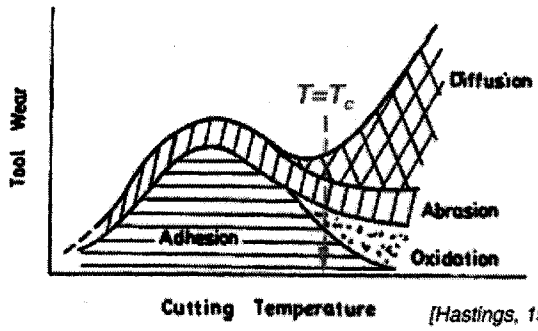

Figure 1-2 Cutting temperature vs. tool wear for carbide cutters [4]

1.2. Prior Art

The classic method for predicting tool wear is the Taylor wear equation (**Eqn 1-1**) developed in 1907 [17]. It was developed to model flank wear and works well for turning applications. Once calibrated for the constants (C) and (n) the Taylor wear equation can give a good approximation of the tool life (T) given the cutting speed (V).

$$T = C \cdot V^{-n} \qquad (1\text{-}1)$$

Attempts to refine this model to include more variables have also been developed as shown in Eqn 1-2a, where the additional variable is feed rate (f) with another constant m to be calibrated by a series of tests as illustrated in Table 1-1. It can be expanded to consider any number of variables (Eqn 1-2b, a= axial depth) but it then requires more tests to calibrate.

$$T = C \cdot V^{-n} \cdot \mathrm{f}^{-\mathrm{m}} \qquad (1\text{-}2a) \qquad T = \frac{C}{V^{n} \mathrm{f}^{\mathrm{m}} a^{p}} \qquad (1\text{-}2b)$$

Table 1-1 Taylor calibration tests for Equation 2a [1]

Test No.	Cutting Speed V (m/min)	Feed Rate (mm/rev)	Measured Tool Life T_t (min)
1	100	0.2	80
2	200	0.2	10
3	200	0.1	40

Taylor type approximations of tool life predict well for a certain ranges of cutting speeds, but it has been shown that over a larger range of cutting speed tool life does not continuously decrease with cutting speed [3]. **Fig 1-3** shows two tool life curves: curve #1 is the Taylor approximation of the time (T) vs. Cutting Speed (V) relation, and curve #2 is an experimental result [3]. This type of phenomena makes it difficult to implement TCM in milling. Milling follows the principles of the Taylor equation, but the addition of other factors like cutter geometry, varying chip thickness, and intermittent cutting causes the Taylor wear equations to be unreliable. "... the complex geometry of the cutters themselves, result in end milling being one of the most complicated types of machining processes" [7]. Since tool life prediction is problematic for milling, it is important to have a TCM system that periodically or continually measures the current state of wear.

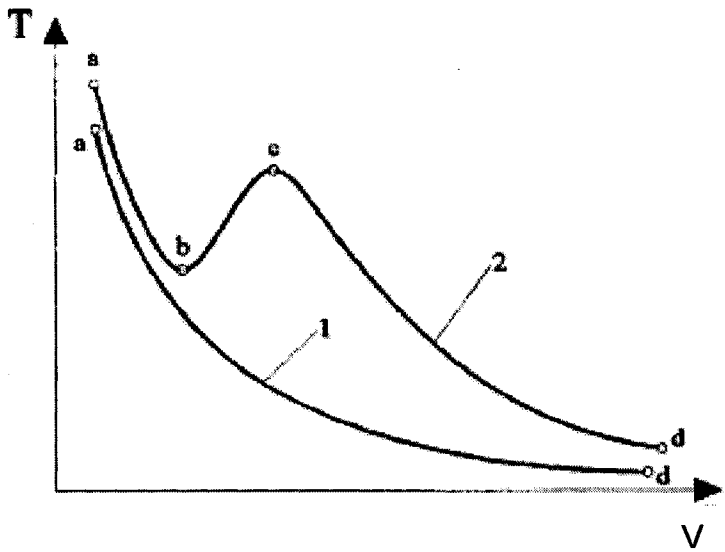

Figure 1-3 Tool life vs. Cutting Speed, Curve 1 = Taylor approximation, Curve 2 = experimental [3]

A review of machine process monitoring and control, was conducted by Liang, in 2004 [16]. They wrote: "As the tool gets worn the geometry changes, thereby impacting the cutting forces." The radial and feed force components were proven to be more sensitive to tool wear [16]. Most force monitoring systems require the use of a work-piece table dynamometer [7]. This can be a problem in milling due to the expense and impracticality of mounting load cells in the cutting zone. One TCM system that used cutting forces in face milling was a neural network based system by H. Saglam and A. Unuvar (2003) [18]. This is an Artificial Neural Network (ANN) system that makes estimations on flank wear (VB) and surface finish (Ra). It requires careful selection of training patterns and model selection. The ANN was trained with 16 experiments, recording 3 min of data for each, and tested with 32 test patterns in order to choose between 19 models. Their system was able to estimate VB and Ra within 23% and 20% respectively. This is a

highly complex system that was applied to the steadiest and most predictable form of milling (face milling) and would be much more difficult to apply to general machining conditions. Using force sensors also becomes problematic due to large entry and exit forces that may result in false alarms based on limits set for tool breakage [7]. Force signals have also been used to detect tool breakage, one such system requires measuring and analyzing the force signal for every revolution [21].

While the radial force may be more sensitive to wear, Liang [16], observed that flank wear correlated with feed and cutting force components [16]. The tangential cutting force component can be directly related to spindle motor power, a quantity that can be easily and inexpensively measured using a non-invasive sensor. To avoid the expense and impracticality of using a dynamometer mounted under the work-piece [18] or a rotating dynamometer clamped between the cutter and spindle [19], commercial systems have opted to use less expensive spindle motor power measurement. One commercial system is TMAC (Tool Monitoring Adaptive Control) developed by Caron Engineering [13]. This system records the cutting power with a sharp tool and sets a threshold for the present power increase to initiate a tool change. The system compares cutting power at selected points in the CNC program to monitor tool wear. This method is most successful with multiple part machining where one tool will last more than one part. In a review of TCM systems [6] a threshold based patent by Jones and Wu [22] with the following comment:

A major limitation of this type of system is that thresholds will vary greatly as the cutting conditions vary. Even simply a change in the radial or axial depth of cut would require the trial cuts be repeated. [6]

The ability to determine the state of wear from power independent of the current or past cutting conditions would improve this type of TCM system.

Under steady conditions like turning, flank wear increases in a third order trend (Figure 1-4). Power has long been known to increase linearly with wear land in turning [20], and this has also been shown to be true in milling (Figure 1-5) [25]. This shows that if a tool experiences identical cutting conditions power can be a good measure of VB. The trouble comes when flank wear is not the dominant mode of wear, something unexpected happens, or the cutting conditions are continuously changing.

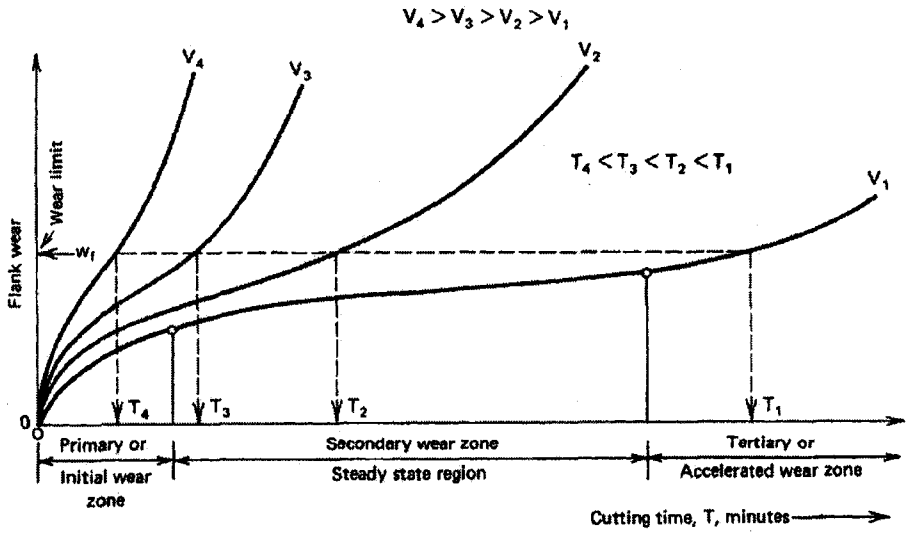

Figure 1-4 Flank wear versus time for various surface speeds [1]

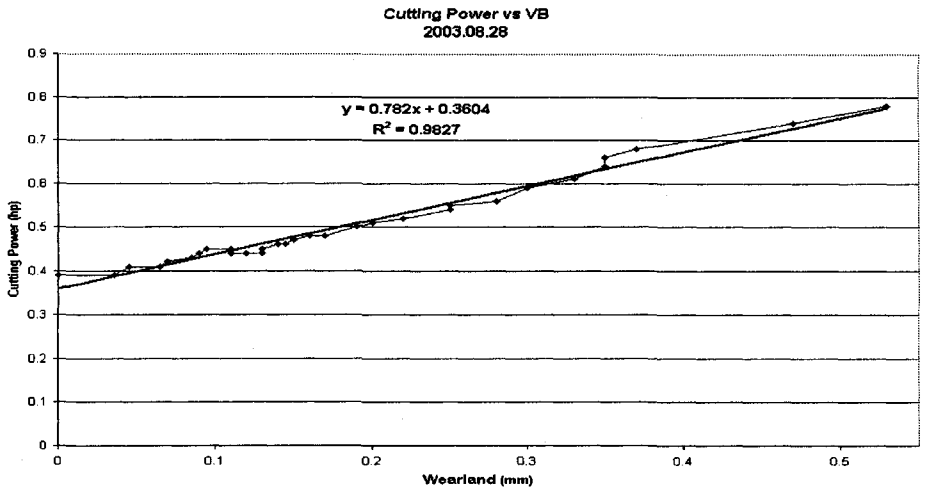

Figure 1-5 Power vs. VB, axial depth = 0.25", radial depth = 0.3", 725 rpm, 2.9 ipm, oil/water coolant, using a 0.5" HSS 4 flute flat end mill [25]

1.3. Vibration and Tool Condition Monitoring

One of the best tools a machinist has to monitor tool wear is his own ear. The increase in sound as the tool wears is a result of increased vibrations. Vibration sensors have been used successfully in TCM [6], but finding a good location for these sensors has been a problem. The main application for vibration signals in TCM has been broken tool detection and chatter diagnosis [6]. Many systems use the familiar Kistler force dynamometer to collect force measurements which are analyzed in the frequency domain. One such system measured the ratio of the amplitude of the tooth passing frequency to the rotational frequency in order to detect a broken tool [25]. Tlusty and Tarng presented a system that considered vibration and accelerometers as a replacement for force sensors [6]. In addition, an accelerometer system was developed that utilized ratios of high frequency content to low frequency content to detect broken tools [23]. Other

systems have successfully used wavelets to analyze vibrations and monitor wear [24].

The most successful mounting location for vibration sensors is on the work piece but this is an impractical location. In addition, when mounting the sensor on the machine bed the recorded vibrations can change in intensity as the distance from the cutter changes. Mounting accelerometers on the structure like the table or spindle has shown bad transmission of the vibrations [7]. "This lack of interest in vibration is most likely due to the fact that it is difficult to put accelerometers near the cutting site, let alone the tool." [7]. This review goes on to say that the success of mounting to the work piece demonstrates that accelerometers could be a very effective "chatter prevention/TCM System." Our research indicates that a contact microphone has good transmutability through the spindle and it may lend itself to the techniques referred to above. (see Chapter 6)

1.4. Motivation

This research will address the limitations of current power based methods of TCM and investigate the use of tangential force model coefficients to improve power based TCM techniques. **Figure 1-6** shows the results from our initial investigation [11, 25, 30] into the idea of using coefficients of a tangential force model to estimate tool wear. This graph shows a gradual increase of the K_{te} coefficient with tool wear and a sharp increase in K_{tc} towards the end of tool life.

This seemed like a promising result but to be practical a TCM system would have to be able to answer three questions reliably under a wide variety of conditions:

- How worn is the tool?
- How much longer will the tool last?
- When is the tool considered to be worn out?

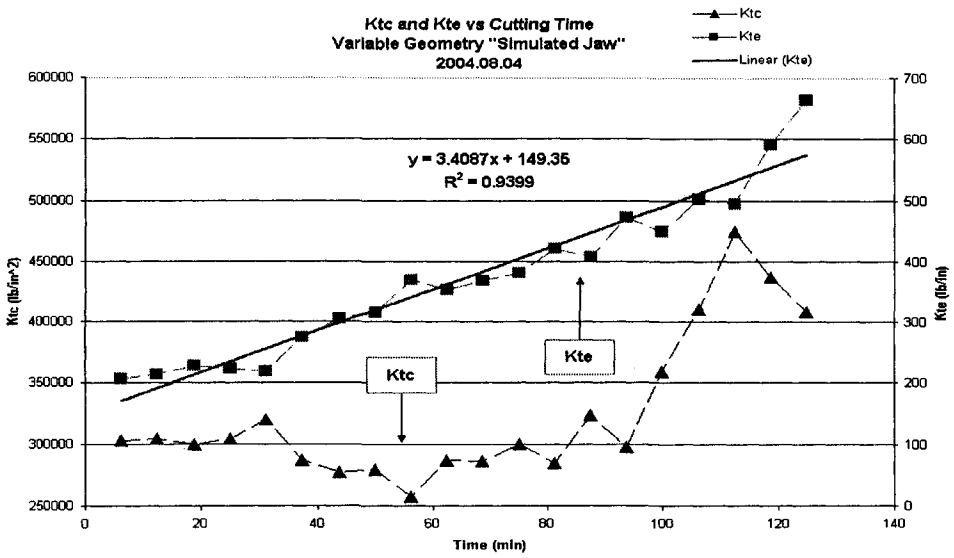

Figure 1-6 Cutting coefficients over time, HSS tool in 1018 steel. Exp A) [25]

1.5. Thesis Outline

In Chapter 2 the experimental methods will be described. The chapter will also discuses the limitations of the current cutting power threshold methods of TCM. An explanation of the tangential force model and the importance of using proper calibration techniques will be discussed. In Chapter 3 the results of the experiments will be presented. The sensitivity of the coefficients to tool wear will be shown. The differences in coefficient behavior with respect to the wear mode

and cutter material will be presented. In addition, the idea of a standard calibration in a sacrificial aluminum block will be tested. Chapter 4 will describe two methods of setting limits on the tangential force model coefficients for an improved power threshold TCM system. Chapter 5 shows an estimation of tool wear in relation to the increase in surfaces finish roughness value Ra. It shows the initial investigation and discuses the potential of using knowledge of K_{tc} and K_{te} in order to improve surface finish models. Chapter 6 will explore the potential of an AKG C411 L vibration pick up known as a contact microphone for TCM. Chapter 7 discuses the feasibility and imitations of the findings from this research and makes suggestions for future work.

CHAPTER 2.

METHODOLOGY

This Chapter will present the experimental methodology used to explore the use of tangential force model coefficients in a TCM system. The behavior of the coefficients and their potential to identify/quantify flank wear and chipping will be explored. The importance of using proper calibration methods for obtaining the model coefficients will also be discussed.

2.1. Tool Wear Experiments and Setup

A number of experiments were designed to test the hypothesis that model coefficients are a reliable indicator of both the amount and type of tool wear. Table 1-1 lists the details of each experiment. The experiments were designed to confirm the result of the initial investigation shown in **Fig 1-6** and published by Xu [11]. This initial experiment is listed as Exp (A) in Table 2-1.

Table 2-1 Experiments

	Experiments											
Reference Letter	A	B	C	D	E	F	G	H	I	J	K	L
Cutter Material	HSS	HSS	HSS	Carbide	Carbide	Carbide	Carbide	HSS	HSS	HSS	HSS	HSS
Work-piece Material	1018 Steel	1018 Steel	1018 Steel	1018 Steel	1018 Steel	1018 Steel	1018 Steel	1018 Steel	1018 Steel	1018 Steel	1018 Steel	1018 Steel
Calibration Material	1018 Steel	1018 Steel	1018 Steel	1018 Steel	1018 Steel	1018 Steel	1018 Steel	1018 Steel	Aluminum	Aluminum	Aluminum	Aluminum
Tool Diameter	0.5"	0.5"	0.5"	0.5"	0.5"	0.5"	0.375"	0.375"	0.3125"	0.3125"	0.3125"	0.3125"
Number of Flutes	1	1	1	4	4	4	1	1	1	1	1	1
*Calibration Cuts	S, 3D	S, D	D @ 50%	S	S	S	S, 3D	S, 3D	S, 3D, C, 3U	S, 3D, C, 3U	S, 3D, C, 3U	S, 3D, C, 3U
**Feed rates (in/min) Calibration cuts	0.8, 1.2, 1.4, 1.7	2.75, 3.0, 3.4, 3.7	2.75, 3.0, 3.4, 3.7	8.02, 16.04, 24.06, 32.09	8.02, 16.04, 24.06, 32.09	12, 24, 36, 48	3.21,3.67, 4.13, 4.58, 5.04	0.8, 1.2, 1.4, 1.7	10.3, 15.5, 18.6, 22.7, 50.0	10.3, 15.5, 18.6, 22.7, 50.1	10.3, 15.5, 18.6, 22.7, 50.2	10.3, 15.5, 18.6, 22.7, 50.3
Spindle Speed for Calibrations (rpm)	1068	1528	1528	2674	4011	4011	3055	1068	5157	5158	5159	5160
***Distance between Calibrations	0'	0"	6"	132"	132"	132"	0"	0'	24"	24"	24"	24"
Feed rate (in/min) between Calibrations	-	-	3.2	32.09	32.09	32.09	-	-	2.444	2.444	3.666	2.444
Spindle Speed between Calibrations	-	-	1528	2674	4011	4011	-	-	2444	2444	3666	2444
*Type of cut Between Calibrations	-	-	D @ 50%	D @ 25%	D @ 25%	D @ 25%	-	-	S	U @ 50%	S	D @ 50%
Additional Notes	Original Experiment	Bad calibration routine	-	-	-	Bad calibration routine	-	-	-	-	-	-
****Photo of tool wear					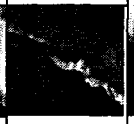						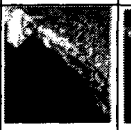	
	FW	FW	FW	CH	CH	CH	CH	FW	FW	FW + CH	FW + CH	FW + CH
	*Types of cut are : S=Slot cut, D=Down Mill, U=Up Mill, C=Center Cut. A number before the letter indicated multiple operations at different radial depth of cut at 75%, 50%, and 25% immersion, unless specified otherwise by an @ and the immersion %.											
	**Each Calibration Cut is taken through multiple feed rates in order to get a range of chip thicknesses for calibration											
	***This is the linear cutting distance between the starting points of consecutive calibrations. This and the type of cut as well as speeds and feeds can be used to calculate Distance in cut.											
	**** FW = Flank Wear, CH = Chipping											

All of the tools were helical end-mills. All experiments used 1018 as the work piece material for wearing the tools, and some utilized 6061 Aluminum as the work piece material for calibration. Most of the experiments were conducted with one-flute cutters in order to eliminate the effects of run out and the need to average the amount of tool wear between multiple flutes. The first attempt at duplicating the results of Exp (A) under different cutting conditions was Exp (B). From Exp (B) we learned the importance of using proper calibration procedures as will be explained in Section 2-3. Exp (C) was virtually the same experiment as Exp (B) with an improved calibration routine. Exps (D), (E) and (F) were designed to see how the coefficients change when using carbide cutters. Exps (G) and (H) were designed to test the sensitivity of the coefficients to a change in cutter diameter. Exps (I), (J), (K) and (L) tested the idea of using a sacrificial block of aluminum for calibration. By using a relatively soft material like aluminum it might be possible to just take a few test cuts at periodic intervals to measure the wear state of the tool. The results of this approach will be discussed in Section 3-4.

The test bed was a Fadal EMC CNC milling machine [34] (**Fig 2-1**) fitted with an open architecture MDSI Controller [35]. Spindle motor power, cutting forces, and vibration data was taken on each test. The power was measured with a UPC power sensor from Load Control Inc. [36] which measures the current and voltage going into the motor (**Fig 2-2**). The forces were measured by a Kistler 3-

axis dynamometer [37] mounted below the work piece (**Fig 2-3**). Vibrations were measured by an AKG C411 contact microphone [38] and a PCB 320C33 accelerometer [39] mounted adjacent to each other on the spindle for most experiments (**Fig 2-4a**) and on the work piece for Exps I, J, K, and L (Fig **2-4b**). All the data was collected with an A/D Board by Computer Board, model DEAS 6402 [40].

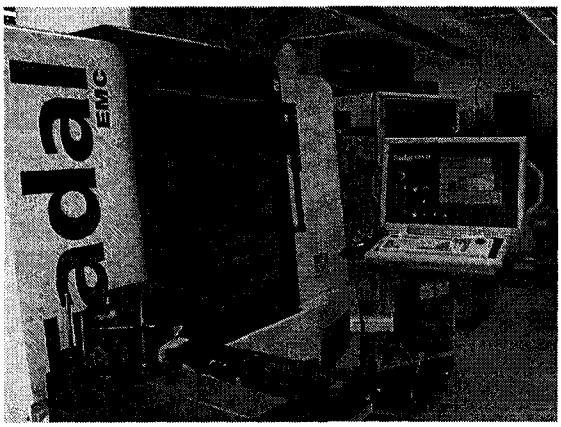

Figure 2-1 Fadal CNC Machine

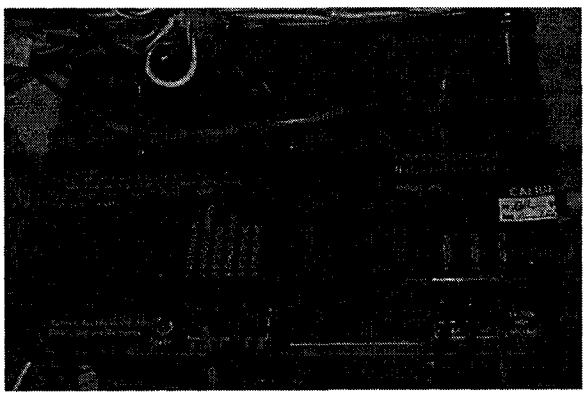

Figure 2-2 Power sensor

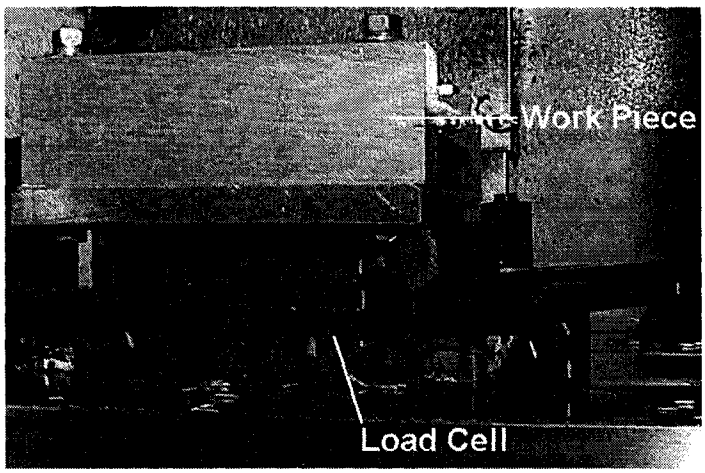

Figure 2-3 Kistler dynamometer (Load Cell)

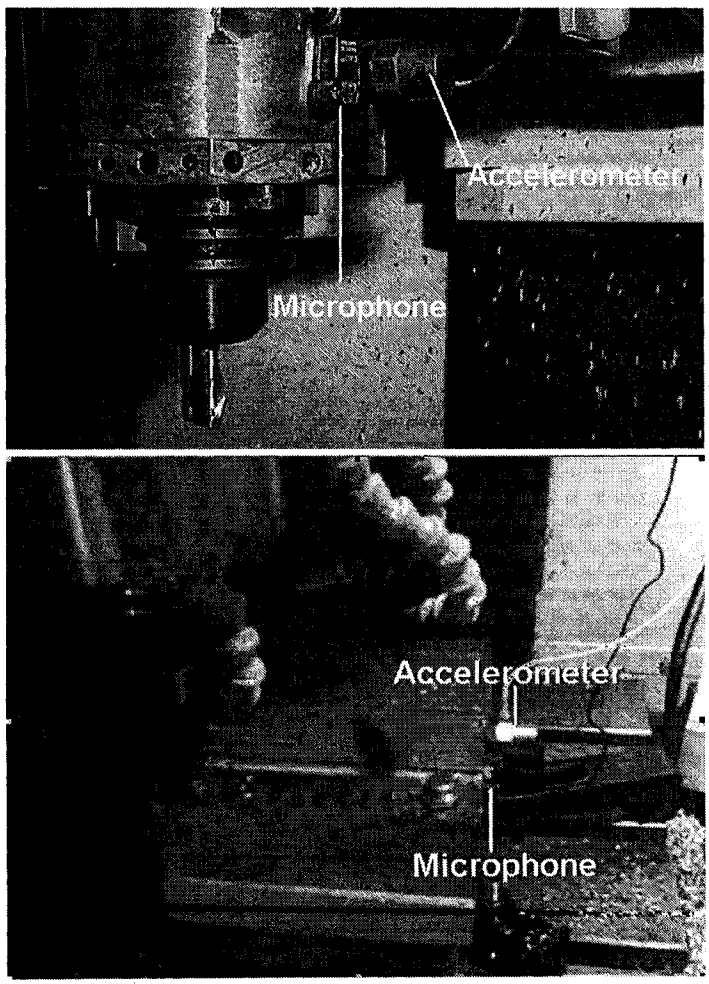

(a)

(b)

Figure 2-4 Microphone and Accelerometer placement

2.2. *Limitations of Power Measurement for TCM*

Fig 2-5 (Exp (G)) illustrates how the spindle motor power changes from cut to cut and over the life of a carbide cutter. The data points are taken at each feed rate of a calibration routine that is repeated until the tool is worn. The calibration cuts consist of a slot cut followed by three down mills (75%, 50%, and 25% radial immersion). Power data was taken at five feed rates ranging from 3.21-5.04 ipm. **Fig 2-5** shows that the variation in power due to changing cutting conditions can far exceed the change caused by wear. Therefore, a wear estimation system based on power must compare identical cuts for power ratio or limit setting. A statistical measure of the standard deviation of these points could also be a method of approximating tool wear but would be very dependent of the cutting conditions like the threshold method. One other thing to note about **Fig 2-5** is the third order trend of power with time, which is similar to that of VB vs. time of **Fig 1-4**.

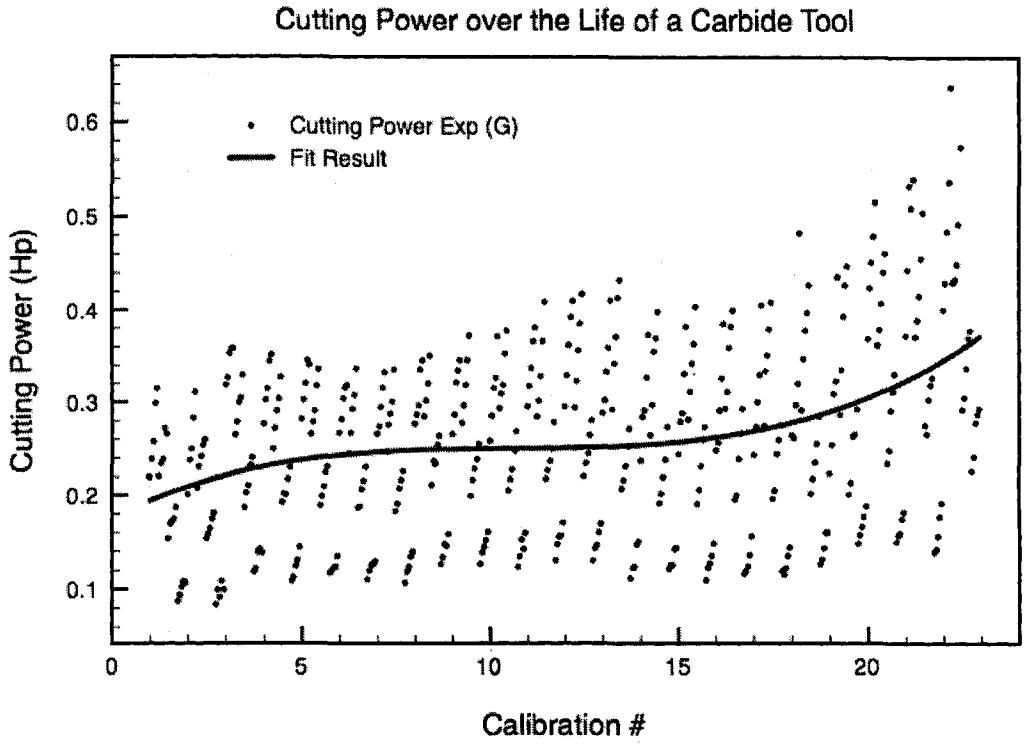

Figure 2-5 Cutting Power (hp) over the life of a carbide tool, Repeated calibration cuts with carbide end mill in 1018 steel, Exp (G)

Another important observation about monitoring power can be seen in **Fig 2-6** which compares the results for Exp E and G. Experiments E and G were performed in 1018 steel with 5/16" HSS cutters. The only difference between tests is the spindle speed. One might expect the two tests to have similar percent increases of power from the first cut to the last, but the 2444 rpm cut shows a 200% increase in power before the tool is completely worn out while the 3666 rpm case only reached about 100% increase in power for the same state of wear. The more aggressive cutting of the 3666 rpm cut resulted in more chipping and a smaller percent increase in power. Each of these tools was periodically

calibrated in aluminum and the average power of these identical calibration routines also reflected a reduction in power **Fig 2-7**.

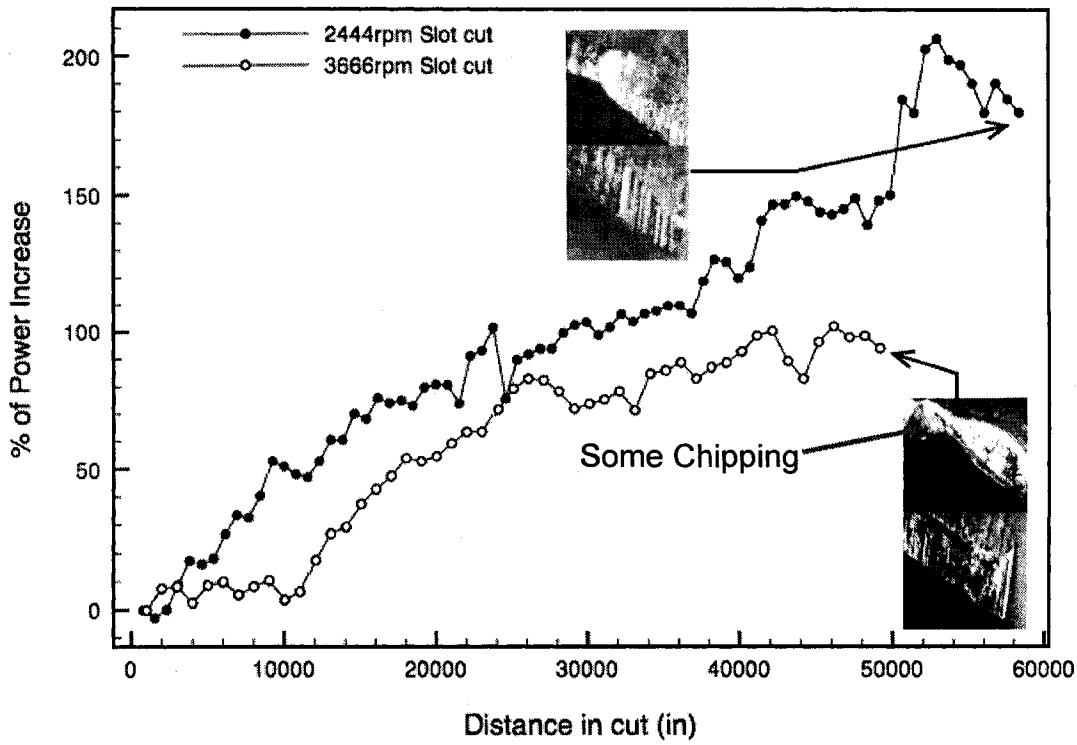

Figure 2-6 Percent power increase vs. Distance in cut, HSS slot cuts in 1018 steel, Exps (I) and (K)

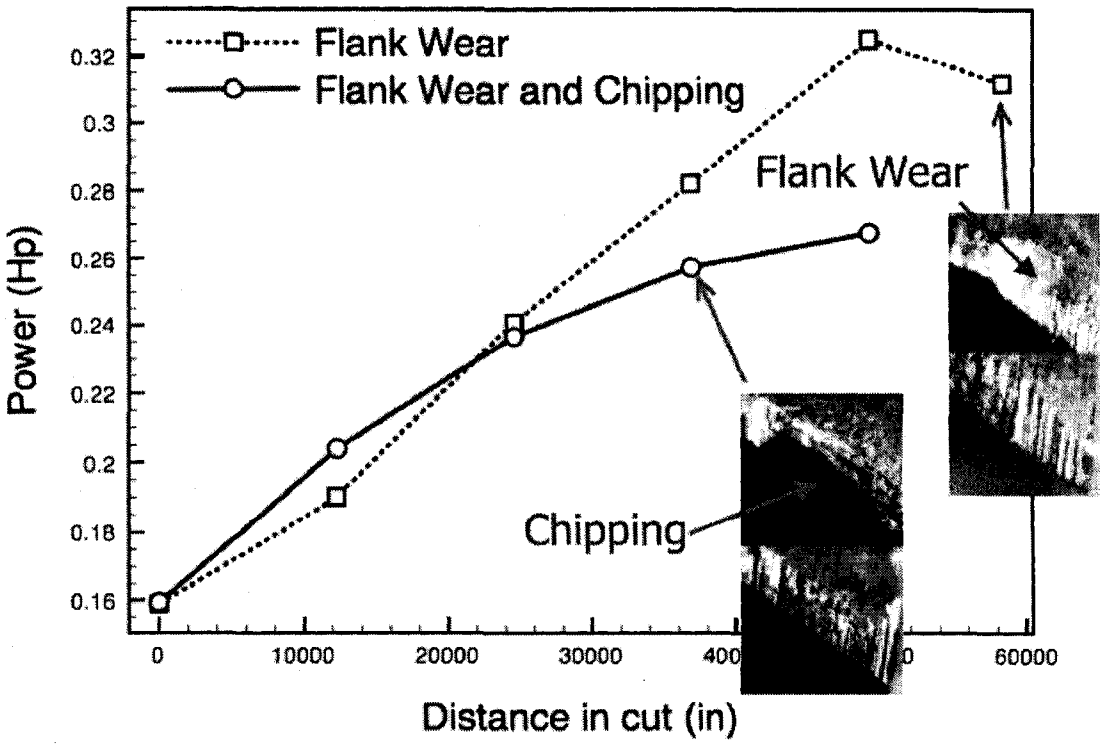

Figure 2-7 Comparison of I identical cutting conditions from tools with different type of wear, Exp (I) = Flank wear, Exp (K) = Chipping and Flank wear

This is an important observation and correlates with one of our primary conclusions, namely that the percent increase in cutting power at the end of usable tool life is dependent on the type of wear experienced by the tool. The difference between the two tests was that the 3666 rpm cut experienced some chipping along with flank wear. This chipping reduced the amount of flank wear land available for rubbing thereby reducing the percent power increase at fully worn condition.

From this observation it can be concluded that using a percentage power increase to assess tool condition is only viable if both the cutting conditions and

the tool failure mode are identical. This imposes a severe limitation on commercial TCM systems. If any process variables are changed, e.g. spindle speed, tool material, tool coating, then it becomes necessary to retrain the system. These observations confirm the results reported by Pickett [6] who noted that the thresholds are a function of cutting conditions.

Another unfortunate aspect of the finding illustrated in **Fig 2-7** is that identical cuts may not always yield the same percent power increase. For example, a threshold for a slot cut at 1000 rpm in 1018 steel with a 0.5" HSS cutter will not be the same for two different part programs because it also depends on the type of tool wear caused by the rest of the part program. Therefore, in the absence of knowledge about the type of tool wear a threshold must be set based on existing knowledge of the final power increases for the given part. Error in this threshold estimate will occur if the tool wear mode changes.

2.3. Tangential Force Model

The cutting force vector consists of radial, tangential and longitudinal components. The tangential forces apply torque to the spindle motor and can be directly related to the spindle motor power, a quantity that can be easily measured with inexpensive power sensors. The radial forces have been reported to be a better indicator of tool wear than the tangential forces [16] but radial force measurement requires the use of an expensive, invasive force

dynamometer and is therefore impractical for industrial use. This research focuses on using tangential force as a wear indicator.

Power data measured by the LCI sensor can be used to estimate the coefficients (K_{tc}, K_{te}) of Eqn 2-1.

$$P_{avg} = K_{tc} \cdot \dot{Q} + K_{te} \dot{A}_c \qquad (2\text{-}1)$$

The particular cutting conditions determine $\dot{\mathbf{Q}}$ the material removal rate and $\dot{\mathbf{A}}_c$ the contact area rate. More information about this equation and calibration procedures are available in [11, 25, 27]. The coefficients show good correlation with the tool wear state for a wide variety of cuts [11]. Equation 2-1 can also be used to accurately estimate the average cutting power and average tangential force for cuts with this tool and material, an ability that has been shown to be beneficial in setting safe and efficient feed rates [26, 29]. Eqn 2-1 can be calibrated with the power from two points that have different chip thicknesses, but it is better to have more points for increased accuracy. The data to perform this calibration can be gathered during the normal procedure of cutting the part or it can be done off-line with periodic calibration in a sacrificial block.

To calibrate the model, the average tangential force is calculated from Eqn 2-2 and plotted versus the average chip thickness calculated with Eqn 2-3. **Fig 2-8** illustrates how the coefficients of Eqn 2-1 are found by obtaining the slope and

intercept of the linear regression of data points obtained from a calibration test. Generally, as the flank wear increases the intercept also increases. Therefore, K_{te} correlates with the portion of cutting power which is insensitive to the variation in chip thickness. K_{tc} is, by definition, that portion of the cutting power which is proportional to the chip thickness.

$$F_{t_{avg}} = \frac{P_{avg}}{\omega \cdot r} \cdot \frac{2\pi}{\phi_{eng}} \qquad (2\text{-}2)$$

($F_{t_{avg}}$=average tangential force, r=radius of cutter, ϕ=angle of cutter, ω=spindle speed, P_{avg}=average power)

$$h_{avg} = \frac{1}{\phi_{eng}} \int_{\phi_{ent}}^{\phi_{ext}} f \cdot \sin(\phi) \cdot d\phi \qquad (2\text{-}3)$$

(h_{avg}=average chip thickness, f=feed/ tooth)

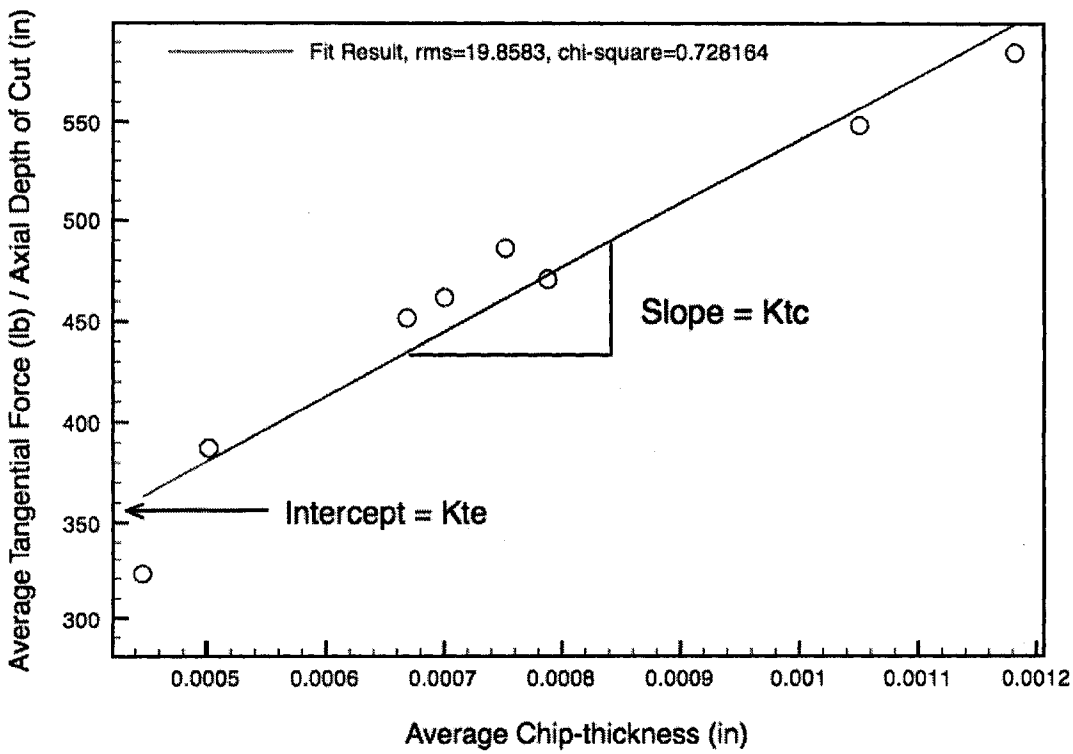

Figure 2-8 Least squares calibration of the tangential force model

From the least squares fit of this data the slope and intercept correspond to the two coefficients for Equations 2-1 and 2-4. These coefficients can be used to estimate the average tangential force and cutting power for any cuts performed with the same tool and material.

$$F_{t_{avg}} = K_{tc} h_{avg} a + K_{te} a \qquad (2\text{-}4)$$

K_{te} is often referred to as the edge coefficient and it would be expected that the increased rubbing caused by wear land growth would increase K_{te}. "Clearance-face (flank or wear-land) wear and chipping almost invariably increase the cutting forces due to increased rubbing forces" [12]. Although these coefficients are referred to in the literature [1] as edge and cutting coefficients, they really represent the portion of energy proportional to chip thickness (K_{tc}) and the proportion which does not change with chip thickness (K_{te}). The value of K_{te} is an artifact of the linear approximation of this model and is typically higher than the true rubbing force at very low chip thicknesses, mostly out of the range of normal cutting. But for normal cutting chip thicknesses K_{te}, the "rubbing coefficient" will be shown to be closely correlated with the increase in cutting power due to an increasing flank wear land rubbing against the work piece. K_{tc}, the slope of the plot shown in **Fig 2-4** should account for changes in cutter geometry that affect the tool's ability to efficiently shear the material, such as a chipped or a broken tooth.

2.4. Calibration of the Force Model with respect to Tool Wear

Estimation of tool wear using the force model coefficients is only possible if the model is accurately calibrated. Getting accurate calibrations of these coefficients can be a challenge. If the calibration procedure is not chosen wisely the coefficients may not behave as predicted. **Fig 2-9** is an illustration of how the coefficients should react due to increased rubbing.

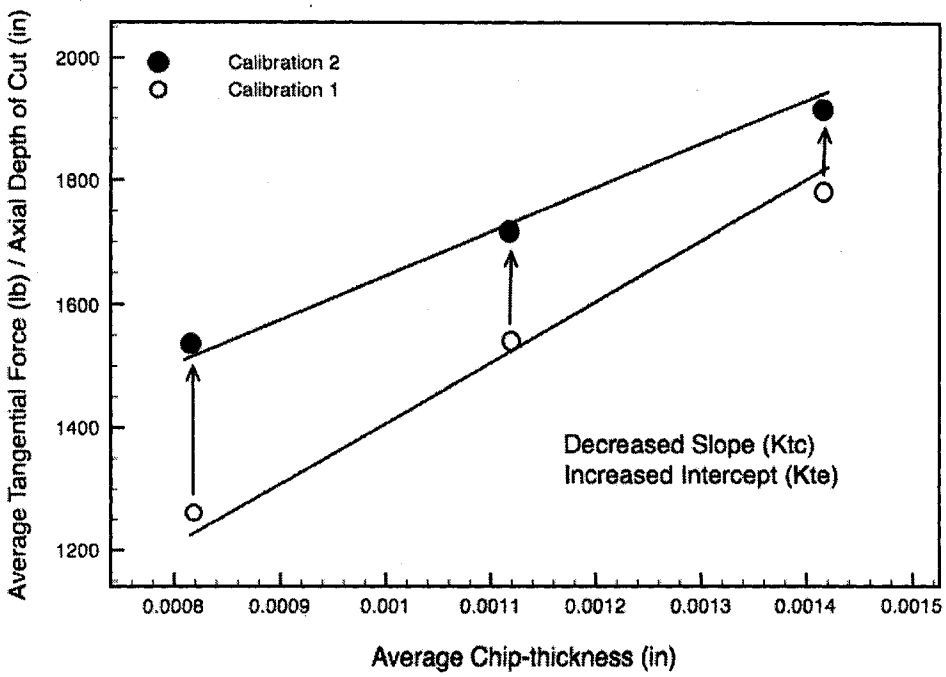

Figure 2-9 Consecutive calibrations with increased rubbing

The increased power due to rubbing will be more significant in smaller chip thickness calibration points causing an additional increase in the intercept (K_{te}) and sometimes a significant decrease in slope (K_{tc}) depending on the range of chip thickness. The reduction in K_{tc} with flank wear that has been observed is not fully understood but it shows that with flank wear the lower chip thicknesses

have a larger absolute increase in power causing the slope of the line to change. It could be that at low chip thicknesses there is more plowing and burnishing of the metal causing higher rubbing contributions to the cutting energy.

Another important change in the cutting coefficients as a function of wear is illustrated in **Fig 2-10**. This figure illustrates what happens if the data points within a single calibration occur at different wear states. In this case there was tool wear between the low chip thickness and high chip thickness data points. It is therefore imperative that the calibration take place over a relatively short period of time and that there not be any significant tool wear between the start and end of the calibration process.

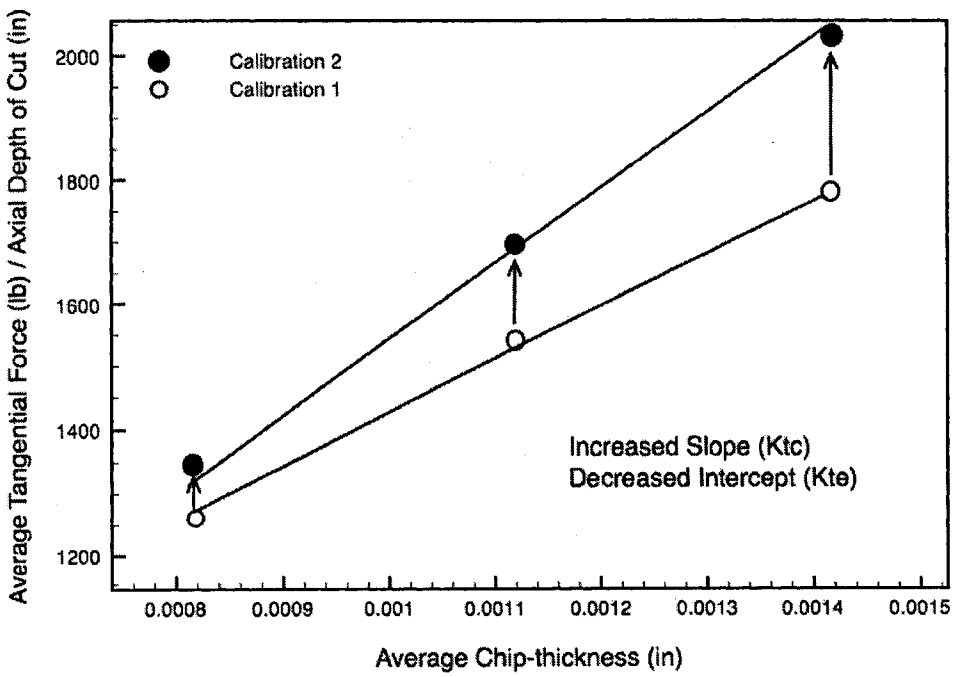

Figure 2-10 Change in slope due to tool wear during calibrations

This effect would continue to happen on each subsequent calibration causing increases in K_{tc}, which should actually be reflected in K_{te}. We have seen this effect often due to each calibration point increasing from low to high chip-thicknesses and the tool wearing significantly between the low and high chip-thickness. If the higher chip-thickness points were taken before the low points the opposite result would occur. An example of this can be seen in **Fig 2-11**. The test was in 1018 steel with a half inch HSS tool. The test consisted of slot cuts followed by a half immersion down mill. The calibrations were calculated from four different feed rates in each down mill operation. The first and last calibration points were more than 5 inches apart in the linear down mill operation.

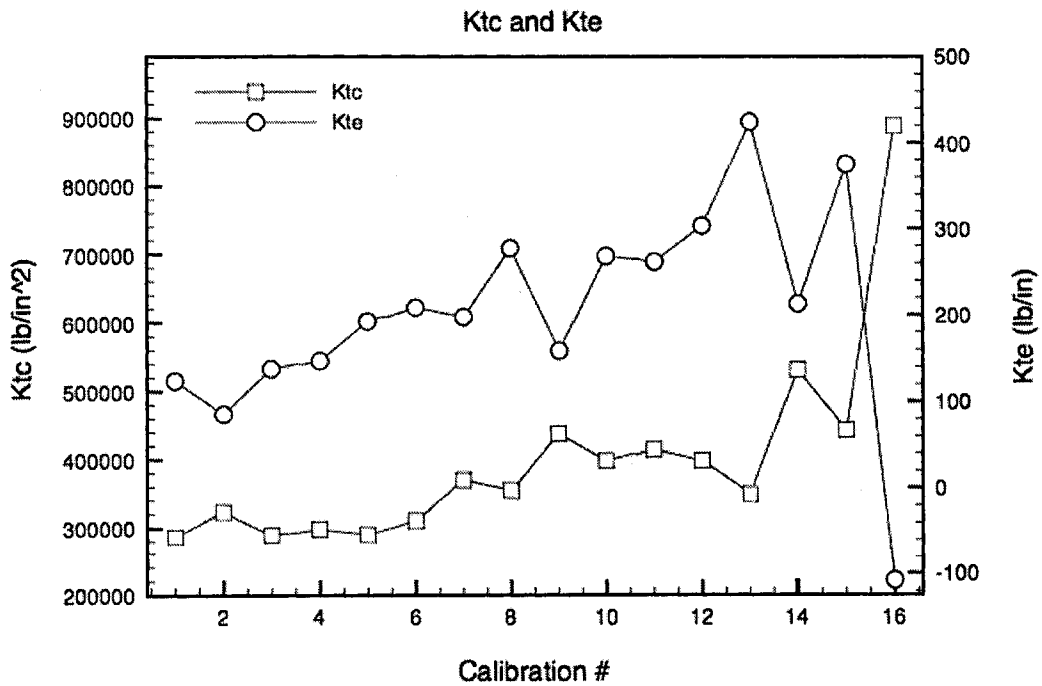

Figure 2-11 Cutting coefficients from a poor calibration routine, 0.5" HSS tool in 1018, Exp (B)

This effect was significant at calibration #16 of **Fig 2-11**. If the last data point of the 16th calibration is left off and calibrated with only three points the last point follows a more reasonable trend (**Fig 2-12**) showing that the effect of wear during calibration for the last calibration point is less significant without that last data point.

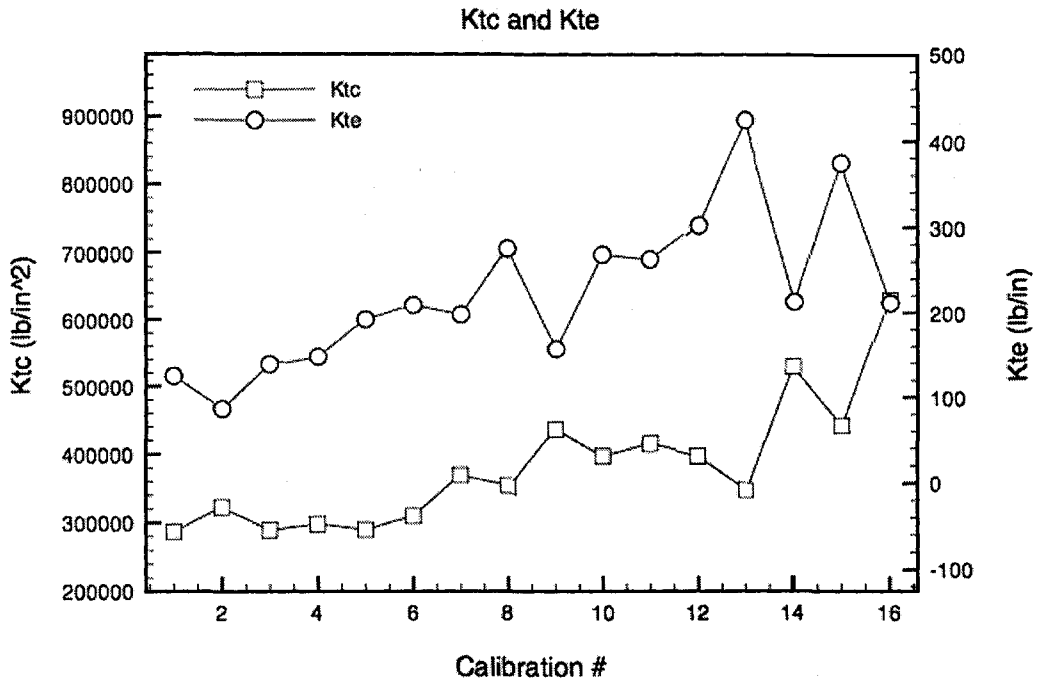

Figure 2-12 Artificially low Kte, Exp (B)

K_{tc} is increasing from the beginning of the test in **Fig 2-12**, which is not consistent with a tool experiencing flank wear as illustrated by **Fig 2-9.** This is the same effect of the tool wearing significantly during the calibrations at every calibration point in **Fig 2-10** just on a smaller scale. The other experiments, done with a more careful calibration process, are consistent with **Fig 2-9**, showing a

strong correlation between flank wear and K_{te}. Incorrect calibration techniques also contribute to the up and down effect of the coefficients seen in **Fig 2-12**. i.e. when K_{tc} goes up, K_{te} goes down and vice versa. We have dubbed this the "see-saw" effect. These effects must be accounted for when creating a calibration routine by keeping the cutting tool at nearly the same wear state.

2.5. Defining a worn tool

Allowed widths of VB have been published which define a worn tool at VB = 0.024-0.031" for rough milling and 0.012-0.016" for face milling [19]. But after interviewing a few machinists it seems that the definition of a worn tool is highly dependent on the task the tool is performing. For roughing, the tool can be used right up until the point of total failure, although it is still beneficial to catch the tool before it breaks or melts to avoid damage to the part or to the spindle bearings due to increased vibrations. Other criteria can be surface finish or part tolerances.

Our research indicates that it may be possible to estimate tool wear by measuring cutting power and calculating the tangential force model coefficients. **Fig 2-13a** is a new, unworn tool. It is not usually a good idea to set power limits with a brand new tool; users often set initial limits on the second or third work piece, after the tool is slightly broken in. **Fig 2-13b** shows the stage at which wear is progressing across the flank face of the tool and K_{te} should be increasing linearly. **Fig 2-13c** shows what the tool edge might resemble when the flank

wear has progressed past the allotted room for cutting and can no longer hold tolerances based on its diameter. At this point the tool can still continue to cut for a significant amount of time and can still perform roughing but the cutting has become much less stable and spindle bearing health may be adversely affected by the excessive vibrations and the risk of an abrupt tool failure. Problems arise for power based TCM systems when the tool wear mode resembles **Fig 2-9d**. Here we see chipping of the cutting edge, resulting in less area for flank wear/rubbing with commensurate smaller increases in power. In this case the TCM user is unaware of the occurrence of this chipping as an increase in the power limits might come suddenly, unexpected, or not at all at the end of tool life.

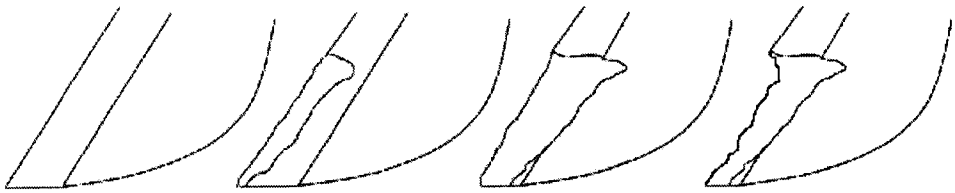

Figure 2-13 Tool Wear Looking at the flank face: a) New Tool, b) Flank wear, c) Worn tool, d) worn tool w/ chipping

CHAPTER 3.

WEAR RESULTS

This Chapter presents and discusses the results of the experiments presented in Table 1-1. Many of the experiments did not result in a uniform progression of flank wear that could be used to relate K_{te} to VB, the flank wear. Initially, our experimental design relied on aggressive cutting so that the tool would wear quickly allowing for more tests to be conducted. This approach generally resulted in more chipping rather than flank wear. It was also found that some types of cuts resulted in more chipping. Generally, up milling produced more chipping than down milling. This led to a somewhat different investigation of the coefficients than was initially expected based upon seeing the results of Exp (A).

The experimental results indicate that selecting thresholds for power or coefficient increase is only part of the problem. Equally important is the task of setting cutting conditions that result in flank wear as the dominant mode. Our findings indicate that small differences in cutting conditions can change the way the tool wears, which in turn affects the percent power increase for a completely worn tool. An effective TCM system should be able to deal with both flank wear and chipping as dominant modes of flank wear.

It should be noted that these results are limited to helical end mills cutting 1018 steel and may not be consistent with other types of cutters and/or other materials. Changes in cutter geometry, e.g. tools with negative rake angles may also change the behavior of the coefficients as the tool wears. Additional testing needs to be conducted to see if consistent results can be obtained with other combinations of tools and materials.

3.1. Flank wear and High Speed Steel

Exp (C) of Table 2-1 was designed to replicate the results of the initial investigation (Exp (A)). Based on the discussion in Section 2.3 flank wear should cause about the same absolute power increase at each chip thickness resulting in an increase in K_{te} and a steady or slightly decreasing effect on K_{tc}. **Fig 3-1** shows the coefficients vs. the distance in cut. This tool experienced predominantly flank wear which can be seen in **Fig 3-2**. The results are similar to that of the original test (Exp (A)) with K_{te} increasing linearly and K_{tc} not increasing until the end of tool life. We took this cutter further than in Exp (A) and continued to cut until it melted into the work piece. Shortly after the multiple pictures taken along the axial depth of cut in **Fig 3-2** were taken the small amount of flank face still left at the tip of the tool wore off and Kte no longer increased linearly. The cutter continued to cut for another 22 calibrations before it melted. For a machinist or TCM system wanting to avoid this region there are three indicators:

1. On average, K_{te} is no longer increasing linearly

2. The scatter or variance of K_{te} is increasing
3. K_{tc} begins to increase

Machinists wanting to continue roughing with a worn tool should consider the effect of increased vibrations on spindle health and may want to set a vibration limit using a contact microphone mounted on the spindle (a method that will be discussed in Chapter 6).

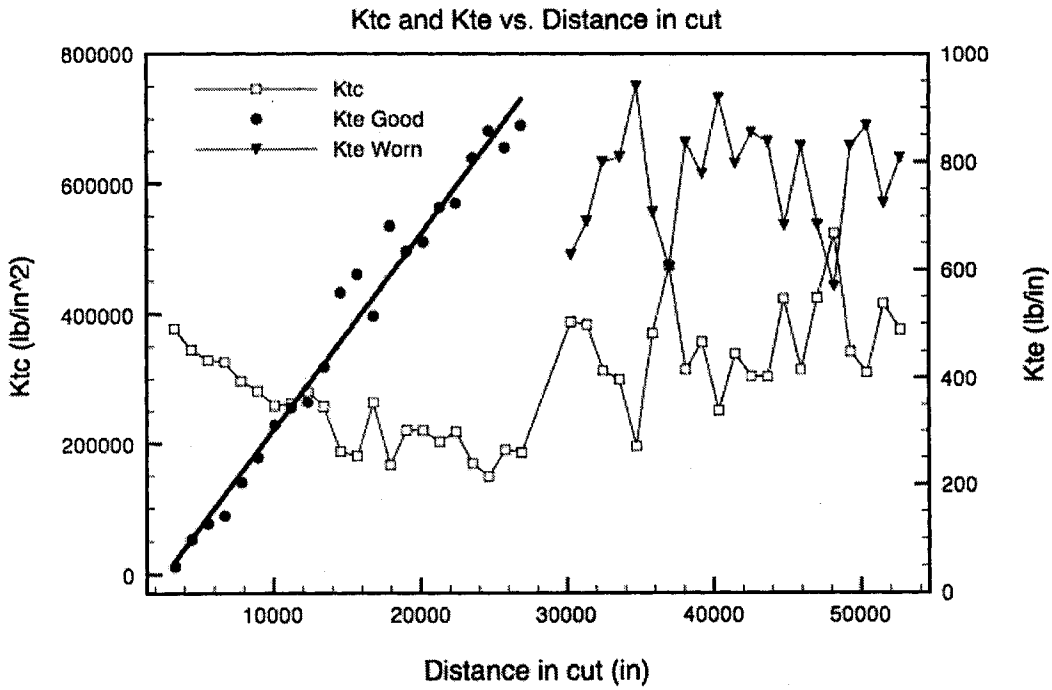

Figure 3-1 Ktc and Kte vs. Distance in cut, 0.5" HSS tool in 1018 steel, Exp (C)

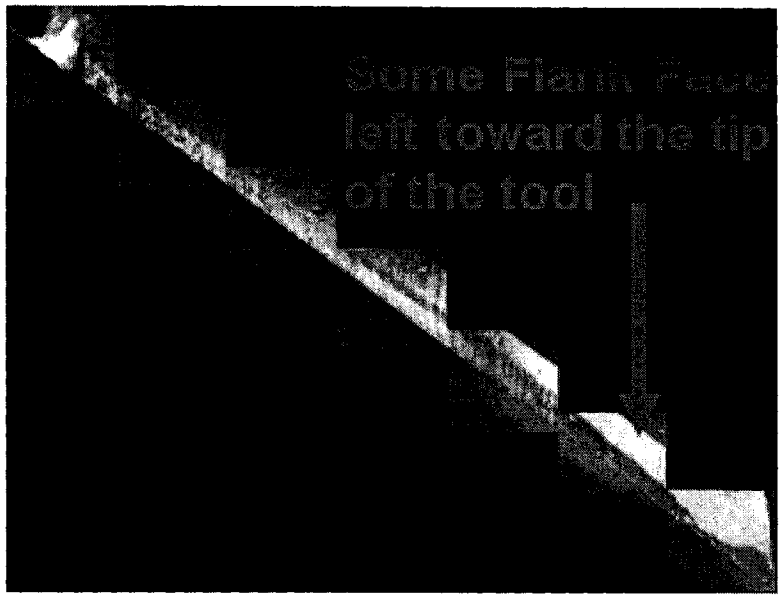

Figure 3-2 Cutting edge just before completely worn (2800" in cut), Exp (C)

We did get a larger decrease in K_{tc} from Exp (C) than Exp (A) but its contribution to the overall power was small. This is shown in **Fig 3-3**, which is a plot of the absolute power increase from the high and low chip thicknesses. The increase in power due to flank wear is almost the same for both low and high chip thicknesses but there is a small separation of the two curves that causes the decrease in K_{tc}, as this difference is ultimately the change in slope of the (Ft_{avg} / a) vs. h_{avg} plots of Section 2.3.

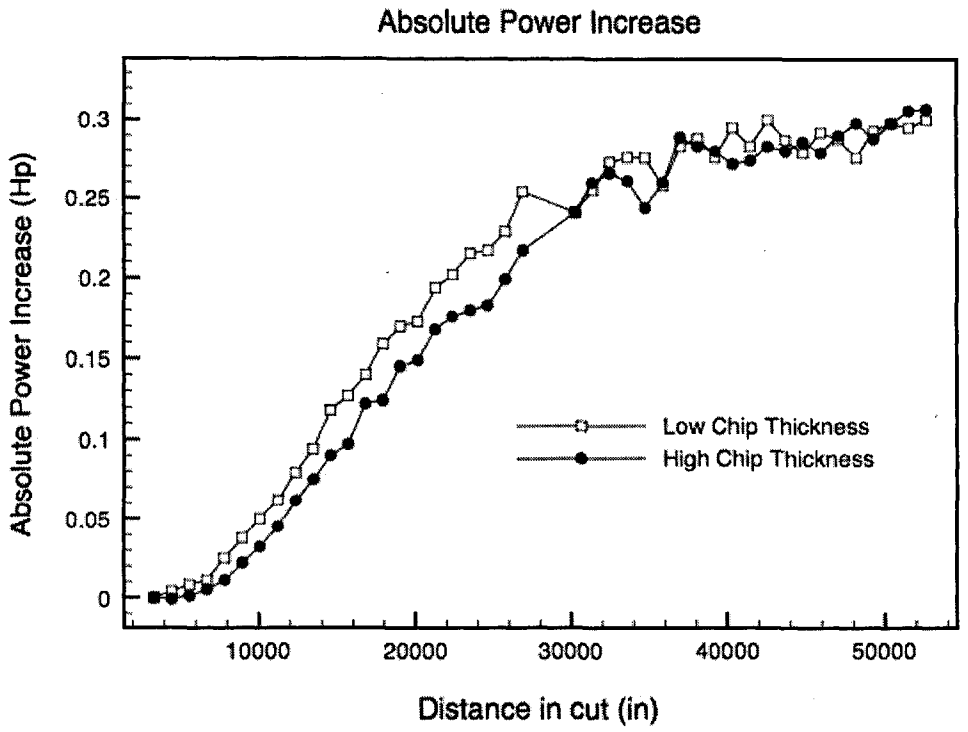

Figure 3-3 Absolute power increase due to flank wear, 0.5" HSS tool in 1018 steel, Exp (C)

The initial values of K_{te} and K_{tc} in Exp (C) were also different than Exp (A) (see **Fig 1-6**). The difference could be related to the difference in cutting speed or to the difference in tool flute geometry. Exp A used a Weldon tool and Exp C used a Niagara tool. These are all sources of error that need to be investigated through further research, but most of this difference in initial coefficients between Exps (C) and (A) could also be related to the calibration routines. The calibration routine for Exp A may have experienced some of the effects caused by significant wear occurring during the calibration routine. The distance between the low and high chip-thicknesses for Exp (A) was about 5" which makes this assumption valid. Had the calibration points been chosen such that wear was

not a factor during calibration the initial and final coefficient values may be closer for these two tests.

Fig 3-4 shows results for Exp (H). The coefficients for a smaller diameter cutter show very similar patterns to the coefficients of the original experiment (Exp (A)). K_{te} is very linear until the end of tool life where there is an increase in K_{tc}. This correlates well with the images of the cutting edge (**Fig 3-5**) which shows that the tool wear mode is flank wear. We can also see that the flank wear has just reached the limit of the allotted flank face by the end of calibration #12, depicted by the arrows pointing out the location of this limit on the previous calibration photos. It is important to note that the linearly increasing nature that we have seen from K_{te} is due to the tests repeating the same cuts. If the cutting conditions were continuously changing the K_{te} increases may not be linear and a TCM system would have to have previous knowledge of K_{te} and K_{tc} limits.

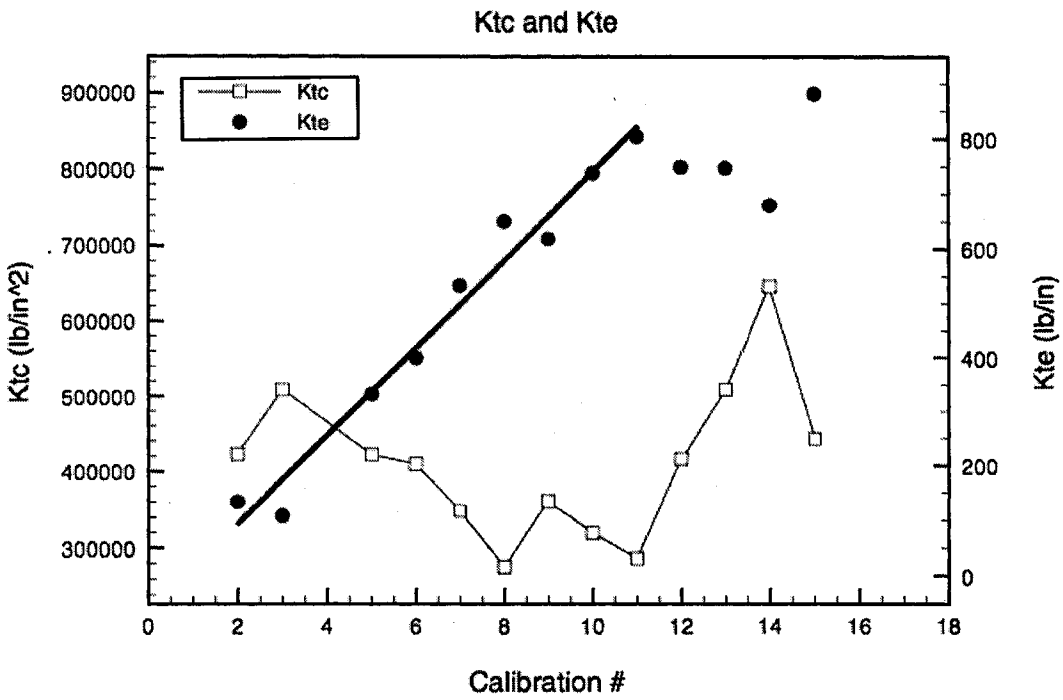

Figure 3-4 Calibration coefficients for a smaller diameter cutter, 0.375" HSS cutter in 1018 steel, Exp (H)

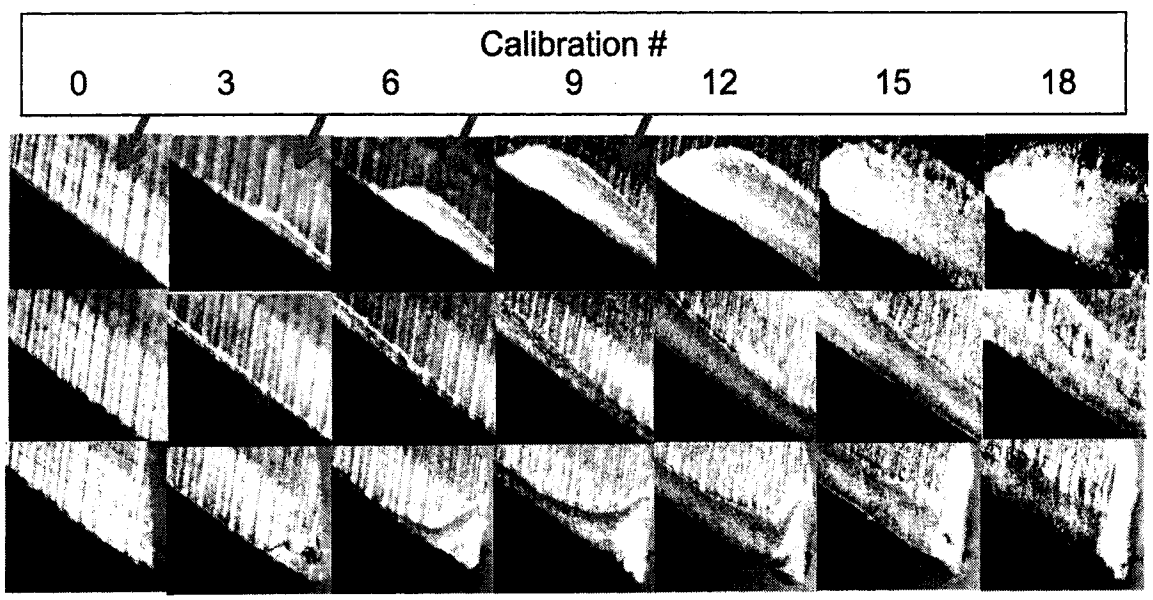

Figure 3-5 Flank wear pictures of Exp (H)

(Pictures are arranged in columns corresponding to the calibration number above with a picture of the tip at the bottom and the highest point of wear land at the top.)

3.2. Chipping and Carbide

We have observed that carbide cutters have a smaller percentage increase in power over the life of the tool. **Fig 3-6** shows how a carbide cutter's power increase is minimal until the end of tool life. This is because the hardness and ability to withstand high temperatures of the carbide cutter makes it more resistant to flank wear but more susceptible to chipping.

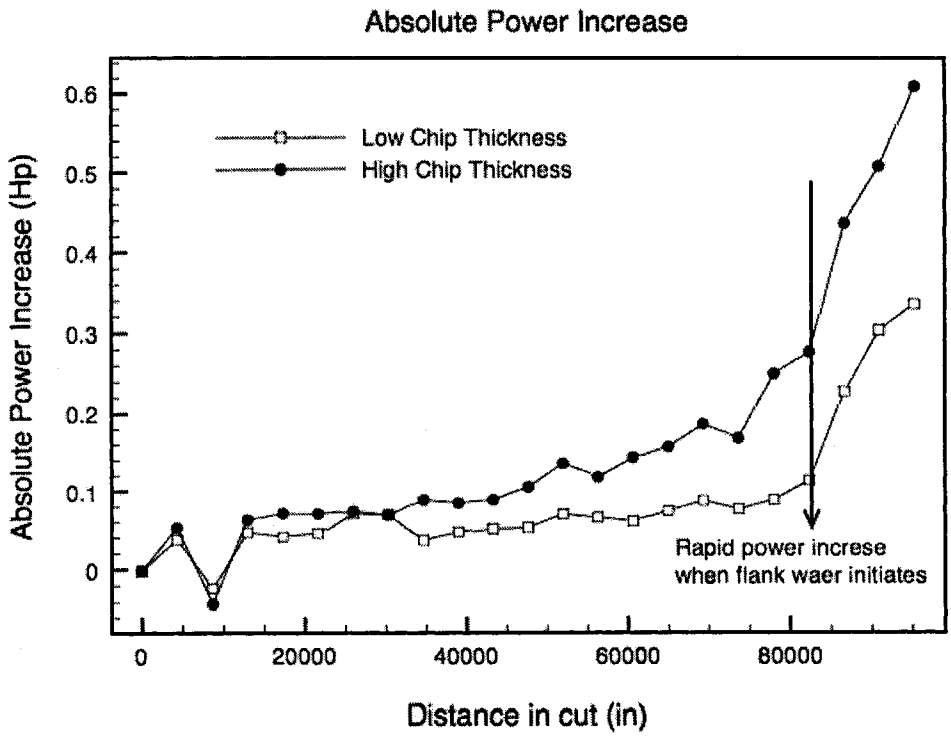

Figure 3-6 Absolute Power increase due to chipping for high and low chip-thicknesses, 0.5" carbide cutter in 1018 steel, Exp (D)

This carbide tool experienced more chipping than flank wear. **Fig 3-6** shows a separation of the high chip thickness curve from the low one that results in an increasing K_{tc}, which does result in significant change in the power increase as compared to the K_{tc} from the flank wear tests. **Fig 3-7** shows that the final

percent increase in power is similar for both the carbide 0.5" tool and the 0.5" HSS tool. This final value of power represents a tool that has completely chipped or worn off its allotted area of flank to resemble either **Fig 2-13c** or **Fig 2-13d**. But the carbide cutter shows a very small increase in power until it jumps to the final power level. This makes using thresholds or a power ratio difficult, because if you exclude the first couple of points of **Fig 3-7b** as a break-in period you are left with less than a 20% increase in power before you should be concerned about changing the tool.

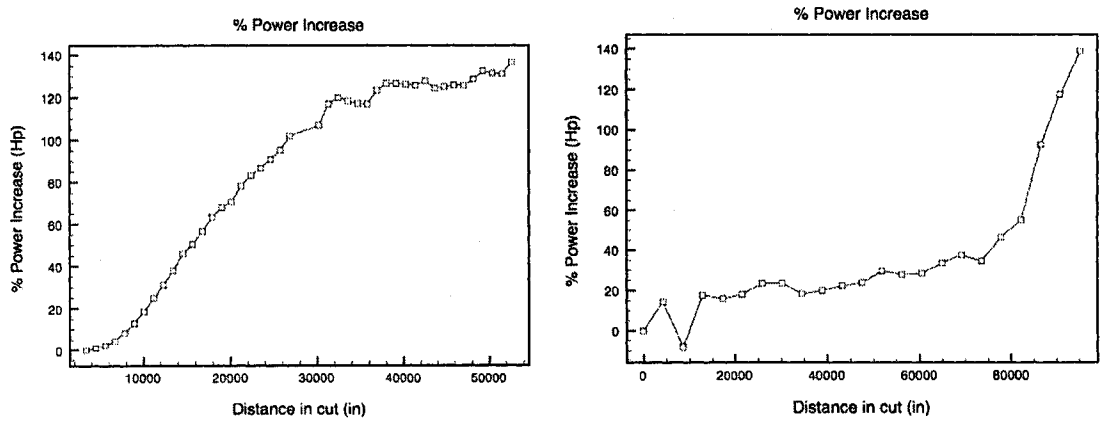

(a) (b)

Figure 3-7 Percent power increase: a) HSS Exp (C), b) Carbide Exp (D)

This difference in **Fig 3-7** between carbide and HSS cutters resulted in almost the exact opposite trend for the coefficients. That is, K_{tc} climbs steadily while K_{te} initially rises and then drop significantly before rising toward the end of usable tool life. **Fig 3-8** shows this for a 0.375" carbide cutter Exp (G).

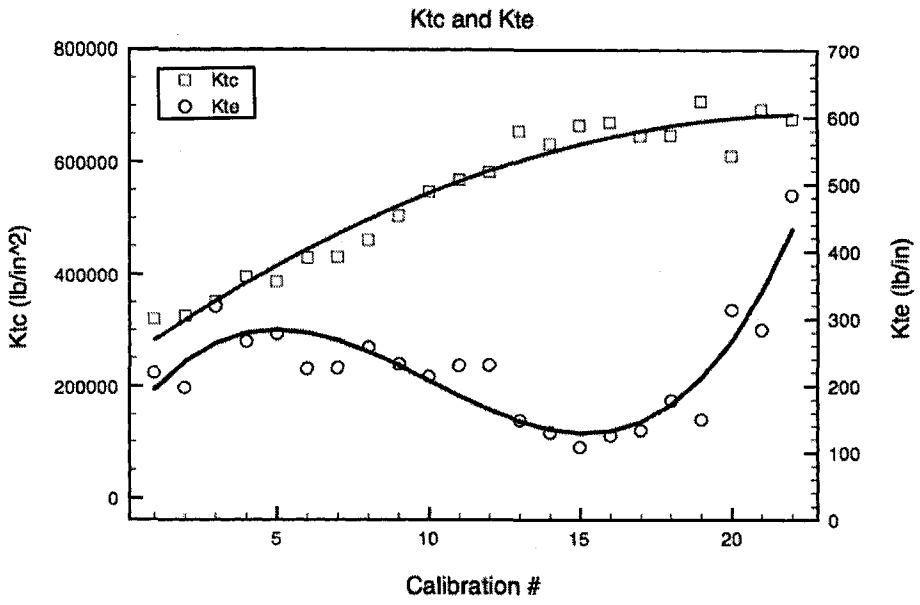

Figure 3-8 Tangential coefficients carbide end mill, 0.375" Carbide end mill 1018 steel, Exp (G)

This particular carbide cutter, under these conditions, seemed to experience more chipping than flank wear. As shown in **Fig 3-9**, the cutter experienced little flank wear and shows mostly chipping represented by the sharp edges and the receding cutting edge. We do see some flank wear in the center of the cutter and some wear land growth at the notch. Flank wear starts to become significant at the #14 and #18 pictures at which point **Fig 3-8** starts to show an increase in K_{te}. Other carbide wear tests showed similar results with K_{te} staying relatively low until the end of tool life when the dominant wear mode was chipping. **Fig 3-10** and **Fig 3-11** show the results of Exps (D) and (E). All the carbide tests showed small percent power increases similar to those shown in **Fig 3-7b**. This opposite trend from the coefficients from HSS to carbide may be an effect of the type of wear occurring rather than the cutter materials; it is expected that when

carbide tools experience flank wear, as they often do with harder materials, the cutting coefficient behavior may be close to what we experienced with the HSS cutters.

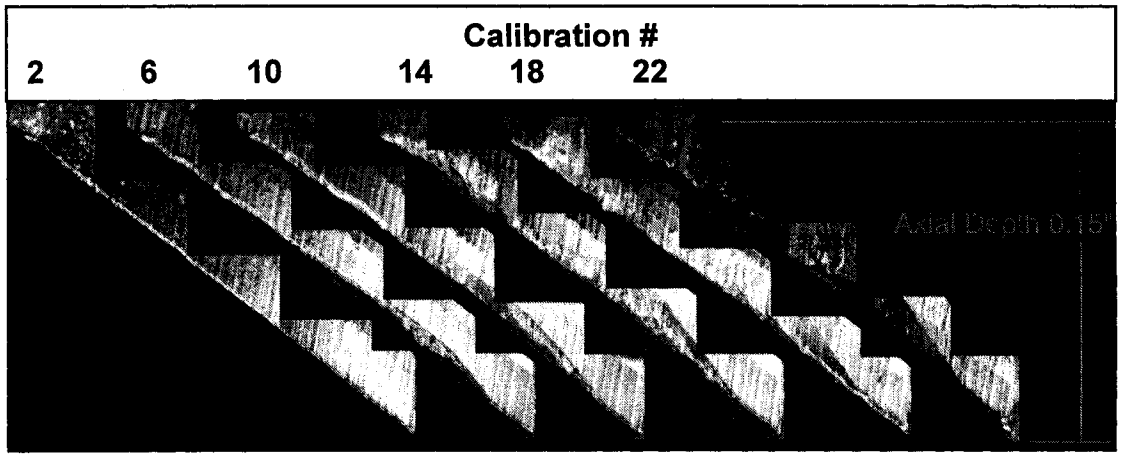

Figure 3-9 Images of cutting edge, Exp (G)

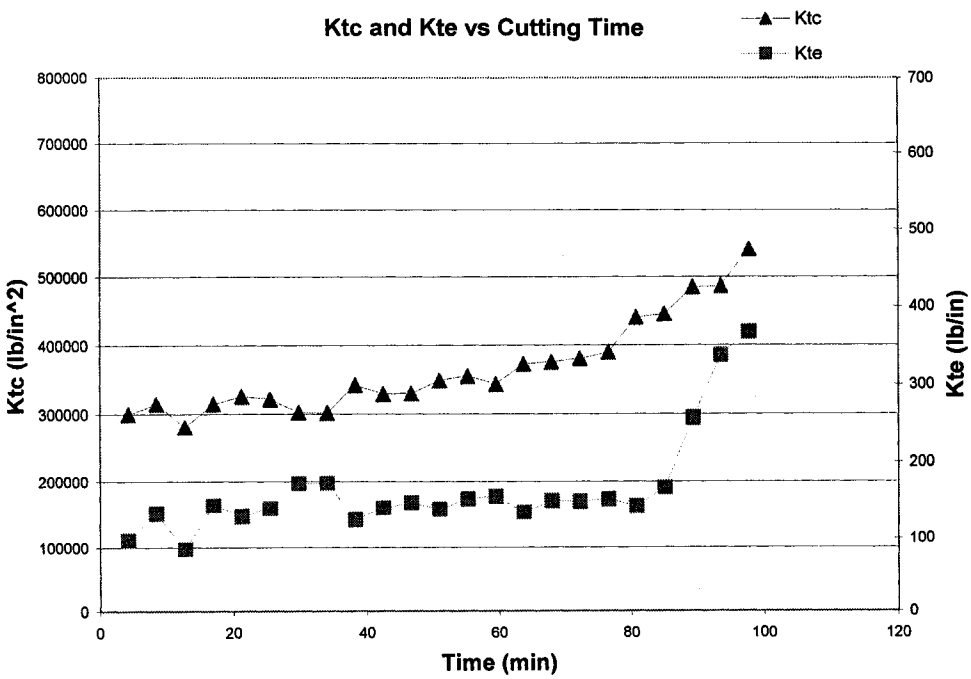

Figure 3-10 Coefficients for a carbide cutter, 0.5" Carbide end mill in 1018 steel, Exp (D)

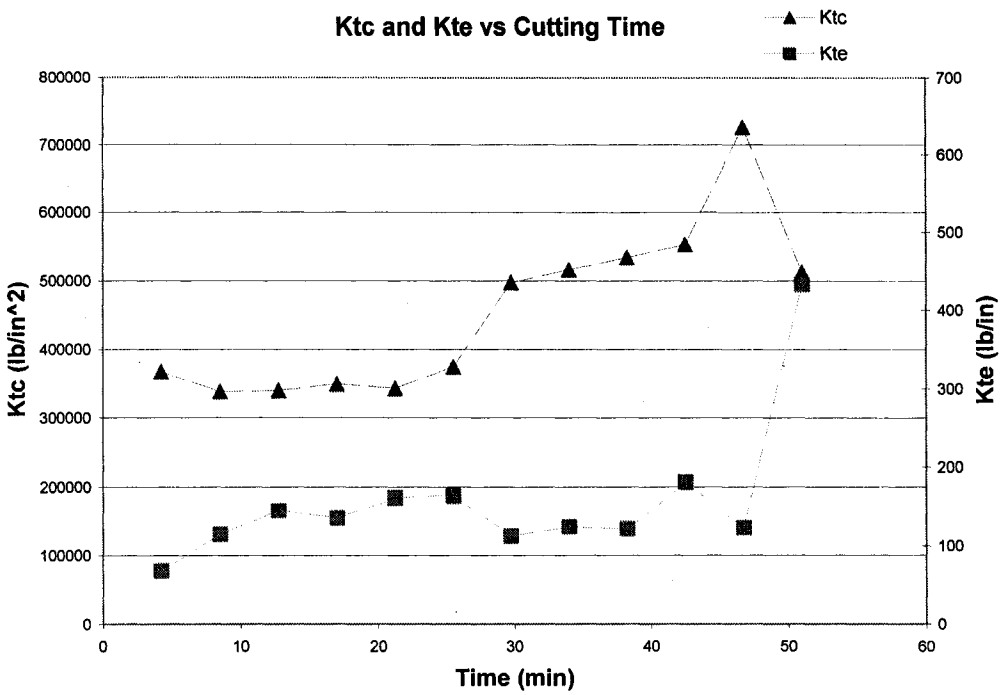

Figure 3-11 Coefficients for a carbide cutter, 0.5" Carbide end mill in 1018 steel, Exp (E)

3.3. Statistical Variation of Calibration with Respect to Wear

The coefficient of determination (R^2) obtained when performing a regression on the data points and defined by **Eqn 3-1** [14], may also be useful in signaling when a tool is approaching the end of its useful life. **Fig 3-12** shows the last three regressions, which are used to calculate the coefficients for Exp (G).

$$R^2 = 1 - \frac{\text{error sum of squares}}{\text{total sum of squares}} \qquad (3\text{-}1)$$

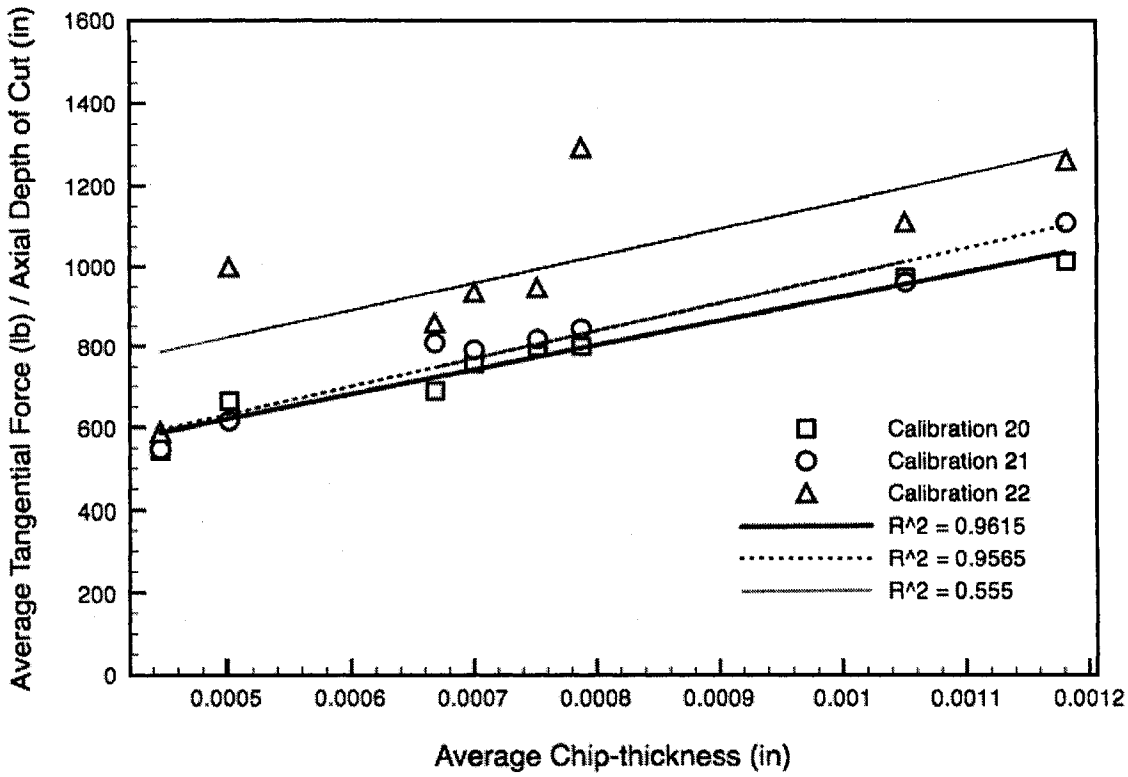

Figure 3-12 Accuracy of calibration at the end of tool life, 0.375" Carbide end mill in 1018 steel, Exp (G)

The data was calibrated with a slot cut and three down mills each at high and low chip-thicknesses. This minimized the regression effects, like an artificially lowered K_{te}, because the data points were taken more randomly and not from low to high chip thickness (see Section 2-4). The data points were close enough together to get a good linear fit of the data until the last calibration, where the coefficient of determination (R^2) value dropped from 0.96, or in other words accounting for 96% of the models observed variability, to about 0.56 and the standard deviation jumped from about 3.6 to 12.8. This shows that there are significant changes to the cutting edge between calibration points resulting in a bad linear regression. This inability for the model to be calibrated within a

reasonable statistical measure may also be a good indicator for identifying the rapid degradation of the cutting edge, which leads to tool failure.

3.4. Sacrificial Block Calibration

Another method of model calibration was also tested. In these tests (I, J, K, L), the model was calibrated in a softer material (6061 Aluminum) periodically while wearing the tool under constant cutting conditions in 1018 steel. The hypothesis was that the tool wear during the calibrations would be insignificant compared to the wear from the steel cuts; this way a TCM user could estimate wear if their cutting process was not good for online calibrations. Each tool was worn until the flank wear and chipping progressed across the flank of the tool, which is about 0.015" for a 5/16" tool. **Fig 3-13** shows the coefficients vs. distance in cut, which is the total distance the tip of the tool travels while engaged with the work-piece. This is calculated based on the tools circumference and the exit and entrance angle of tooth. Distance in cut allows you to compare a slot cut to a peripheral cut with respect to tool life.

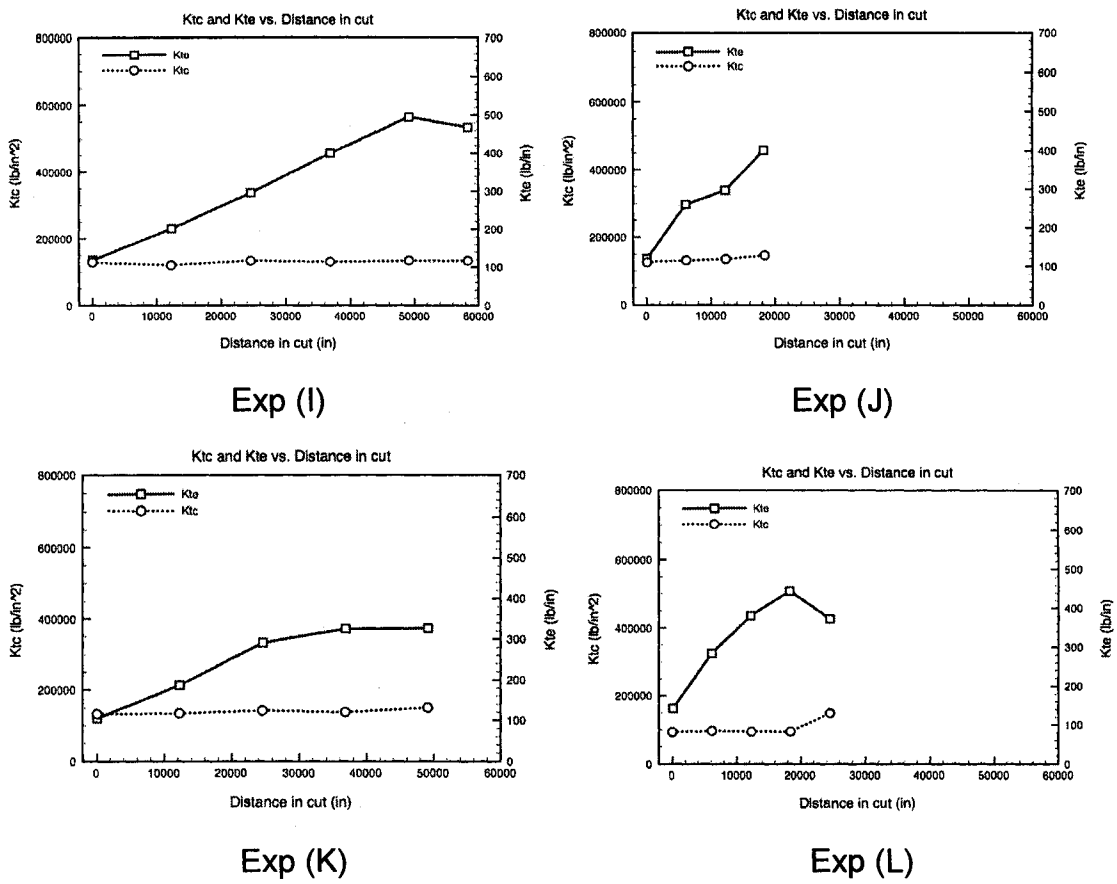

Figure 3-13 Coefficients from sacrificial block calibrations

From **Fig 3-13** we can see that Exps (J), (K), and (L) did not reach the same power level as Exp (I). Lower values of K_{te} and K_{tc} are directly related to lower levels of power. Looking at the photos of the tool wear for each case shown in Table 2-1, we see that Exp (I) failed with flank wear as the dominant mode while the other three tests show both flank wear and chipping. Close inspection of the cutting edge shows that the level of K_{te} was qualitatively related to the flank wear and the tools with more chipping had lower values of K_{te} and ultimately smaller increases in power. This can also be seen in the images of the cutting edge for Exp (K) in **Fig 3-14.** In this figure we see the first image taken when the flank

face is still new. The second image shows the tool with a small amount of flank wear and a small amount of chipping at the notch near the top of the cut. In the third image we see some of the cutting edge has broken away starting at the notch and including the tip. The flank wear has reached the limit of the allotted manufactured flank face, but the edge has been chipped back about half way to the limit of the manufactured flank face leaving less area for rubbing and losing the ability to reach a K_{te} of 400 lb/in that the other tests reached. Even though this flank wear area is less than the other tests VB has still tripled near the tip since the second calibration and we can see this increase in VB reflected by a 56% increase in K_{te}. In picture 4 we can see a large chip has broken off near the top of the cut, removing some of area available for rubbing, resulting in a smaller increase of K_{te}. The length of VB does increase significantly at the tip, which is why we still see some increase in K_{te}.

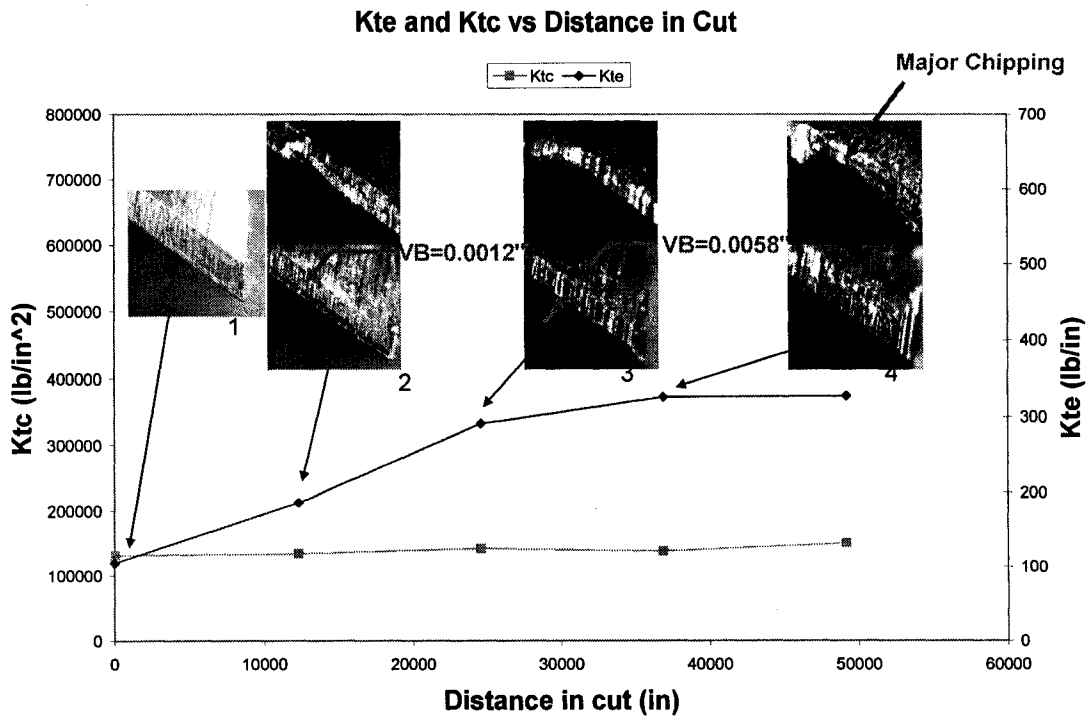

Figure 3-14 Pictures with coefficients, chipping and flank wear, 5/16" HSS end mill calibrated in 6061 Aluminum, Exp (K)

Each of the other three tests show the same relation of VB to K_{te}. Exp (I) experienced predominantly flank wear without chipping. As can be seen in **Fig 3-15**, when the flank wear reached the limit of the manufactured flank face the edge was still free of chipping, resulting in a much larger length and total area of VB, and in turn a larger value of K_{te}.

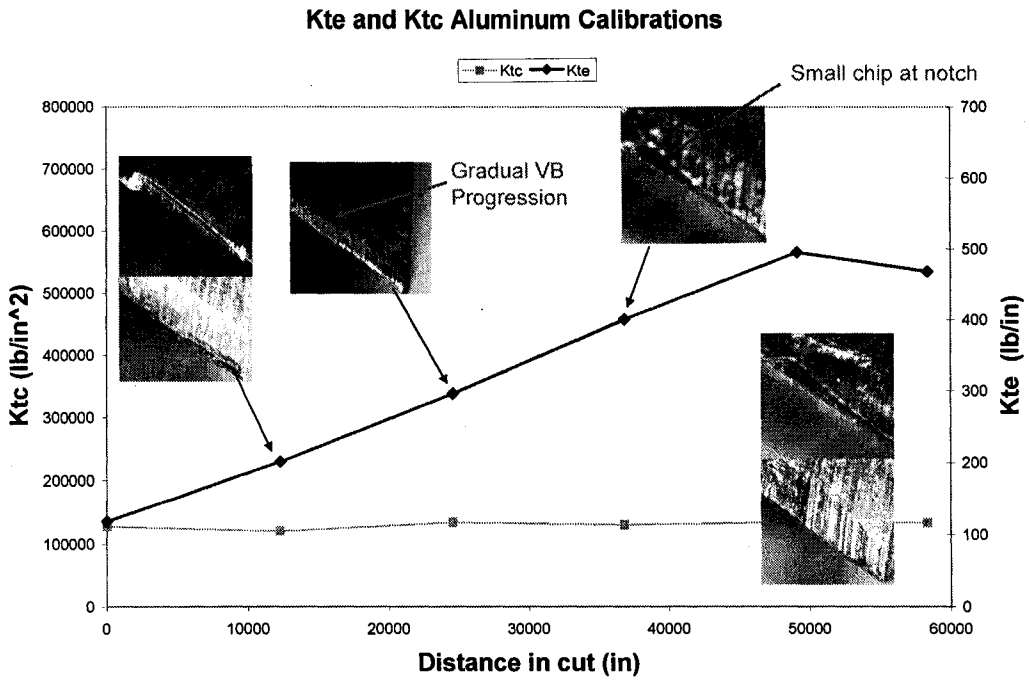

Figure 3-15 Pictures with coefficients, predominantly flank wear, 5/16" HSS calibrated in 6061 Aluminum, Exp (I)

In **Figures 3-16** and **3-17** we can see pictures of the cutting edge for the remaining two tests where aluminum was used for calibration. For each experiment a K_{te} value of about 400 lb/in represented the point at which the flank wear had reached the limit of the manufactured flank of the tool, with the exception of Exp (K), which had a significant chip that reduced its potential rubbing surface. We did not see as much of an effect on K_{tc} due to chipping as we did for the steel cuts; this may be due to a smaller shearing energy for aluminum and/or the chipping being masked by a built up edge (aluminum sticking to the chipped area – perhaps even filling it in). Since the chipping occurred in steel this may not be a problem for a tool that is solely worn in

aluminum, but does raise a point against using aluminum as the sacrificial block material for tools experiencing chipping.

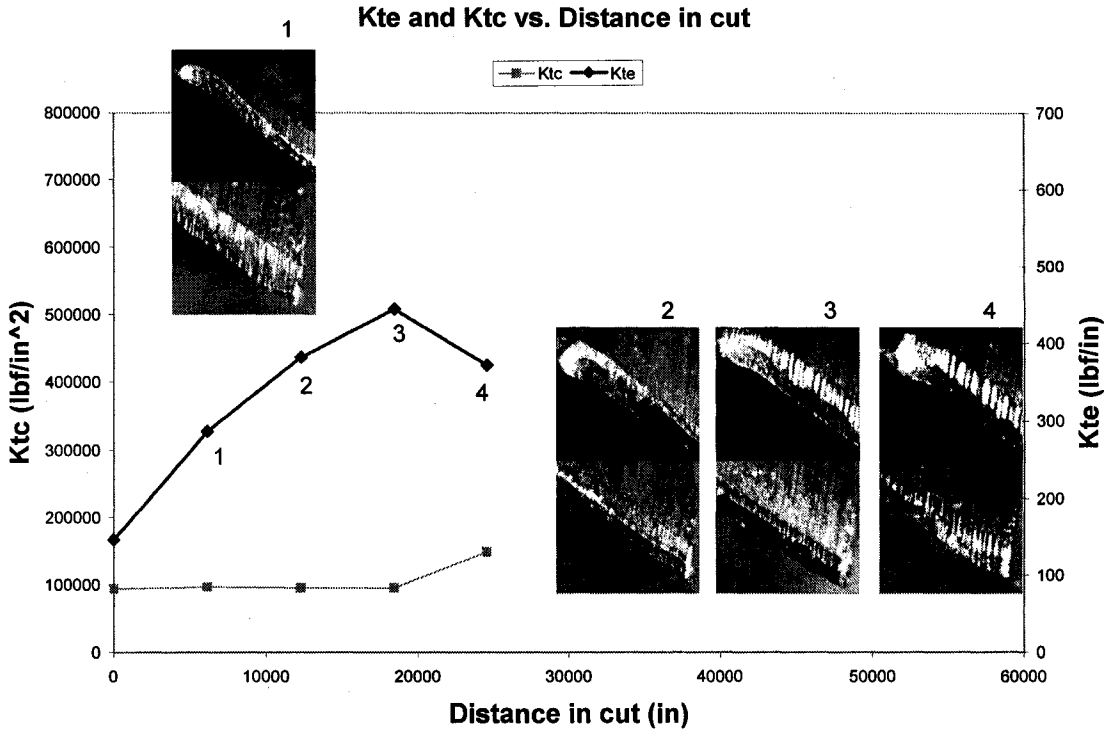

Figure 3-16 Pictures with coefficients, flank wear w/ some chipping, 5/16" HSS calibrated in 6061 Aluminum, Exp (L)

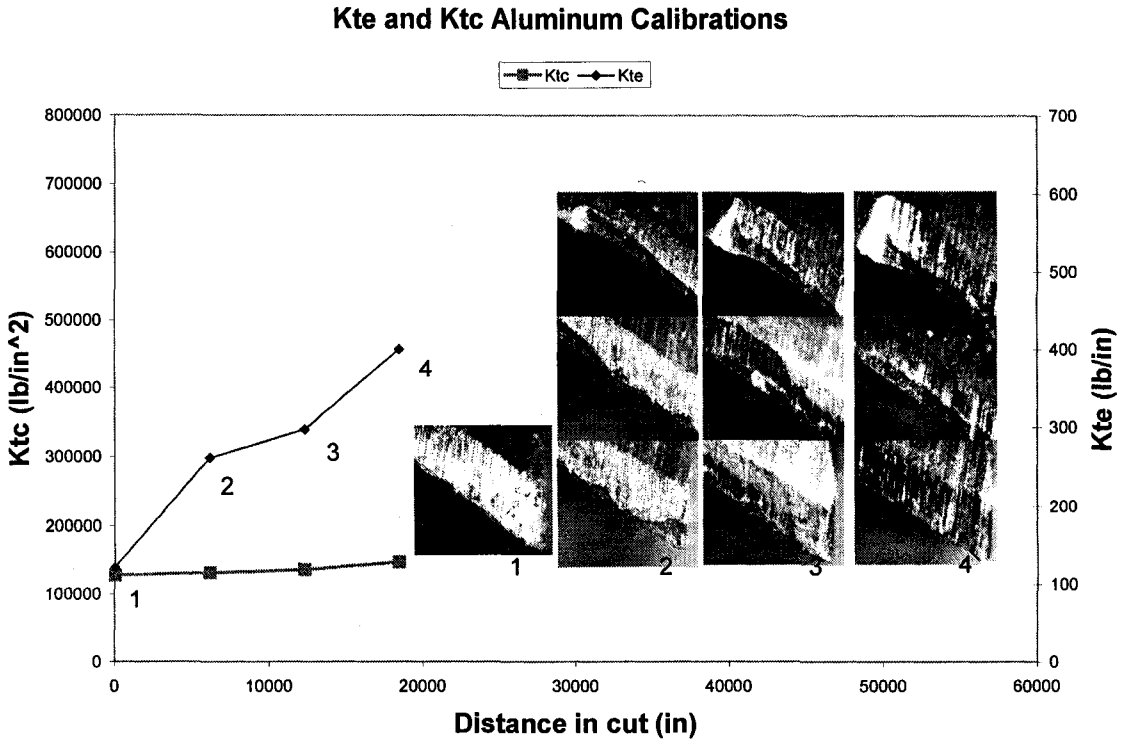

Figure 3-17 Pictures with coefficients, chipping and flank wear, 5/16" HSS calibrated in 6061 Aluminum, Exp (J)

3.5. Radial Coefficients

Tangential forces can be estimated using **Eqn 2-4**, and the behavior of the coefficients of that equation as a function of tool wear is the basis for much of this investigation. A similar equation can be used to relate cutting conditions to radial forces as shown in **Eqn 3-2**.

$$F_{r\,avg} = K_{rc} h_{avg} a + K_{re} a \qquad (3\text{-}2)$$

The radial coefficients (K_{rc} and K_{re}) can be calibrated by measuring the average forces in the X and Y direction using a Kistler dynamometer as described by Altintas [1 pg 41-46]. The method is described in more detail in Appendix C.

The wear sensitivity of the radial coefficients compared to the tangential can be seen in **Fig 3-18**, a pure flank wear test in 1018 steel (Exp (H)). The results are similar to that of the tangential coefficients except at the end of tool life. K_{rc} did not show the same increase at the end of tool life as K_{tc}. Instead the model calibration yielded negative values for K_{rc}. If you follow the curve of the K_{te} and K_{re} coefficients you can see the sensitivity is almost the same with the curves separating at the end, where there is an increase in K_{tc} signaling a worn tool, K_{rc} continues to decrease, not providing any usable information about tool wear.

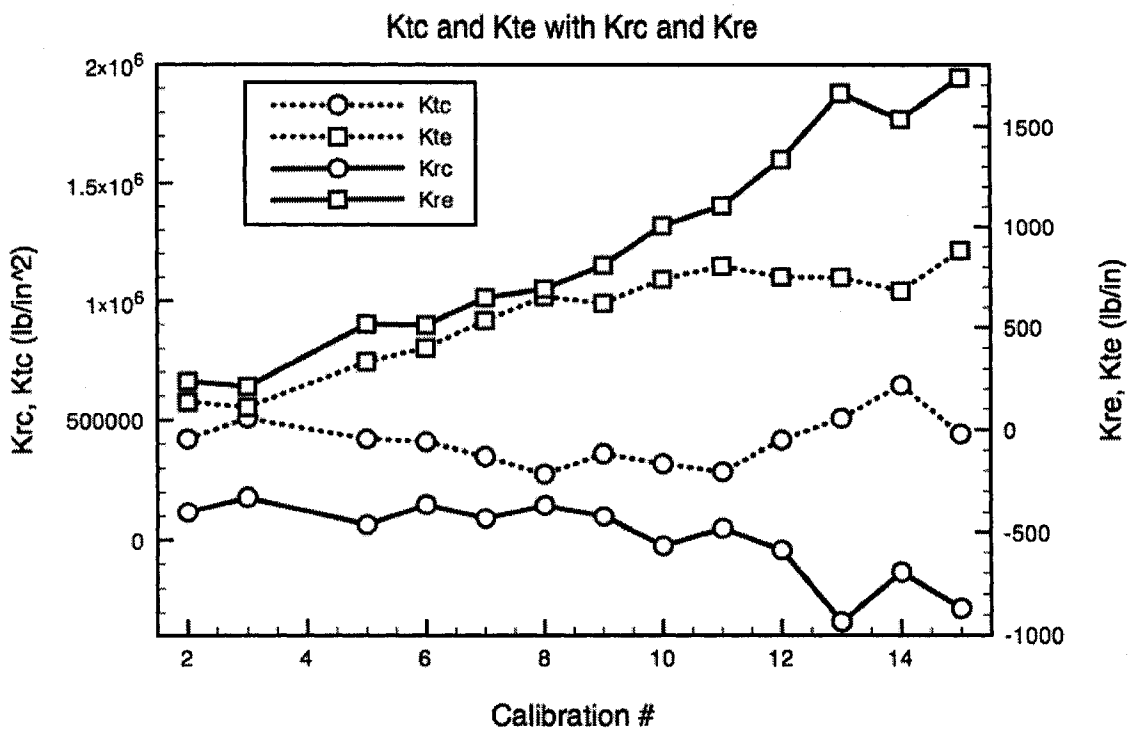

Figure 3-18 Radial and tangential coefficients for steel calibrations, Pure flank wear, Exp (H)

In order to explore the behavior of the radial coefficients with the type of tool wear. Specifically, when using aluminum for calibration (Exp I, J, K, L) K_{tc} did not appear to be as good an indicator of tool chipping as when calibrating in 1018 steel. The lack of K_{tc} sensitivity with respect to chipping from the aluminum calibrations can be explored by looking at the radial force coefficients. **Fig 3-19** shows the same experiments as **Fig 3-13** but with radial coefficients plotted along with the tangential coefficients. **Fig 3-18** shows that the radial coefficients are more sensitive than the tangential coefficients, but K_{rc} also doesn't change much on the tests where chipping occurred. This confirms that aluminum may not be the best sacrificial block material and even the radial coefficient doesn't

identify the chipping effect. These cases did show increased sensitivity with tool wear for the radial coefficients vs. the tangential.

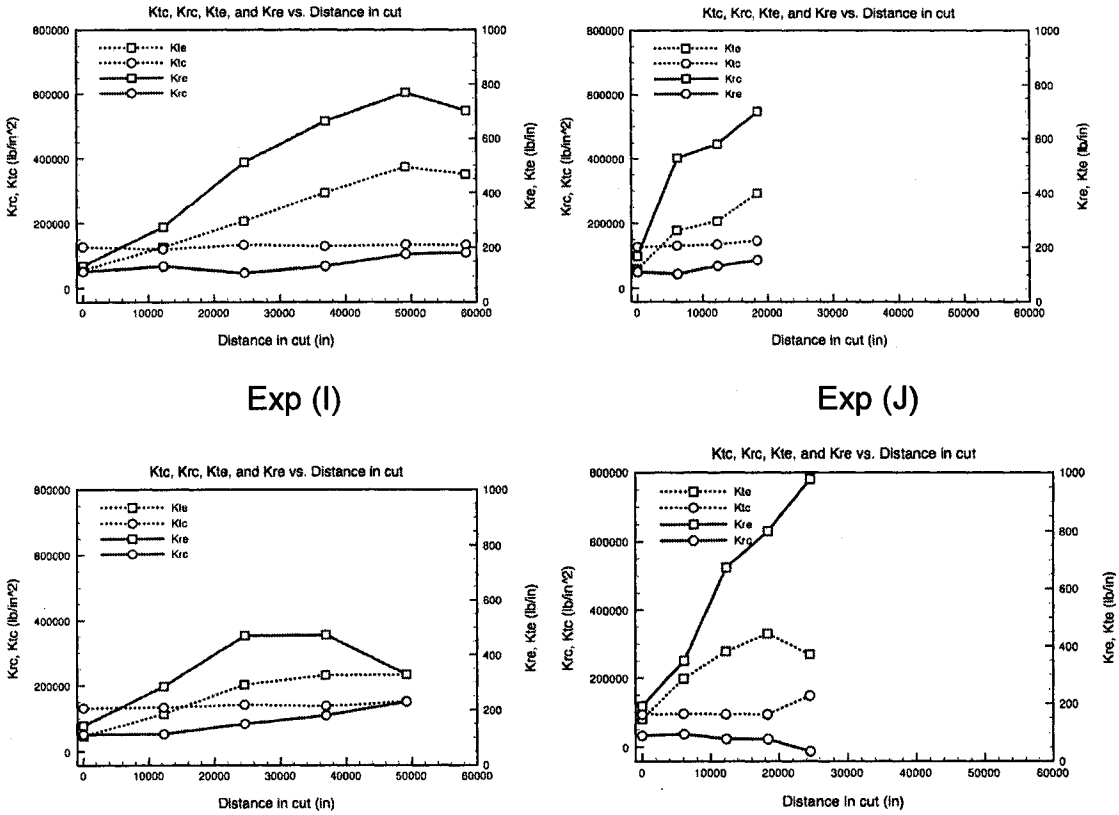

Figure 3-19 Radial and Tangential coefficients, Aluminum sacrificial block calibrations, Radial coefficients = solid lines, Tangential coefficients = dotted lines

CHAPTER 4.

ESTIMATING WEAR

A primary goal of this research is to find a method for indirectly measuring the percentage of tool life that has been expended. This is vital for unattended machining where a "smart cnc" will know when to change the cutting tool. One significant finding that has been repeatedly shown throughout this investigation is that when flank wear is not the dominant mode the percent power increases are lower and a power based TCM system may experience difficulty. A second important finding is that the percent power increase at fully "worn out" condition is dependent on the average chip thickness and therefore a conventional TCM system must set different thresholds for different cutting conditions. We have also have seen that the model coefficients behave differently based on the mix of flank and non-flank wear on the tool edge.

With good calibration methods a user could learn how the coefficients react to specific machining conditions, and then use this information to improve their cutting process in order to achieve a wear mode that is as close to pure flank wear as possible. This will manifest itself in an increase in K_{te} with K_{tc} remaining unchanged until catastrophic failure at the end of tool life. The TCM system should still be effective even if unexpected chips are taken out of the cutting edge

and power levels change. In order to accomplish this, the TCM system should reduce the power threshold based on the amount of chipping.

4.1. Setting Limits on Kte and Ktc Cutting Constants

One method of quantifying a worn tool could be to set limits on K_{te} and K_{tc}. To do this we would have to correlate a certain level of wear with each set of coefficients. Since we are trying to account for both chipping and flank wear there is no easy way of accomplishing this task. But one thing that can be identified with a good level of certainty is a completely worn tool, whether it be flank wear that has completely passed the allotted space or a combination of the edge breaking down due to chipping and a sharp increase in power. This point was identified for all of the half inch cutters and was considered to be 110% worn at this point in time (**Fig 4-1**). Note that experiments (A) and (C) are for HSS cutters and (D) and (E) are for carbide. Characteristically, the HSS cutter experiences larger increases in K_{te} than the carbide cutters, while the carbide cutters experience larger increases in K_{tc}.

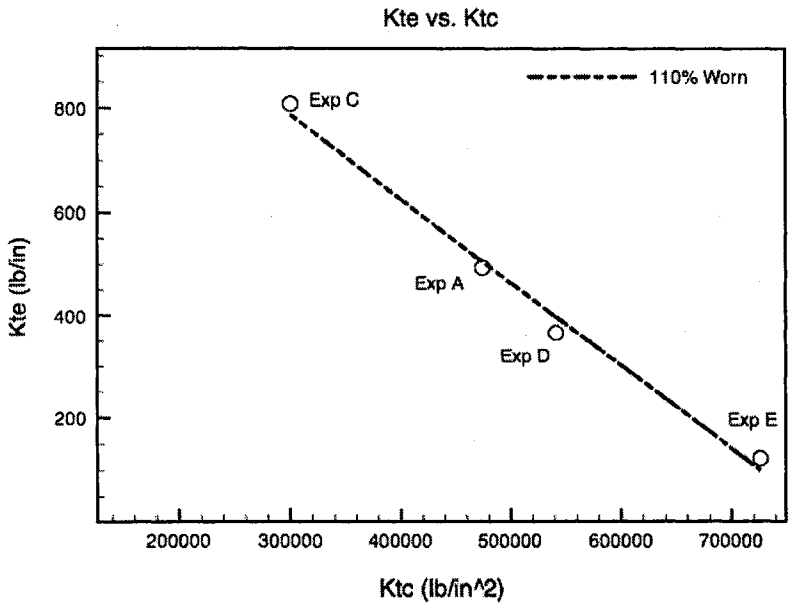

Figure 4-1 110% worn definition of Kte and Ktc combination

Now we can use this line and a 10% offset of 100% as our limit and see the progression of the coefficients toward this new K_{te} and K_{tc} limit as the tool wears. **Fig 4-2** shows the progression of Ktc and Kte as the tool goes from sharp to unusable for the same four tests.

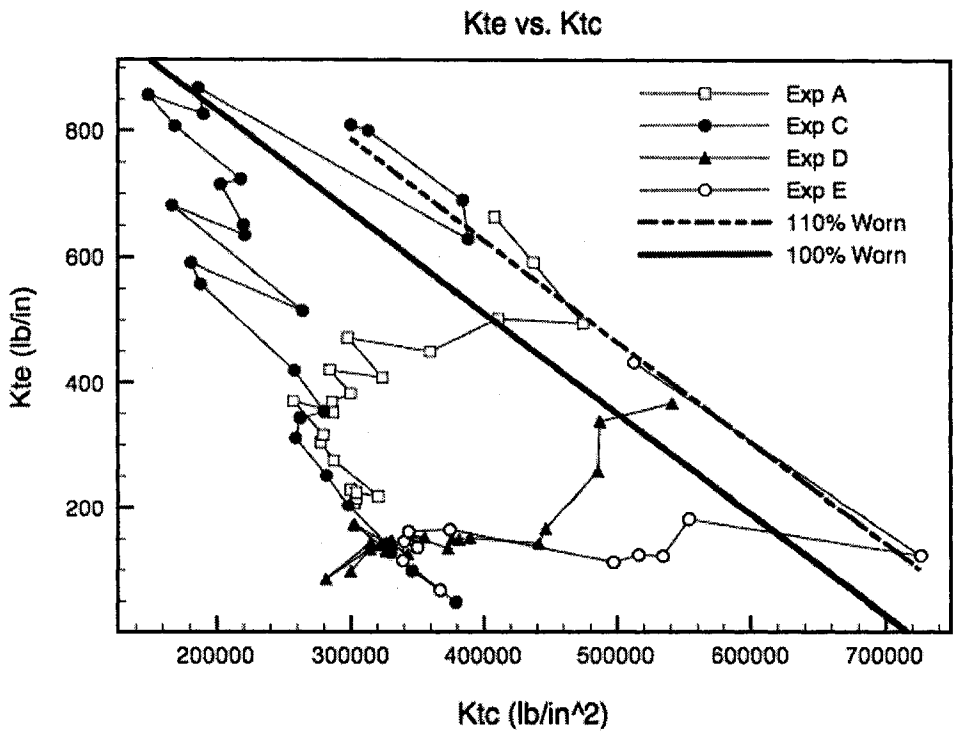

Figure 4-2 Progression towards the threshold of Kte and Ktc

As shown in **Fig 4-2** all the unworn tools start with roughly similar coefficient values. The paths traced by the coefficients begin to separate as wear occurs at different levels of chipping and flank wear. The assumed 110% wear line seems to be quite consistent with a completely worn tool with none of the tests exceeding this line by more than 4%. **Fig 4-2** was created to help understand the next section which involves the same basic principle of creating a linear regression that will ultimately set limits on K_{te} and K_{tc} such that flank wear and chipping can be estimated together in order to get an measure of the tool life. Section 4-2 will present this information with an improved graphical representation.

4.2. Multiple Regression

A classic method of estimating tool life is to use a multiple linear regression based on cutting conditions such as cutting speed and any other variable deemed important [14]. Multiple regressions have also been used in TCM to model the force measured by a dynamometer [7]. If we assume that the value of the coefficients are predominately dependent on the cutter geometry and work-piece material and independent of spindle speed and cutter material for the tests in this report, the coefficients could be used in a multiple linear regression to balance the fluctuations in Ktc and Kte that are due to changes in cutter wear mode (chipping vs. flank wear). This would be accomplished by fitting a plane to data points of Ktc and Kte vs. percent of cutting edge used. Data points from two extreme cases could be used to calibrate this model. The extreme cases would be a predominately flank wear case and a predominantly chipping case for a given cutter geometry and work-piece material. This way tool life could be estimated for a cutter experiencing any combination of chipping and flank wear based on their current Kte and Ktc values. Eqn 4-1 represents tool life based on a planar regression of the coefficients, where L=percent of cutting edge used and the $\beta_{0,1,2}$ are calibration constants.

$$L = \beta_0 + \beta_1 \cdot Ktc + \beta_2 \cdot Kte \quad \textbf{(4-1)}$$

A measure of the percent of usable tool edge left is needed to calibrate this multiple regression. Since it is very difficult to get an exact measure of wear

when both chipping and flank wear are present we will assume that the cutting power increase is directly proportional to the wear land as illustrated in Fig 1-5. It would be better if there was a way to quantify the amount of wear using a microscope, but for lack of a better method we will use the trend of the power data to represent the trend of the percent of tool life used.

This was accomplished by identifying the point at which the tool has completely worn its flank face away and scaling the power data such that this point = 110% of the cutting edge used. This will give us our estimation of percent tool edge used with each set of coefficients for a multiple regression. Exps (C) and (D) were used to calibrate for the β coefficients and yielded β_0=-95.33, β_1=2.58-4, β_2=0.1607. The resulting equation can be plotted as a plane as shown in **Fig 4-3**.

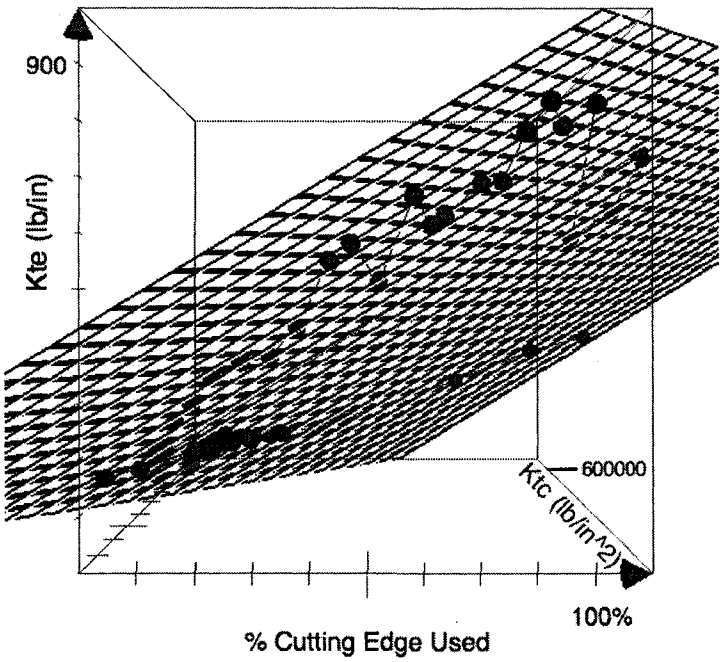

Figure 4-3 Multiple linear regression with Kte and Ktc values of Exps (C) and (D)

The effect that we get from this surface is simply that with a lack of increase in Kte the increase of Ktc becomes more significant. Ultimately the idea is that a tool that experiences flank wear should have higher power limits than a tool experiencing chipping. The regression does this by giving a different weight to Ktc and Kte when determining the percent tool edge used.

The resulting equation was then used to estimate tool life for the remaining half-inch end mills experiments in 1018 steel. We can see the resulting trend for each experiment in **Fig 4-4** and its resemblance to the plot of VB vs. time (**Fig 1-3**). The error between each, the wear estimation, and wear predictions are in

Fig 4-5 and can be seen in tabular form in the Appendix A. The multiple regression was calibrated with Exp (C) and (D) which is why the error is so low in **Fig 4-5**, but when using the resulting equation to estimate wear for Exp (A) and (E) the error is still low and predicts well. Exp (E) was the worst case where the error reached 20.73%, with the exception of the last point when the tool is completely worn and reaches almost 100% error, which is the same effect we saw in **Fig 4-2** with the last point traveling up the 110% worn line. Further refinement of this model and constantly updating the regression with more data will hopefully show that this method will work for a given tool size and shape in a given material with any combination of chipping and flank wear. Further Investigations may use statistics for further refinement of this multiple regression by testing different interactions between the variables.

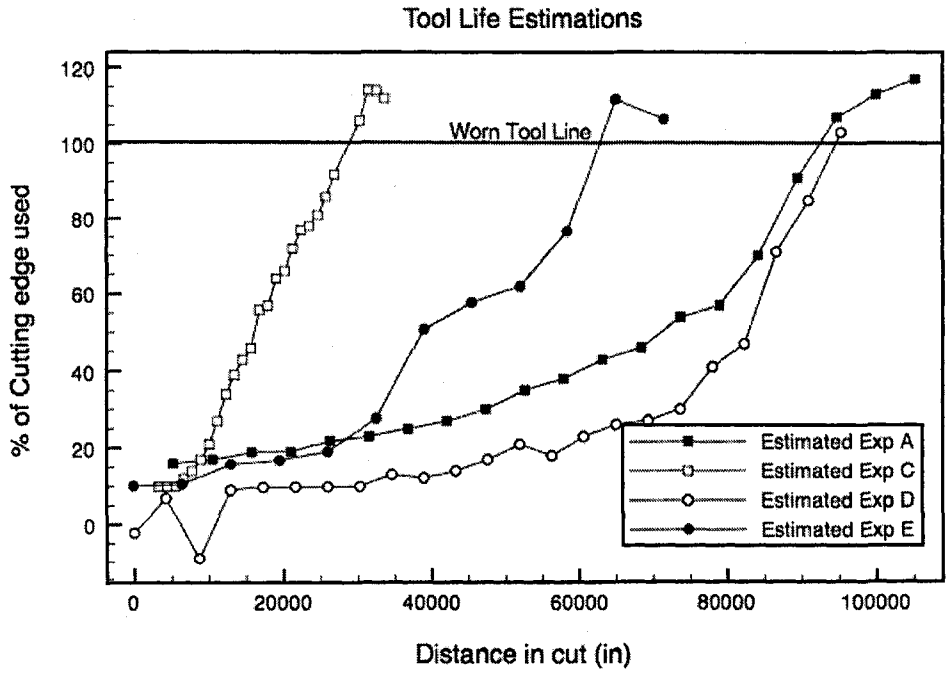

Figure 4-4 Predicted percent of edge used

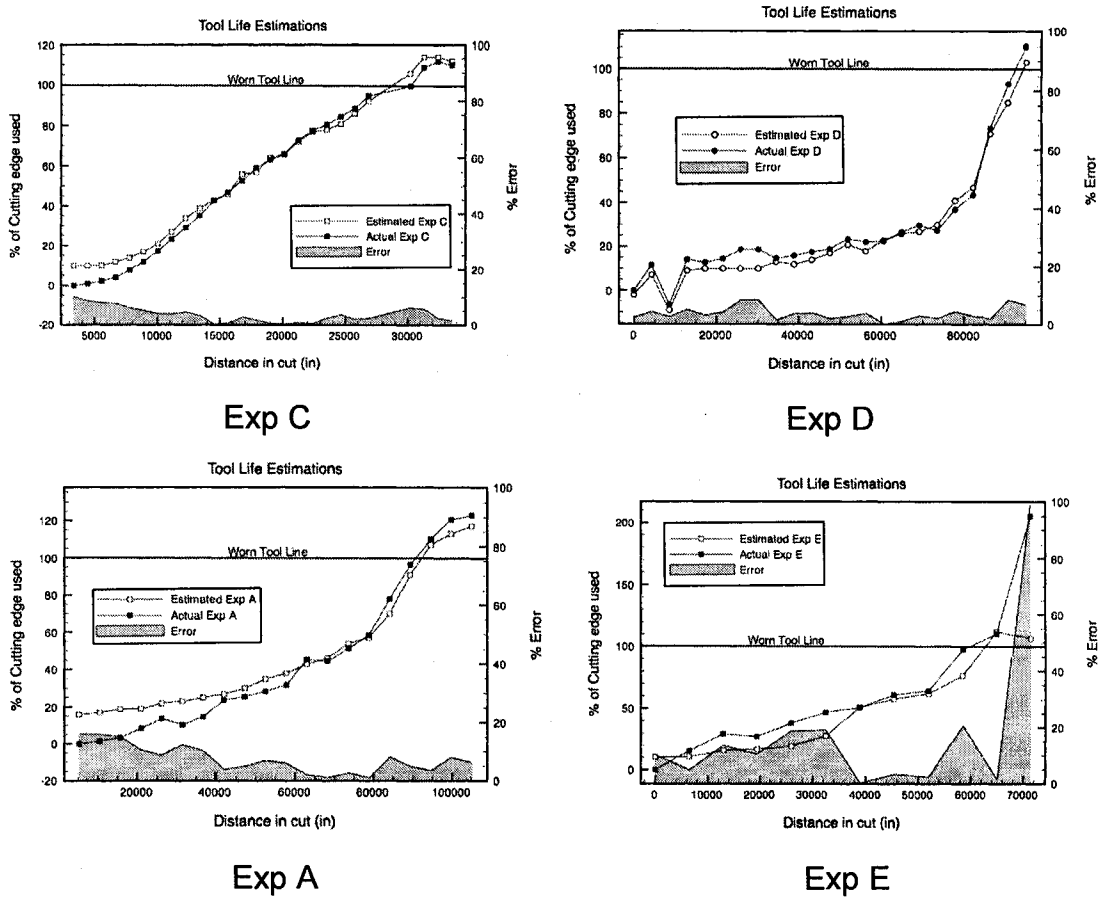

Figure 4-5 Estimation plots with error

This is ultimately the same method of setting power limits that has proved to be reliable in commercial TCM systems, with the difference being that once calibrated it has the potential to work with a wide variety of cutting conditions. It has been shown that the values of Ktc and Kte work for a given tool and material combination and can be used to predict cutting power for a wide variety of cuts [11]. Each of the four tools shown in **Fig 4-4** were calibrated at different spindle speeds and with different calibration routines yet the method of estimating wear still holds. This method also has the ability to react to an unexpected chipping problem that results in smaller power increases. Once calibrated the user does

not have to train with the first part, the wear state can be tracked from the beginning. Not having to compare identical cuts would allow more flexibility when trying to choose the time between calibration points. This would make the system more reliable in the cases where the distance between similar cutting conditions does not occur as frequently as needed for traditional power threshold systems.

The best way to calibrate Eqn 4-1 would be to gather K_{tc} and K_{te} data over the life of a tool for what is considered the extreme cases of chipping and flank wear for a given application. The method shown here used two extreme cases of flank wear and chipping to calibrate. New data that is known to be accurate could be added to recalibrate and increase the accuracy of the calibration. If it's found that the tool life relates in a more complex regression, an experiment between the two extreme cases may be needed to estimate any curvature of the regression plane. This regression will be limited by the cutter geometry and work piece material and may or may not hold if things like cutter coatings are introduced. A different regression would have to be performed for each cutter diameter due to the difference in flank face area available for flank wear, and because the cutting coefficients have not been shown to be interchangeable with different cutter diameters.

Another challenge for this method is to come up with online calibration methods in order to track the coefficients. One simple method would be to periodically

select an appropriate G move in the G-code to split into four or five quick moves at different feed rates to get a variety of chip thicknesses. The feed rates could be at 85%, 95%, 100%, 105%, and 110% of the original feed rate so that the part quality and cutting time are not affected by any significant amount. If you wanted to be conservative the feed rates could all be below the original at the expense of cutting time. Other more complicated methods of online calibration have been attempted that involve splitting all the G-moves into smaller moves and grouping certain ones together for calibration [11].

4.3. Constant K_{tc} Wear Estimation

The method in section 4.2 requires the part program to accommodate calibrations. It also has the problem in that there is no information gathered between calibrations. Another method of estimating the tool wear would be to calculate the K_{te} with an assumed constant K_{tc}. From Eqn 2-1 in section 2.3, if K_{tc} is assumed constant, K_{te} can be calculated from each power data point as often as we can collect data, without a calibration. The advantage of this method over a power threshold method would be that the K_{te} value could be calculated from any cut geometry and/or speeds and then compared to the original, which may be at different cutting conditions.

This method could also be used with the 100% worn line (Eqn 4-2), calculated by offsetting the 110% line from section 4.1 **Fig 4-2**.

$$Kte\_Limit = -0.0016 \cdot Ktc + 1158.455 \qquad (4\text{-}2)$$

If a K_{tc} value could be calibrated before cutting or at the beginning of the part, it could be used to calculate a worn tool K_{te} based on the Eqn 4-2. Then Kte could be calculated continuously without a calibration routine, and monitored in relation to the worn K_{te} value. If an opportunity presented itself in the G-Code or scheduled down time which allowed for a standard calibration, a new K_{tc} could be found and the worn tool K_{te} limit could be adjusted. **Fig 4-6** illustrates this technique on Exp (C) (see **Fig 3.1** for K_{tc}, K_{te} plots). K_{te} is calculated continuously with all the data assuming K_{tc} hasn't changed since the first calibration. The original set of data shows the calculated K_{te}'s and the limit assuming that the only opportunity to calculate K_{tc} was at the beginning of the test. The adjusted set of points are K_{te}'s from the same power data that shows new K_{te}'s and the adjusted limit based on the new K_{tc}, assuming there was an opportunity to calibrate a new K_{tc} halfway through the test. **Figure 4-6** shows that the first limit would have predicted the end of tool life sooner had there been no chance for re calibration of K_{tc}. The second limit is a bit more accurate remembering from **Fig 4-5** the tool was worn at about 28000" in cut. This strategy worked well for the pure flank wear case and was able to predict the end of tool life fairly closely with only the one calibration of K_{tc}, but for a tool that experiences some unexpected chipping the second calibration would be important.

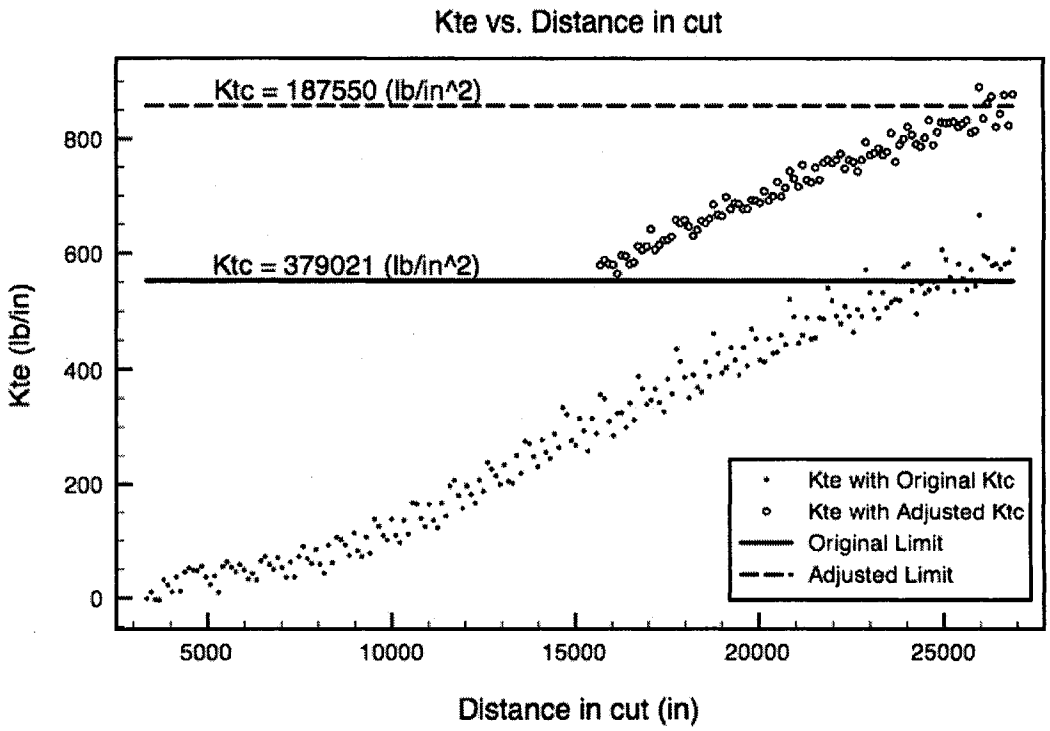

Figure 4-6 Constant Ktc tool wear estimation, Exp (C)

If the tool was known to wear on the other extreme with mostly chipping and no flank wear this strategy could be used in the exact opposite fashion in that K_{te} would be held constant and K_{tc} calculated continuously. This method should be implemented with any strategy including the multiple regression method in section 4.2 in order to calculate an estimated tool wear value in-between calibration points by assuming the K_{tc} to be that of the most recent calibration. This would help detect sudden problems that may happen between calibrations.

CHAPTER 5.

SURFACE FINISH

Surface finish is another important area that is affected by tool wear. Surface finish is highly dependent on the geometry of the cutter and its state of wear.

> *The surface finish produced in a machining operation usually deteriorates as the tool wears. This is particularly true of a tool worn by chipping and generally the case for a tool with flank-land wear - although there are circumstances in which a wear land may burnish (polish) the work piece and produce a good finish. [12]*

It might be possible to relate an increase in motor spindle power to surface finish quality through experimental analysis but using the cutting coefficients to distinguish between flank wear and chipping may have some additional value. Current surface finish models, like the one described in [28], are based on the geometry of the cutter and can predict surface finish for worn tools. Knowledge of the tool wear mode (flank or chipping) may allow for more accurate estimates of the surface finish. At the very least, knowing the amount of flank wear vs. chipping could estimate the probability of the burnishing effect mentioned in the above quote. In this chapter a preliminary study of the relationship between our TCM system and the surface finish is presented.

5.1. Preliminary Surface Finish Experiment

The surface finish was measured with a Mitutoyo SJ-400 surface roughness tester [41] (**Fig 5-1**). The G-code for wearing the tool periodically would step over and leave a strip of material behind which could be measured after the wear test was complete. **Figure 5-1** shows the block of 1018 steel that was used for the wear test with the periodic ledges left behind for calibration. The surface that was rubbing against and created by the flank face of the tool is the surface of interest rather than the surface created by the bottom of the cutter. **Figure 5-2** shows the percent of cutting edge used for Exp (G) plotted with the surface roughness measurement. Recall that Exp (G) is for a carbide cutter with a significant amount of chipping (See Fig 3-8). The percent of cutting edge used was calibrated with the multiple regression method described in Chapter 4 using the coefficients from Exps (G) and (H). The figure shows a good correlation between the changes in slope of each third order polynomial fit. The cutter is able to hold a pretty consistent surface finish until the end of the tool life. This initial test shows good correlation between the percent of cutting edge used (calculated from coefficients) and surface roughness, which shows the potential for using power measurements to estimate surface finish quality. The fact that the cutter is experiencing chipping (and little flank wear initially) may explain why we get a good correlation between surface finish and the estimation of cutting life.

Future investigations should include surface roughness in relation to flank wear in order to investigate the effects of burnishing described by [12]. It may be found that the level of K_{te} can be used with surface finish models to update the predicted surface finish based on an estimate of VB. One such model in [25] calculates the path of the tool tip as well as the flank heal (back side of flank wear land) passing through the work piece to estimate surface quality.

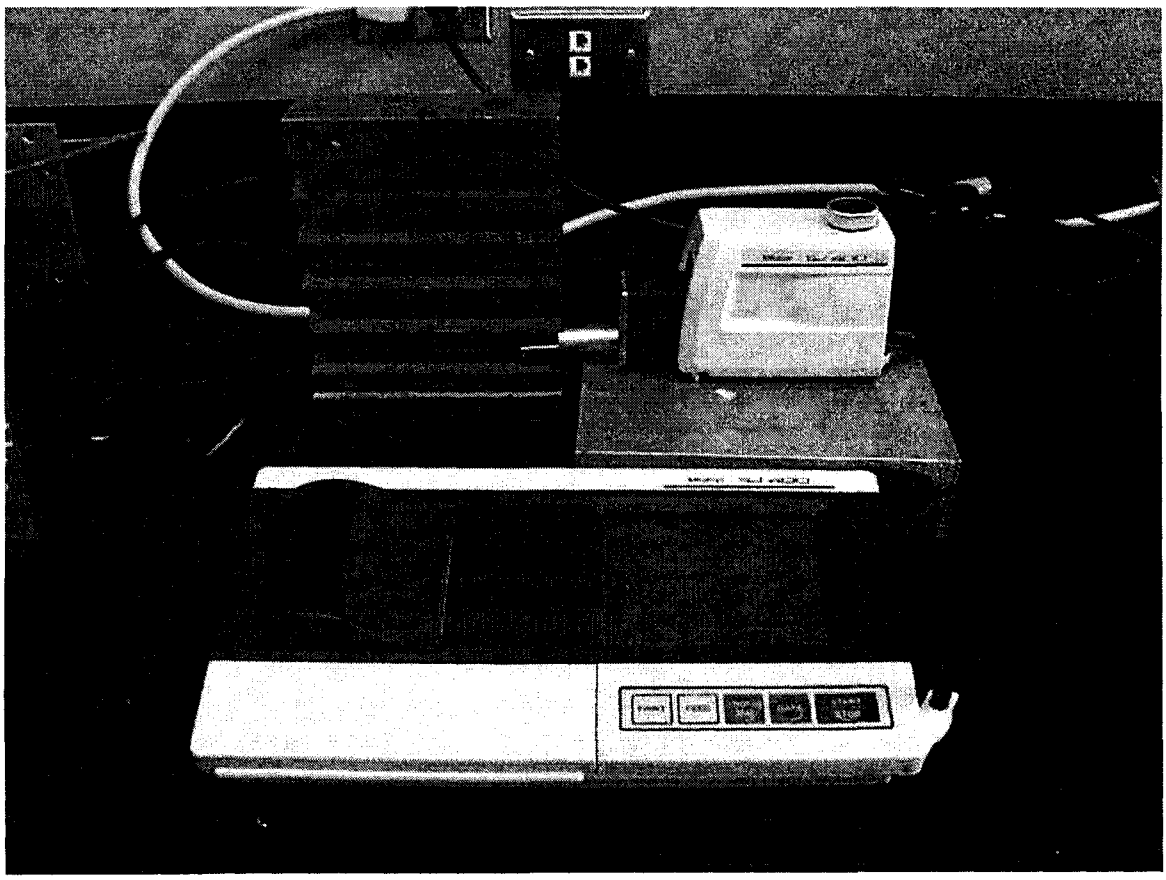

Figure 5-1 Mitutoyo Surface roughness tester with probe and work-piece setup

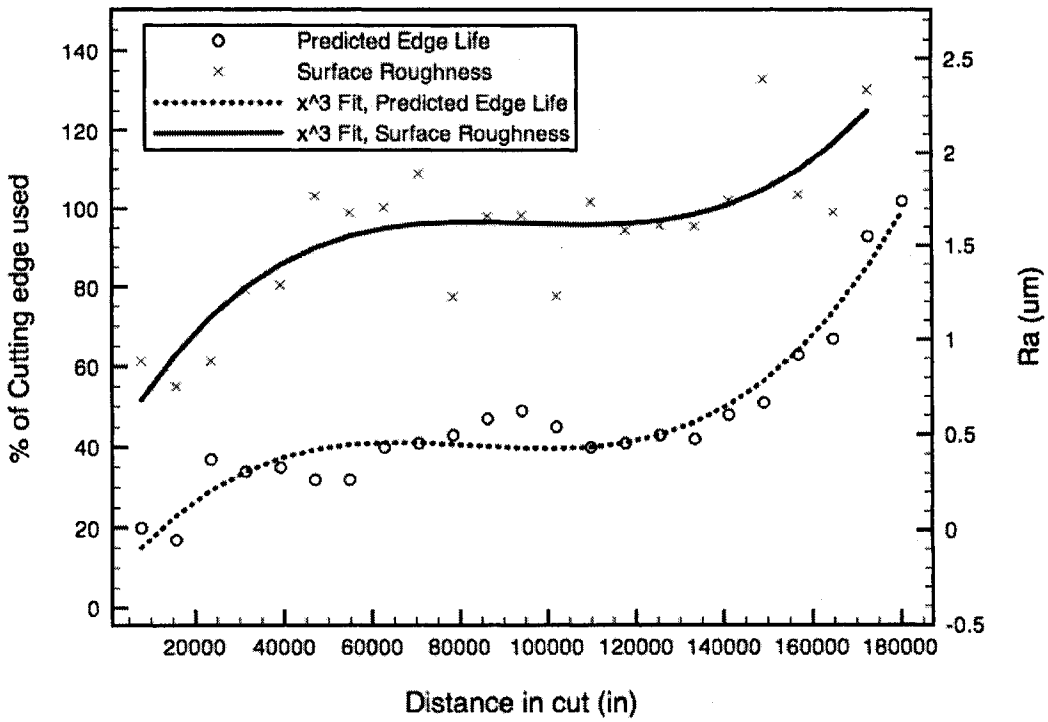

Figure 5-2 Predicted edge life Plotted with surface Roughness (Exp G)

CHAPTER 6.

CONTACT MICROPHONE

An AKG C411 L contact microphone is an instrument designed to pick up the vibrations of musical instruments. It has a range of 10Hz to 18,000Hz and a sensitivity of 1mv/msec-2. This chapter presents a preliminary exploration of the capabilities of this sensor for use in a TCM system. An added benefit to using this sensor is its cost. It can be purchased for around $150 as compared to the $550 dollars of the PCB accelerometer used in these tests.

It is well known that the trained ear of a skilled machinist can quickly determine when something is wrong with the machining process. An analysis of the frequency and magnitude of the signal from a contact microphone may lead to a similar capability. The output of the sensor can be analyzed for frequency and RMS content (see **Fig 2-4** for experimental set-up). Vibrations and acoustic emissions have been used for tooth breakage, chatter detection and tool wear estimation [23, 24, 31, 9].

6.1. Microphone RMS and Average Power

For Exp (G) (carbide tool – significant chipping – see **Fig 3-8**); we can look at the average spindle motor power, average microphone RMS, and the amplitude at

the tooth passing frequency of the microphone FFT for each calibration. That is to say, that we found the average of the 20 tests (5 speeds at four radial depths) taken at each calibration point. **Fig 6-1** shows that these values were proportional and follow the same trend.

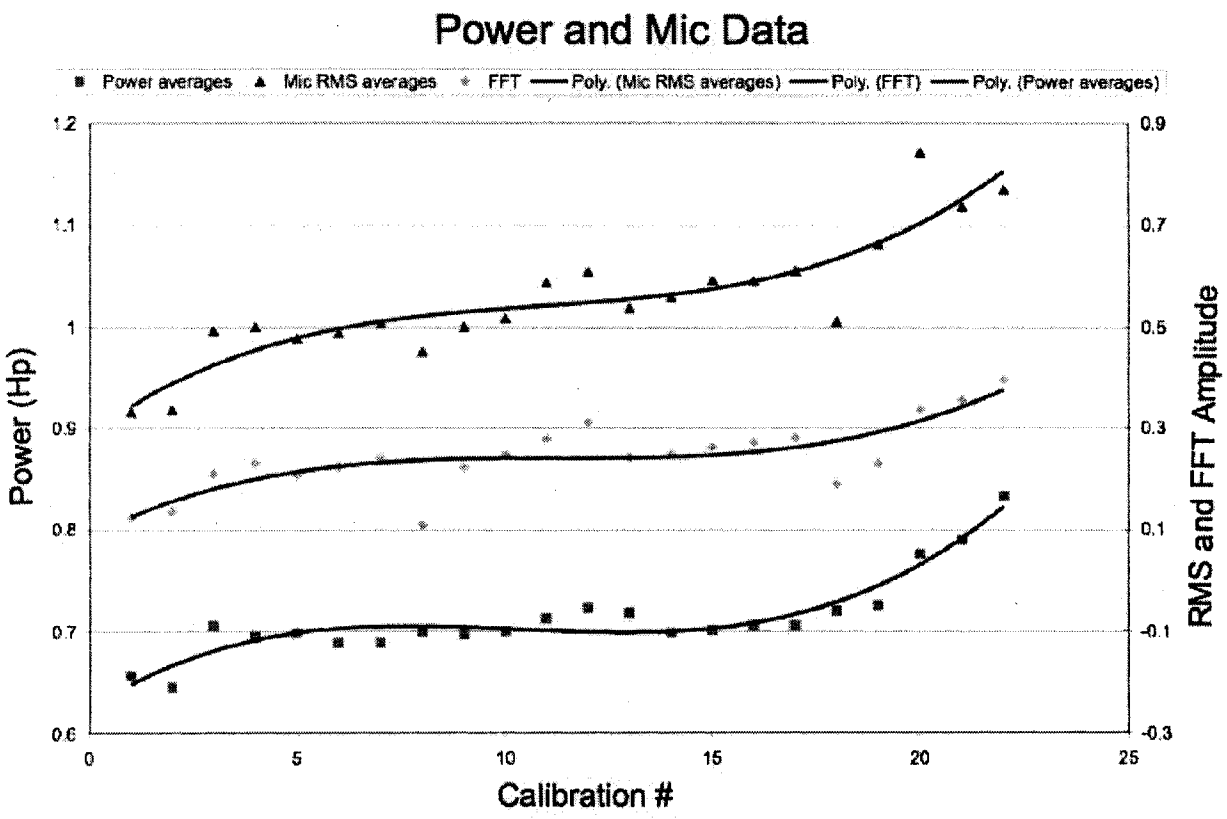

Figure 6-1 Average cutting power, microphone RMS and Max FFT frequency peak value from microphone FFT, Exp (G)

This shows that for this particular test the vibrations transmitting through the spindle are related to the cutting power. However, saying that the average values correlate doesn't guarantee that the values for a specific cutting condition also are correlated. **Fig 6-2** plots the average power, and RMS from the contact microphone and accelerometer mounted on the spindle, for each feed rate of calibration #12 for Exp (G). This figure

shows a strong but not perfect correlation between power and the rms value of the contact microphone output.

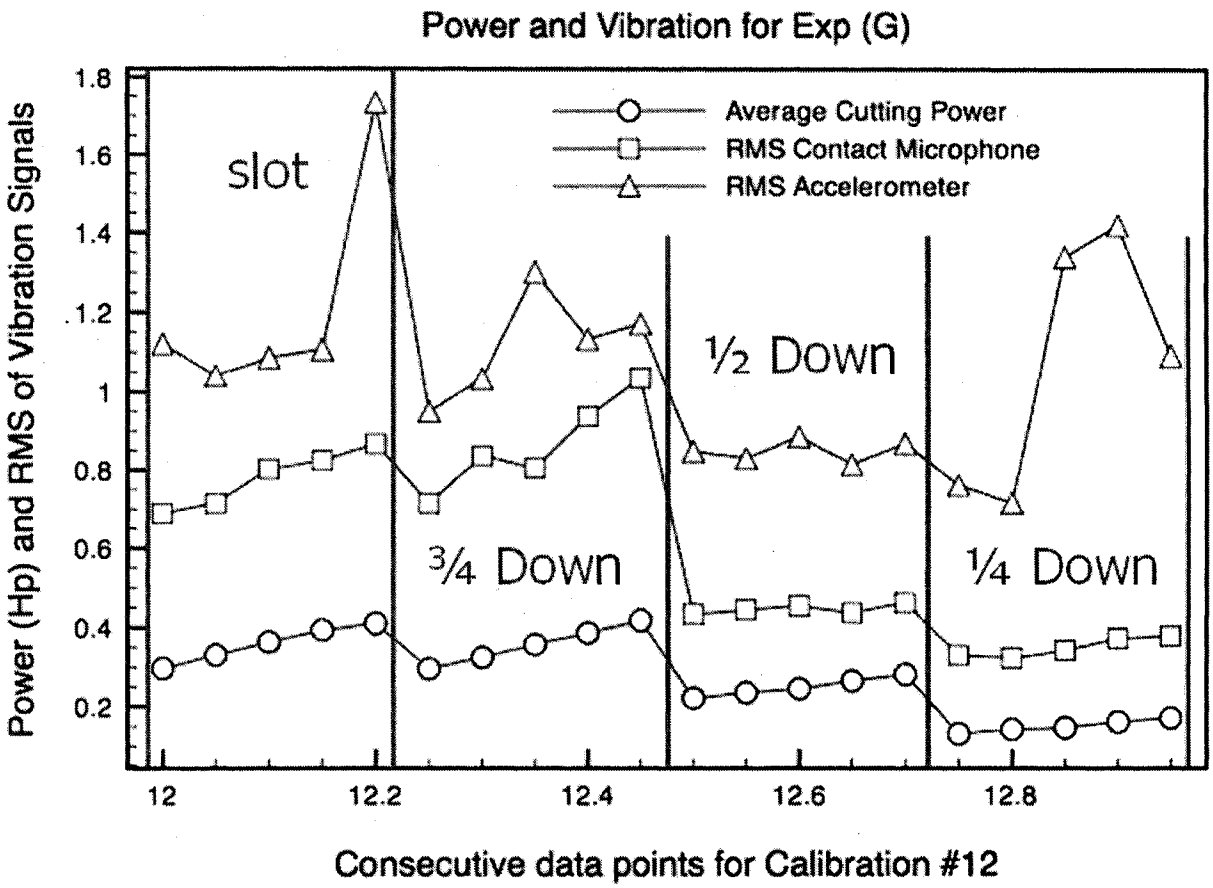

Figure 6-2 Comparison of Microphone RMS and average power data, Exp (G)

For each radial immersion (**Fig 6-2**) the feed rate was set to 3.21, 3.67, 4.13, 4.85 and 5.04 ipm. The increased feed rate should increase the measured spindle motor power, which is true for all points in the power data. The first 5 points were a slot cut that had slightly slower feed rates that put its power level at about the same as the ¾ immersed down mill. The RMS of the accelerometer output did not correlate with motor spindle power as well as that of the contact microphone. The contact microphone values seem to correlate very well with the power, with two noticeable exceptions. The first is that

the RMS of the slot cut is actually lower than that of the ¾ immersed down mill. This makes sense from a vibration and tool wear stand point. A slot cut has material on ether side of it preventing the tool from vibrating in the direction perpendicular to the feed. This explains why the slot cuts tend to perform the same or better than most peripheral cuts at the same spindle speed and feed rate, as shown in Exps (I) and (J) (see **Fig 3-13**). This phenomenon was related to the exit angle by Tlusty [2, 8]. The other difference is that the RMS value dropped by a larger percent between the 10^{th} and 11^{th} point as compared to the power signal. This provides information about the increased vibrations when going from a ½ immersion down mill to a ¾ immersion down mill that cannot be obtained from the power signal. This data can lead to further investigation of cutting geometry in relation to increased vibration and tool wear. **Fig 6-2** suggests that exit angles more than 90 degrees produce excessive vibration that may be detrimental to tool life and surface finish. Programmers may want to select half immersion or less down-mills or slot cutting over down-mills with an exit angles over 90 degrees. Experienced machinists already know this, but it is an example of the type of information and investigations the contact microphone may be used for.

Fig (6-3) is a plot of the microphone RMS vs. the power from the data points in Fig 6-2. This correlation between power and RMS (**Fig 6-3**) of the contact microphone shows that vibration thresholds may be set the same as power thresholds, or in conjunction with a power based TCM system.

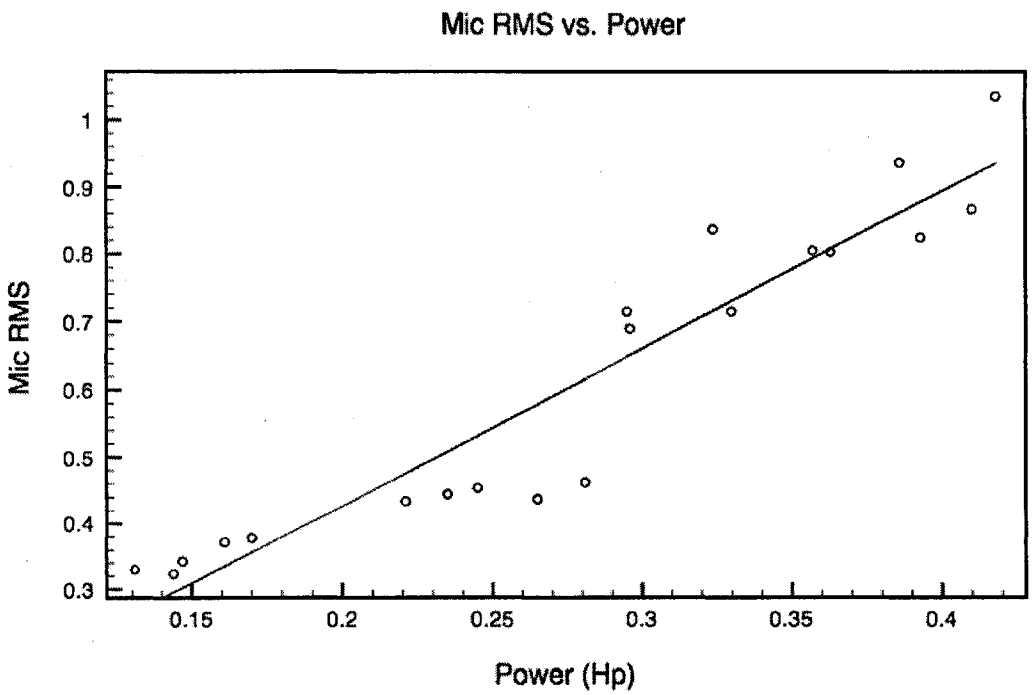

Figure 6-3 Microphone RMS vs. Power, Exp (G)

Experiments (I) through (L) experienced different levels of chipping and flank wear, as explained in Section 3-4. This caused some experiments to last a longer "distance in cut" than others. Chipping causes smaller increases in power, making it more difficult to determine when the tool was worn. But if we look at the RMS value from the contact microphone in **Fig 6-4** we see that there was a significant increase in vibration that may have caused or is the result of the Exp (J) tool to wearing faster than the others.

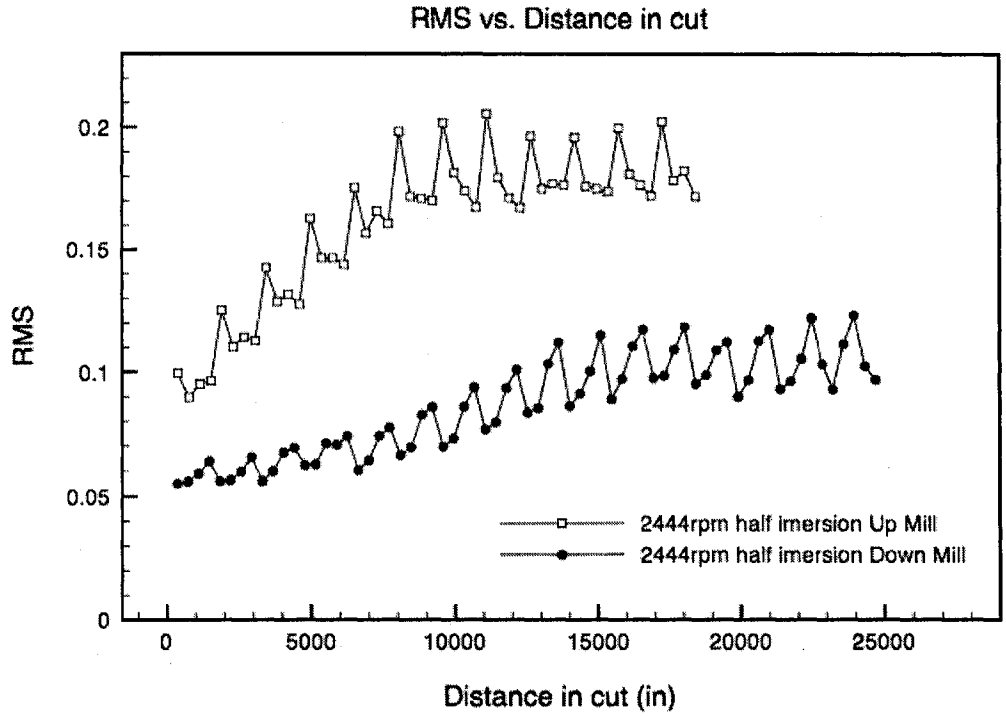

Figure 6-4 RMS vs distance in cut for constant geometry tests, Exps (J) and (L)

Note that the microphone was mounted on the machining bed, causing the signal to change with the position of the cutter even though the cuts were at constant geometry and speed for both tests. This is why mounting to the spindle became our standard practice in later tests.

In **Fig 6-4** the material removal rate for the up mill is the same as the down mill, which causes the power to be about the same for each case, but the contact microphone picked up additional vibrations that may lead to an undesirable pattern of wear. These extra vibrations could show up in any type of cutting and are caused by poorly chosen chip thicknesses and cuttings speeds as well as the dynamics of the machine. When choosing cutting conditions, it is important to choose a chip thickness that is not too

small so that the cutter has a "good bite" of material which keeps the cutter engaged with the part. In our tests the down mill (Exp L) had a longer tool life than the up mill (Exp J) for the exact same feed rates and spindle speed. The down mill starts off with a large chip thickness then gradually decreases to zero, providing a good bite which pulls the cutter, keeping it engaged. The up mill starts at zero chip thickness causing it to be more difficult for the tooth to engage the part. This results in the cutter having to be forced into the cut causing burnishing, increased rubbing, and higher temperatures [15]. The burnishing can actually work harden the surface causing trouble for the next tooth [15]. The difficulty in engaging and cutting a work hardened surface could be the reason for the increased vibrations felt from the contact microphone and is valuable information for TCM or process monitoring systems.

6.2. Frequency content

The frequency content can provide additional information for a TCM system that a power sensor can't provide. Accelerometers and force dynamometers have been used for these purposes but have limitations of high expense and location for mounting. **Fig 6-5** and **Fig 6-6** shows the frequency content of the X-Force signal collected by the force dynamometer for new and worn tool data from Exp (G). **Fig 6-7** and **Fig 6-8** shows the same information from the contact microphone mounted on the spindle and **Fig 6-9** and **Fig 6-10** is from the accelerometer mounted adjacent to the contact microphone. The spindle speed was 3055rpm which translates in to a 50.9 Hz spindle and tooth passing frequency for the one tooth carbide cutter.

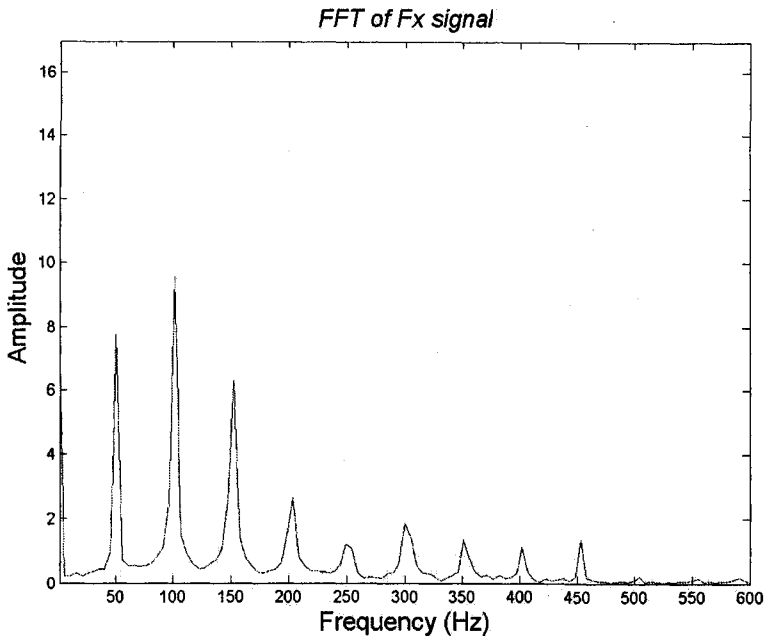

Figure 6-5 FFT of Fx signal for new tool, Exp (G)

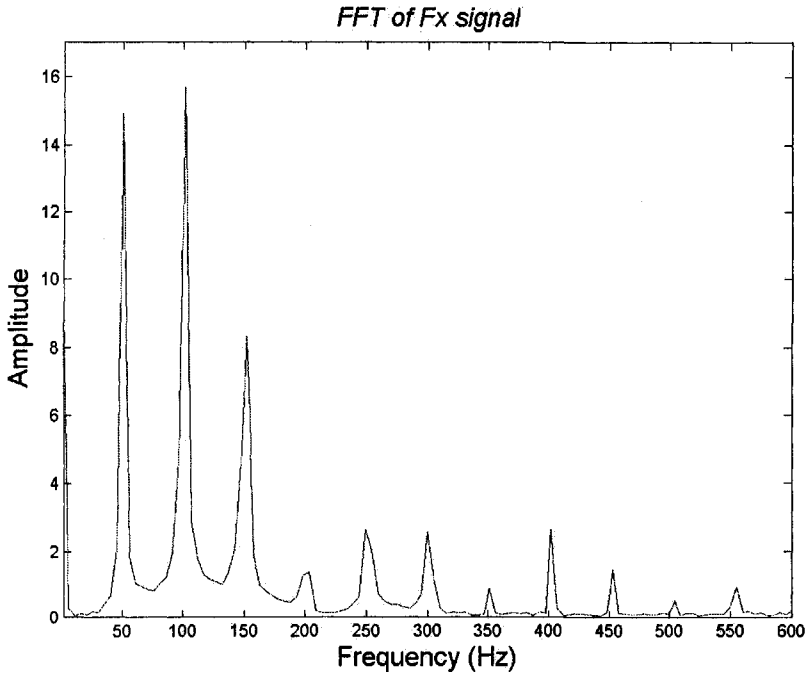

Figure 6-6 FFT of Fx signal for worn tool, Exp (G)

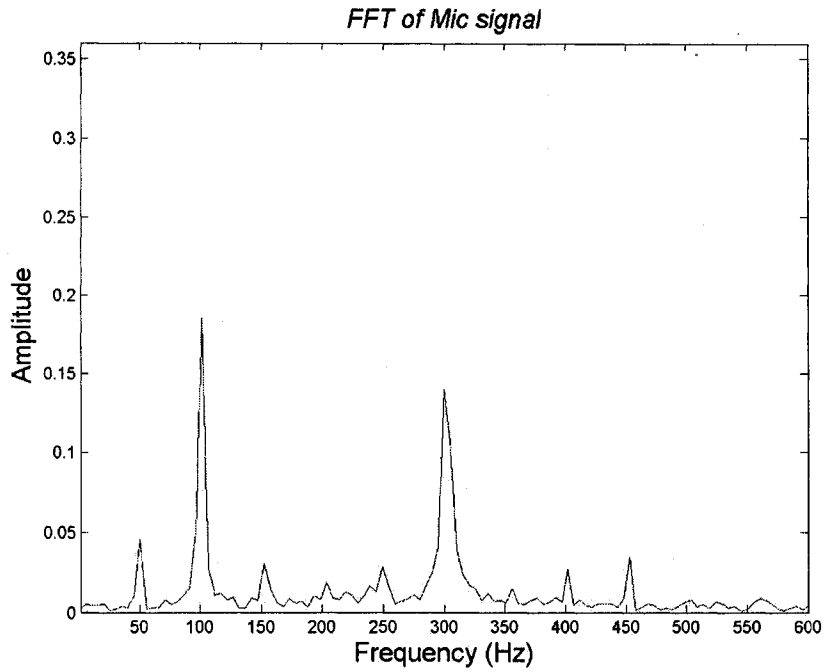

Figure 6-7 FFT of Microphone signal for a new tool, Exp (G)

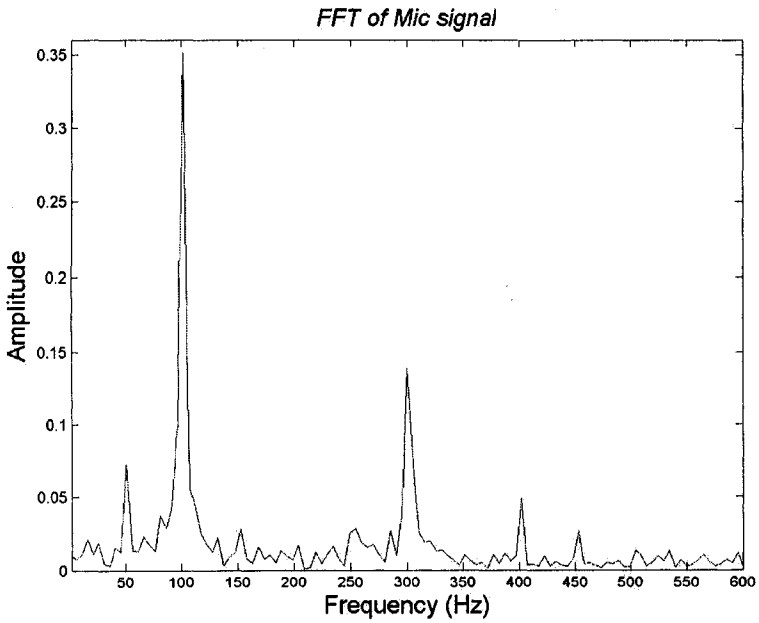

Figure 6-8 FFT of Microphone signal for a new worn, Exp (G)

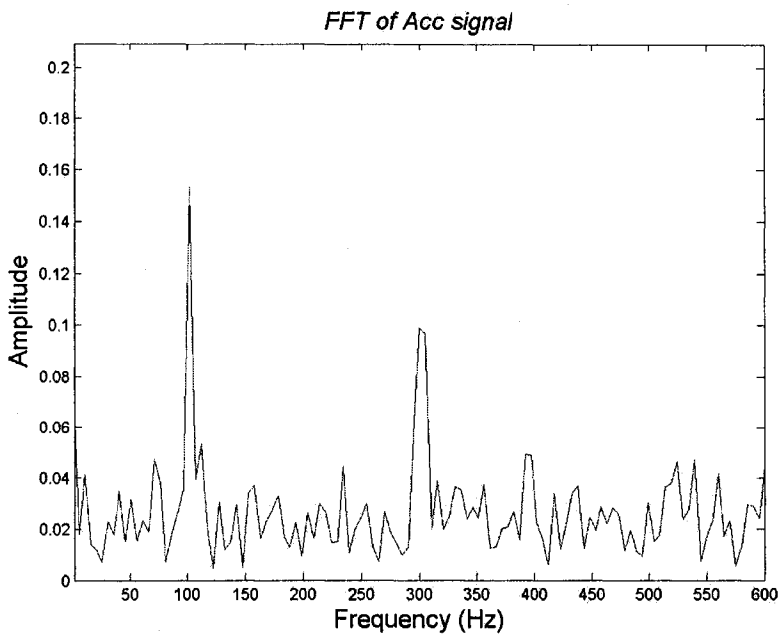

Figure 6-9 FFT of Accelerometer signal for a new tool, Exp (G)

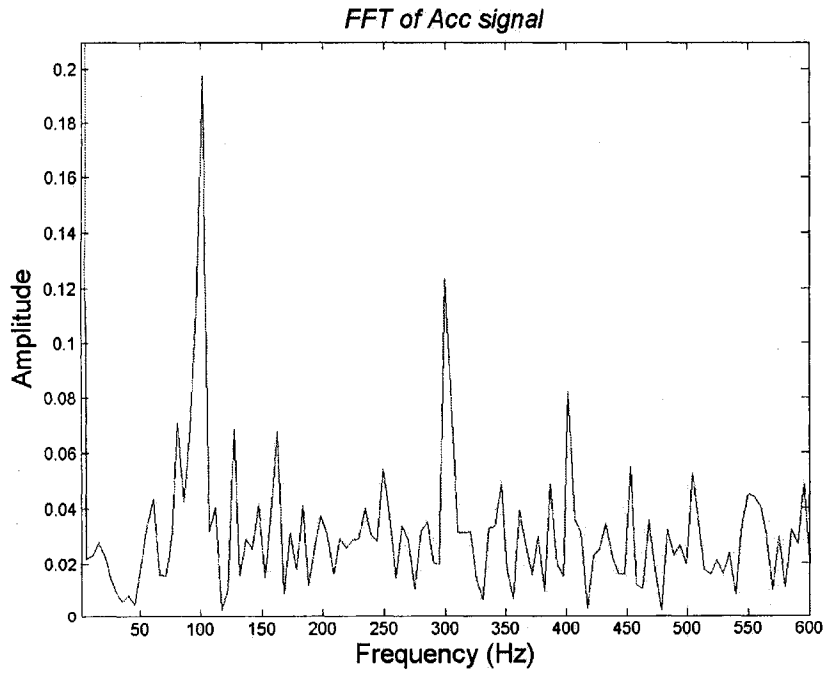

Figure 6-10 FFT of Accelerometer signal for a worn tool, Exp (G)

The contact microphone showed more sensitivity and better frequency information than the accelerometer. The accelerometer didn't show any distinguishable peak at the spindle frequency. The contact microphone was able to show distinguishable peaks at most of the same frequencies as the force signal. The FFT at the spindle frequency increased by about 75% and its first harmonic increased by more than 90% from new to worn tool conditions. In contrast, the force signal had the largest percentage increase at the spindle frequency. For a flank wear case (Exp (H)) increases were seen from the 2^{nd},3^{rd},4^{th}, and 5^{th} harmonics as well as the first (**Fig 6-11**). A ratio of the energy in at the first harmonic vs. the rest of the signal or the spindle frequency may be a good place to start a tool wear investigation with the contact microphone. The contact microphone may be a good sensor for the method described in a patent [31], that uses frequency threshold limits for vibration sensors for milling. It may also be useful in another patent [33], which uses vibrations in three dimensions along with wavelet signal processing to monitor tool wear. A contact microphone has an advantage compared to a standard microphone in that there should be less interference from the many sources of sound found in a noisy shop floor.

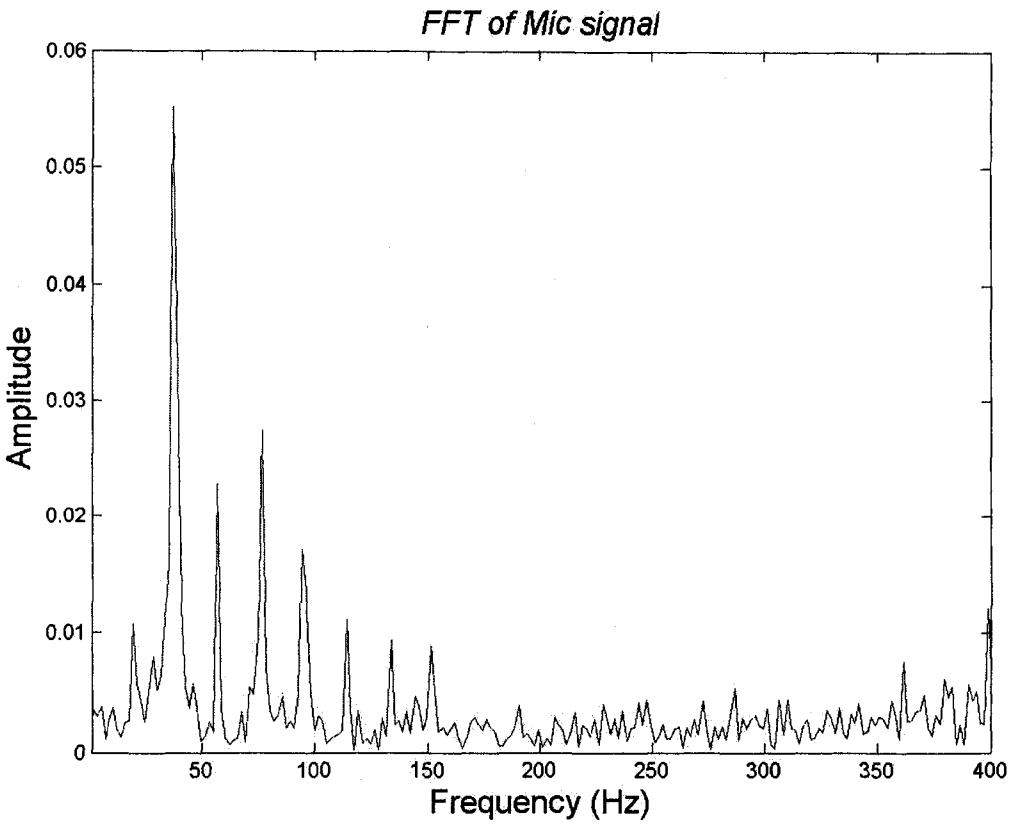

Figure 6-11 FFT of Mic signal for a worn tool with flank wear, Spindle frequency = 17.8 Hz, Exp (H)

The contact microphone shows a good ability to pick up vibrations through the spindle giving an RMS that correlates well with cutting power as well as frequency information. It is an inexpensive alternative to PCB accelerometers and is worthy of further investigation. A challenge when using the contact microphone is that it does not sit on important frequency nodes of the spindle. Experimentation to find the best location on the spindle would be beneficial. One possible method would be to use an accelerometer hammer tap test described in [1] in order to find the natural frequency and harmonics. Then running the spindle at these frequencies and experimenting with the placement of the microphone.

CHAPTER 7.

CONCLUSIONS AND FUTURE WORK

7.1. Conclusions

The use of dynamometers and other load cells to gather information about the cutting conditions in milling is standard practice for researchers but has proved to be impractical for commercial use. The dynamometers introduce unwanted compliance and expense. In addition, users are not willing to place a $30,000 piece of equipment in range of a high velocity cutting tool. "It is clear to see that, as the more expensive and complicated a TCM system becomes, the less value it will have to the industry."[7]. The two power and microphone sensors presented in this report are inexpensive, non-invasive, and less complicated than their alternatives. Power has been the method of choice for commercial TCM users, but its methods of power ratios and limits are restricted to identical cutting conditions and are not well equipped to deal with the unexpected changes milling cutters sometimes experience.

The results from the HSS Exps A, E, F, G, J and K all show a good correlation between VB and K_{te}. For cutting processes that exhibit pure flank wear, using K_{te} to estimate VB will expand the range of applications in which power can be

effectively used. Using K_{te} may allow the TCM system to estimate VB without a necessity for comparison to new tool values of that specific tool. For less stable cutting processes where the mode of wear is unknown or changeable, both coefficients (Ktc and Kte) together might serve as a good diagnostic tool to identify the tool wear mode. The coefficients could be used to identify bad cutting conditions that do not achieve a gradual flank wear, thereby allowing the machinist to fine tune the part program until cutting conditions are found that achieve the desirable mode of gradual flank wear.

There has been a gap between academia and the machining industry when it comes to tool wear in milling. Commercial users prefer to use non-invasive power sensors. Academic studies claim that radial forces are more sensitive to wear and therefore the correct sensor to detect wear is an expensive, invasive force dynamometer. The behavior of the tangential coefficients with respect to chipping and flank wear are revealing, and our studies indicate that the lack of sensitivity of the tangential forces may be linked to the occurrence of chipping. Furthermore, monitoring both of the coefficients may allow a TCM system to determine whether an increase in power is related to flank wear or chipping.

The regression method described in Chapter 4 showed good predictions of wear level for a wide variety of cuts. This method is basically an automatic way to set power limits based on the tool's current state of wear. It assumes that the cutter's change in geometry is the driving factor in increasing the power and that

the rubbing due to flank wear has a larger effect on cutting power increase than the effect of a chipped cutting edge. Even if further testing of this method determines that carbide and HSS should be used separately in the analysis, it is still is a great improvement over the power thresholds that have to be changed for every variation in cutting conditions.

The regression method will work best when calibrated with two extreme cases: one of pure chipping and the other pure flank wear. It would also be helpful to add data points from the combinations of Ktc and Kte in the region that the system is being used. This will allow the equation to react to un-expected changes in the coefficient as well as the expected ones. The trend of the cutting power over the life of the tool seems to be the best way to estimate a tool life curve. Since power is ultimately what the industry uses to define a worn tool this should be an acceptable method for calibration.

One simple method of defining a worn tool with the coefficients and power that was universal for all experiments was the statistical variation of the data once the tool was worn. The increases in variation were due to a rapidly changing cutting edge. Although only briefly described in this thesis it is definitely a universal indicator of a worn tool and could be used to stop cutting before complete tool failure. These variations may be too late for many cases but could be used as a good fail safe measurement.

The contact microphone poses the same problems as a power sensor for TCM with a few additional challenges and advantages. Methods to account for the uneven frequency response need to be explored, but it's cost and ability to pick up transmissions through the spindle make it worthy of continued consideration as one element of a comprehensive TCM system. The microphone could certainly be used as a simple reference for a machinist trying to minimize vibrations. If the initial and final vibration levels are recorded for a repeatable cutting process the contact microphone could be used in place of a power sensor for threshold TCM. The contact microphone can also give frequency content information that could be used in the same way accelerometers and force dynamometers have been used for tooth breakage detection.

The testing in this report was limited to standard helical end mills with 30 degree helix angles with positive rake angles. Most of the research was conducted with half inch end mills wearing in 1018 steel in order to be able to compare values to the original investigation of the coefficients. Some testing at different cutter diameters was conducted with similar results. Changes in the cutter geometry (like a negative rake angle) may cause contributions of flank wear and chipping to show up differently in each of the force components. Our results may not be consistent with those of a radically different tool shape and tool coatings and additional research is warranted.

7.2. Future Work

Future work should address the following issues.

1. Testing with other tools and materials
    - This research focused on tool wear of 30 degree helical end mills in 1018 steel. The use of tangential force coefficients to monitor wear was successful but the methods may not hold up with all cases. More testing should be done with other work-piece materials and tools. Tools with coatings and insert cutters with negative rake angles may exhibit the most drastic difference from the patterns shown in this research.
2. Find a better method to quantify VB in order to get a good VB vs. Kte calibration.
    - The current microscope and camera technique can be difficult to work with at times resulting in bad records of the cutting edge. The method of shining a focused beam of light at the cutting edge can result in strange shadows and shiny reflections that blind the camera. The best images came from a very well lit room with light hitting the tool from all angles. A good place to start would be the imaging and analysis techniques of reference [32].
3. Further investigation of the 110% wear limit and multiple regression estimations.

- The 110% limit based on a weighted combination of K_{te} and K_{tc} described in Section 4-1 may be a very promising method for setting a new type of power threshold that is much more universal. Note that the weightings are probably dependent on the type of tool and the workpiece material. More tests should be done with other tool diameters and materials in order to justify a practical use of this method.
- For the multiple regressions an alternative method of quantifying the wear land should be explored to improve calibration and accuracy of the model.
- These methods should also be explored with the radial coefficients due to their increased sensitivity to wear. The use of feed drive power to replace the Kistler dynamometer should also be explored.

4. Refine calibration techniques for online calibration.
    - The coefficients can tell you a lot about the nature of tool wear if good calibration techniques are practiced. The amount of tool wear from the start to finish of a calibration routine should be minimal. A good range and multiple data points are good for any regression. A program that modifies G-code to accommodate for periodic calibration without adversely affecting part quality or machining time would be helpful, e.g. varying feedrate to achieve different levels of average chip thickness. Different techniques could be developed

based on the user's needs; e.g. quantify VB, identify chipping, or using a sacrificial block.

5. Further investigation into the coefficients and surface finish.
    - There are many models that predict surface finish based on the cutting conditions and the geometry of the tool. If the coefficients could give insight into the changing geometry of the tool, new or existing models should be able to predict surface finish accurately.

6. Temperature effects
    - The largest factor in tool wear is temperature yet it was not measured in the experiments of this thesis and could be a large source of error for all experiments. For the techniques in this research tool temperature should not have an effect as long as there is no significant wear between calibration points. But the effect of work piece temperature on the coefficients is unknown. During wear tests with repeated cutting the work piece was observed to heat up significantly measured only by touch. Whether or not this temperature increase affects the machineablity of the material enough to change the coefficients should be explored. A temperature sensor on the work piece may provide useful information about these effects.

REFERENCES

[1] Altintas, Y., (2000), Manufacturing Automation: Metal Cutting Mechanics, Machine Tool Mechanics, Machine Tool Vibrations, and CNC Design, Cambridge University Press, ISBN 0-521-65973-6.

[2] Tlusty, J., (2000), Manufacturing Processes and Equipment, Prentice Hall, Upper Saddle River, New Jersey, ISBN 0201498650.

[3] A. G. Mamalis, J. Kundrak, and M. Horvath, (2005), "On a Novel Life Relation for Precision Cutting Tools", Journal of Manufacturing Science and Engineering, Vol. 127, DOI 10.1115/1.1794158

[4] Carsten Schmidt and Eugene Y.-C. Yen, (2006), "Tool Wear Prediction and Verification in Orthogonal Cutting", Engineering Research Center for Net Shape Manufacturing (ERC/NSM), The Ohio State University. http://nsmwww.eng.ohio-state.edu/6thCIRP_toolwear_Toronto.pdf, April 14, 2007

[5] Tien-Chien Jen, Aloysius U. Anagonye, (2001), "An Improved Transient Model of Tool Temperatures in Metal Cutting", Journal of Manufacturing Science and Engineering, Vol. 123, DOI 10.1115/1.1334865

[6] Prickett, P. W. and C. Johns, (1999), "An overview of approaches to end milling tool monitoring", International Journal of Machine Tools and Manufacture, Vol. 39, pp. 105-122.

[7] Rehorn, A. G., J. Jiangand, and P. E. Orban, (2004), "State-of-the-art methods and results in tool condition monitoring: a review," International Journal of Advanced Manufacturing Technology, DOI 10.1007/s00170-004-2038-2.

[8] E. Orady and J. Tlusty, (1981), "Effect of Thermal Cycling on Tool Wear in Milling", Ninth North American Manufacturing Research Conference Proceedings, Vol 9, May 19-22,

[9] R. H. Osuri, S. Chatterjee, and S. Chandrashekhar, (1991), "On-line Condition Monitoring of Tool Wear in End Milling Using Acoustic Emission", Taylor and Francis, Vol. 29, NO. 7, pp. 1339-1353.

[10] K. Jemielniak, (1999), "Commercial Tool Condition Monitoring Systems", International Journal of Advanced Manufacturing Technology, Vol 15, pp 711-721

[11] Min Xu, Robert B. Jerard and Barry K. Fussell, (2007), "Energy Based Cutting Force Model Calibration for Milling", Computer-Aided Design & Applications (In press)

[12] The University of Melbourne, (2007), Department of Mechanical and Manufacturing engineering, http://www.mame.mu.oz.au/manuf-sci3/436413/tool_wear.htm, April 14, 2007

[13] Caron Engineering, Tool Monitor Adaptive Control System (TMAC), http://www.caron-eng.com/measuring_tmac_7.php, April 14, 2007

[14] Douglas C. Montgomery, George C. Runger, and Norma F. Hubele, (2004), Engineering Statistics, Third addition, John Wiley & Sons Inc.

[15] Modern Metal Cutting: A Practical Handbook, Sandvick Coromant, Fair Lawn, New Jersey,1996

[16] Steven Y. Liang, Rogelio L. Hecker, Robert G. Landers, (2004), "Machine Process Monitoring and Control: The State-of-the-Art", Journal of Manufacturing Science and Engineering, Vol. 126, pp. 297-310

[17] B. W. Niebel, A. B. Draper, R. A. Wysk, (1989), Modern Manufacturing Process Engineering, McGraw-Hill, Inc. United States

[18] H. Saglam and A. Unuvar, (2003), "Tool Condition monitoring in milling based on cutting forces by a neural network", International Journal of Production Reserch, Vol. 7, pp. 1519-1532.

[19] E. Kuljanic, M. Sortino, (2005), "TWEM, a method based on cutting forces – monitoring tool wear in face milling", International journal of machine tools & manufacture, vol. 45, no1, pp. 29-34

[20] D. Cuppini, G. D'Errico, and G. Rutelli, (1990), "Tool Wear Monitoring Based on Cutting Power Measurement," Elsevier Sequoia/Printed in the Netherlands, Wear 139, pp.303-311

[21] J. H. Tarn and M. Tomizuka, (1989), "On-Line Monitoring of Tool Conditions in Milling", ASME Journal of Engineering for Industry, Vol. 111, pp. 206-211

[22] J. Jones, Y. Wu, Cutting tool's power consumption measured, US Patent, US 5 587 931. 1996

[23] Joseph C. Chen and Wei-Liang Chen, (1999), "A tool breakage detection system using an accelerometer sensor", Journal of Intelligent Manufacturing, vol. 10, no. 2, pp. 187-197

[24] Gaoyong Luo, David Osypiw, and Mark Irle, (2001), "Tool Wear Monitoring By On-Line Vibration Analysis With Wavelet Algorithum", 3rd International Conferavnce on Metal Cutting and High speed machining,

[25] Schuyler, C. K., (2005), Feedrate Optimization and Tool Condition Monitoring of Flat-End Milling Operations Utilizing Spindle Motor Power, Master's Thesis, Dept. of Mechanical Engineering, The University of New Hampshire.

[26] Min Xu, C. K. Schuyler, B. K. Fussell, R. B. Jerard, (2006), "Experimental Evaluation Of A Smart Machining System For Feedrate Selection And Tool Condition Monitoring", Transactions of the North American Manufacturing Research Institution/SME (NAMRC) Volume 34, Marquette University, May 23-26.

[27] Min Xu, (2007), Smart Machining System Platform for CNC Milling with the integration of a power sensor and cutting model, PhD Dissertation, Dept. of Mechanical Engineering, The University of New Hampshire.

[28] F. Ismail, M. A. Elbestawi, R. Gu, and K. Urbasik, (1993), "Generation of Milled Surfaces Including Tool Dynamics and Wear," Journal of Engineering for Industry, Vol. 115, pp. 245-252

[29] Jerard, R. B., B. K. Fussell, M. Xu, C. Yalcin, (2006), Process Simulation and Feedrate Selection for Three-axis Sculptured Surface Machining, International Journal of Manufacturing Research, 1(2), pp. 136-156.

[30] Min Xu, C. K. Schuyler, B. K. Fussell, R. B. Jerard, (2006), Patent Provision Application, Method to Measure Tool Wear from Process Model Parameters, Filed on 12/2/2006

[31] David A. Anderson, William A. Dias, Method for monitoring cutting tool wear during a machining operation, US Patent, US 4 744 242. 1988

[32] David Kerr, James Pengilley, and Robert Garwood, (2006), "Assessment and visualization of Machine tool wear using computer vision", International Journal of Advanced Manufacturing Technology, Vol 28, pp781-791

[33] Werner Wilhelm Kluft, Martin Josef Reuber, Heinz-Hubert Kratz, Method and device for monitoring the wear condition of a tool, US Patent, US 6 732 056. 2004

[34] Fadal Machining Centers, LLC, EMC Machining Center, Chatsworth, CA http://www.fadal.com/, April 14, 2007

[35] MDSI, Manufacturing Data Systems Inc.., Ann Arbor, MI http://www.mdsi2.com April 14, 2007

[36] Load Controls Incorporated, Universal Power Cell, Sturbridge, MA http://www.loadcontrols.com, April 14, 2007

[37] Kistler Instrument Corp., 3-Component Dynamometer, Amherst, NY http://www.kistler.com/, April 14, 2007

[38] AKG Acoustics, C411 Vibration Pick up Microphone, Vienna, Austria www.akg.com, April 14, 2007

[39] PCB Piezotronics, Inc., 320C33 Accelerometer, Depew, New York http://www.pcb.com/, April 14, 2007

[40] Measurement Computing, DEAS 6402 A/D Board, Norton, MA http://www.measurementcomputing.com/, April 14, 2007

[41] Mitutoyo, SJ-400 surface roughness tester, Japan, http://www.mitutoyo.co.jp/eng/index.html, April 14, 2007

APPENDICES

APPENDIX A

Wear estimation results

Table A-1 Tabulated results of multiple regressions (Exp A,C,D,E)

	Kte (lb/in)	**Ktc (lb/in^2)**	**Actual % of cutting edge used** (based on power trend)	**Estimated % cutting edge used** (based on %edge=-95.33 + 0.161*Kte + 0.00026*Ktc)	**Absolute difference (Error)**
Experiment A	207.07	303070	0.00	16.14	16.14
	213.96	303950	1.45	17.47	16.02
	228.43	299620	3.41	18.68	15.27
	223.73	304070	8.47	19.07	10.60
	218.17	320350	13.71	22.38	8.67
	274.68	287160	10.43	22.9	12.47
	304	277490	14.73	25.12	10.39
	315.81	279300	23.64	27.48	3.84
	369.79	257230	25.45	30.47	5.02
	352.38	287050	28.49	35.36	6.87
	368.54	286040	31.76	37.7	5.94
	382.32	299720	45.37	43.44	1.93
	420.25	284410	44.49	45.59	1.10
	407.99	323820	51.20	53.79	2.59
	471.7	297660	58.34	57.28	1.06
	449.98	359720	77.85	69.8	8.05
	502.24	410850	96.35	91.39	4.96
	494.47	474510	110.06	106.56	3.50
	591.56	437290	120.64	112.56	8.08
	663.79	408480	123.22	116.74	6.48

Experiment C	48.64	379020	0.00	10.27	10.27
	98.3	346150	1.00	9.77	8.77
	126.71	330480	2.28	10.29	8.02
	141.78	327460	4.13	11.94	7.8
	203.31	297610	7.82	14.13	6.31
	249.88	281630	12.09	17.49	5.4
	310.47	259310	17.28	21.47	4.19
	342.95	262030	23.34	27.39	4.05
	352.94	280120	29.08	33.66	4.58
	418.84	258410	35.31	38.65	3.35
	557.49	187550	42.80	42.66	0.14
	591.1	181220	47.03	46.43	0.6
	514.61	264140	52.72	55.53	2.81
	681.57	166750	59.02	57.24	1.78
	634.17	220720	63.13	63.54	0.41
	650.9	220120	65.79	66.07	0.28
	715.22	203230	72.85	72.06	0.8
	723.13	218310	77.54	77.22	0.32
	806.7	168860	80.55	77.89	2.66
	856.7	148960	84.48	80.79	3.68
	826.1	189960	88.52	86.45	2.07
	867.7	186340	94.74	92.21	2.54
	627.95	388070	99.47	105.71	6.25
	689.74	383540	108.82	114.48	5.66
	799.43	313290	111.59	113.98	2.39
	808.47	299720	110.10	111.94	1.84
Experiment D	67.69	367040	0.00	10.24	10.24
	114.7	338810	15.42	10.51	4.9
	145.48	339940	29.41	15.75	13.66
	135.81	349890	27.29	16.76	10.53
	161.69	343210	38.06	19.2	18.86
	164.68	374340	46.92	27.71	19.21
	112.33	497130	50.83	50.98	0.14
	124.01	516170	61.16	57.77	3.39
	121.79	534020	64.40	62.01	2.38
	181.19	553490	97.32	76.58	20.74
	122.67	726310	110.05	111.76	1.72
	432.45	512600	205.43	106.42	99.01
Experiment E	97.48	299830	0.00	-2.31	2.31
	133.5	314480	11.46	7.26	4.2
	85.28	281390	-6.47	-9.03	2.55

	143.72	315020	14.00	9.04	4.96
	129.65	326110	12.72	9.64	3.08
	139.86	322050	14.36	10.23	4.12
	172.4	302540	18.74	10.43	8.31
	172.87	302020	18.69	10.37	8.32
	125.33	342630	14.60	13.21	1.39
	140.38	329620	15.88	12.27	3.61
	147.18	330450	17.65	13.58	4.07
	138.44	348910	18.96	16.93	2.02
	152.11	355110	23.51	20.73	2.78
	155.49	343720	22.14	18.34	3.81
	134.62	373010	22.55	22.54	0.01
	149.69	376020	26.72	25.74	0.98
	148.75	381150	29.85	26.91	2.94
	151.67	389560	27.48	29.55	2.06
	142.58	441040	36.96	41.37	4.4
	166.4	446210	43.71	46.53	2.82
	257.48	485510	73.47	71.31	2.16
	337.71	486900	93.20	84.56	8.64
	367.08	541330	110.10	103.32	6.78

Table A-2 Tabulated results of multiple regressions (Exp H,G)

	Kte (lb/in)	**Ktc (lb/in^2)**	**Actual % of cutting edge used** (based on power trend)	**Estimated % cutting edge used** (based on %edge=-56.04 + 0.1403*Kte + 0.000113*Ktc)	**Absolute difference (Error)**
Experiment H	134.27	423287.50	15.63	10.64	4.99
	109.12	508647.20	20.12	16.76	3.36
	330.88	421985.80	39.71	38.08	1.64
	398.62	410247.50	47.90	46.26	1.64
	532.60	349150.60	59.24	58.15	1.09
	650.53	275798.40	67.67	66.40	1.26
	618.70	361427.60	74.31	71.62	2.69
	737.41	320107.30	86.53	83.60	2.93
	803.59	286381.20	87.54	89.07	1.53
	749.54	417405.20	95.69	96.30	0.61
	747.31	509121.00	106.41	106.35	0.06
	680.31	647572.30	109.40	112.60	3.20
	882.93	443573.90	114.51	117.97	3.46
	1007.36	193931.30	110.22	107.21	3.01
	870.59	467040.40	109.56	118.89	9.33
	235.91	1249212.20	106.61	118.25	11.64

Experiment G	220.47	320419.00	0.00	11.11	11.11
	198.47	326075.00	-2.80	8.66	11.47
	318.86	352053.00	25.49	28.49	3.00
	267.23	396653.00	22.15	26.28	4.14
	277.59	388095.00	23.25	26.77	3.52
	226.58	429353.00	20.26	24.28	4.02
	227.78	431265.00	19.78	24.66	4.88
	258.09	461459.00	40.69	32.33	8.36
	232.81	504166.00	33.37	33.61	0.23
	214.73	546836.00	36.75	35.89	0.85
	231.12	568188.00	41.81	40.61	1.20
	231.69	582729.00	46.08	42.33	3.75
	149.22	656288.00	38.27	39.07	0.80
	130.26	633022.00	31.64	33.78	2.14
	109.43	666662.00	35.86	34.66	1.19
	125.98	672376.00	39.75	37.63	2.12
	134.07	647048.00	38.29	35.90	2.39
	179.06	648402.00	39.97	42.37	2.39
	150.50	709663.00	44.72	45.28	0.56
	314.40	611965.00	66.23	57.24	8.99
	284.34	694230.00	75.62	62.32	13.30
	484.65	676986.00	98.10	88.47	9.63
	707.00	472000.00	100.06	96.50	3.56

APPENDIX B

Experiment reference index

The experiment index is in reference to table 2-1 in section 2-1. All the raw data can be found in the computer in the DML know as Fadal at extension: \\Fadal\experimental data\Data\Bennett

followed by the extension in table AB-3.

Table B-3 File extensions

Experiment	File extension
Exp (A)	2004.08.03_Thesis_experiment_A
Exp (B)	2007.2.08_Thesis_experiment_B
Exp (C)	2007.2.13_Thesis_experiment_C
Exp (D)	2004.8.10_Thesis_experiment_D
Exp (E)	2004.8.16_Thesis_experiment_E
Exp (F)	2004.8.13_Thesis_experiment_F
Exp (G)	2006.12.12_Thesis_experiment_G
Exp (H)	2006.8.21_Thesis_experiment_H
Exp (I)	2006.7.5_Thesis_experiment_I
Exp (J)	2006.7.14_Thesis_experiment_J
Exp (K)	2006.7.14_Thesis_experiment_K
Exp (L)	2006.7.14_Thesis_experiment_L

APPENDIX C

Code for radial coefficients

This is the MatLab code written by Min Xu, a Ph-D student in the UNH Design and Manufacturing Laboratory. There are several methods in which the code calculates the radial and tangential coefficients based on force and power data from a calibration routine. This thesis used case 3 defined on the third line of non commented code, which utilizes Fx and Fy for the calibration.

```
%This file is used to calibrate the Ktc, Kte, Krc, Kre, where Ktc and Kte come
% from the formular Ftc = Ktc*ChipArea, Fte = Kte*ToolLength, Frc and Fre
% respectively are the tangential force for shearing and ploughing
% materials. Krc and Kre come from the formular Frc = Krc*ChipArea, Fre =
% Kre*ToolLength, Frc and Fre respectively are the radial force for
% shearing and ploughing materials.
%
% Use Altinatas's model, add runout to the mode,
% Use different methods to calibrate Ktc, Kte, Krc, Kre,
% and then use Ktc, Kte, Krc, Kre to predict
%
% Created by MinXu
%
% First define some variables for the tool
close all;
clear;

% choose calibration mode
CalibrateModel = 3;        % use which method to calibrate
% 1 ---- with Avg Ft and Fx,   2 ---- with Avg Ft and Fy,
% 3 ---- with Avg Fx and Fy,   4 ---- with Avg Ft, Fx and Fy
% 5 ---- with Avg Fx,          6 ---- with Avg Fy
% 7 ---- with Avg Ft first to get Kt, then use Fx and Fy to get Kr

Nt = 1;            % number of teeth
D = 0.375;         % tool diameter
Phi = 30*pi/180;   % tool helix angle
n = 0.94;          % motor efficiency
DataPoints = xlsread('Copy of two.xls');  % data file name
NumToStart = 1;    % Use this variable to choose
NumToEnd = 12;
```

```
NumToStartCalibration = 1;  % Use this variable to choose the data point to start
calibration
NumToEndCalibration = 12;  % Use this variable to choose the data point to end
calibration

RD = DataPoints(NumToStart:NumToEnd,10);
AD = DataPoints(NumToStart:NumToEnd,11);
Feed = DataPoints(NumToStart:NumToEnd,14);
w = DataPoints(NumToStart:NumToEnd,7);
Yo = DataPoints(NumToStart:NumToEnd,24);
Pe = DataPoints(NumToStart:NumToEnd,20);
Fxy_Max_Act = DataPoints(NumToStart:NumToEnd,21);
Fx_ave = DataPoints(NumToStart:NumToEnd,22);
Fy_ave = DataPoints(NumToStart:NumToEnd,23);
%Mrr_1 = DataPoints(NumToStart:NumToEnd,12);   % contact area, unit: inch^2
%Ac = DataPoints(NumToStart:NumToEnd,13);   % contact area, unit: inch^2
Dimensions = size(RD);
NumOfDataPoints = Dimensions(1);

% Use the info to calibrate
P = n*Pe;
fpt = Feed./w/Nt;                % the feed per tooth - inches/tooth
Theta_Enter = acos(1-2*Yo);        % entrance angle
Theta_Exit = acos(1-2*(Yo+RD));     % exit angle
Ac = AD.*(Theta_Exit - Theta_Enter)*D^2/2;   % contact area
Delta_Theta = 2*tan(Phi)*AD*D;        % Angle between the leading edge and top
of engaged flute
Mrr_1 = Feed.*RD.*AD*D^2;          % Material removal rate - cubic inches/min
Mrr_2 = Mrr_1./w;                % Material removed per revolution of the cutter -
cubic inches/rev
Ft_ave = 6600*P./w/pi/D*60;        % Ft_ave = 6600*P./w/2/pi/D/Nt*120;

% define some constants
C1 = D*AD.*(cos(Theta_Enter)-cos(Theta_Exit))/2/pi*Nt;
C2 = D*AD.*(Theta_Exit-Theta_Enter)/2/pi*Nt;
C3 = D*AD.*(cos(2*Theta_Exit)-cos(2*Theta_Enter))/8/pi*Nt;
C4 = -D*AD.*(sin(Theta_Exit)-sin(Theta_Enter))/2/pi*Nt;
%C5 = D*AD.*(2*Theta_Enter - 2*Theta_Exit + sin(2*Theta_Exit) -
sin(2*Theta_Enter))/8/pi;
C5 = D*AD.*(2*Theta_Enter - 2*Theta_Exit + sin(2*Theta_Exit) -
sin(2*Theta_Enter))/8/pi*Nt;
C6 = D*AD.*(cos(Theta_Exit)-cos(Theta_Enter))/2/pi*Nt;

% build the matrix to calibrate
NumToUseForCalibration = NumToEndCalibration - NumToStartCalibration + 1;
switch CalibrateModel
```

```
% 1 ---- with Avg Ft and Fx,    2 ---- with Avg Ft and Fy,
% 3 ---- with Avg Fx and Fy,    4 ---- with Avg Ft, Fx and Fy
% 5 ---- with Avg Fx,          6 ---- with Avg Fy
% 7 ---- with Avg Ft first to get Kt, then use Fx and Fy to get Kr
   case 1    % use Avg Ft and Fx
   for i = 1:NumToUseForCalibration;
      iDataIndex = i + NumToStartCalibration - 1;
      M_C(i, 1) = C1(iDataIndex, 1)*fpt(iDataIndex);
      M_C(i, 2) = C2(iDataIndex, 1);
      M_C(i, 3) = 0;
      M_C(i, 4) = 0;
      M_F(i, 1) = Ft_ave(iDataIndex);
      M_F(i+NumToUseForCalibration, 1) = Fx_ave(iDataIndex);
      M_C(i+NumToUseForCalibration, 1) = C3(iDataIndex, 1)*fpt(iDataIndex);
      M_C(i+NumToUseForCalibration, 2) = C4(iDataIndex, 1);
      M_C(i+NumToUseForCalibration, 3) = C5(iDataIndex, 1)*fpt(iDataIndex);
      M_C(i+NumToUseForCalibration, 4) = C6(iDataIndex, 1);
   end;

   % output file name
   ForceProfileFileName = sprintf('%s', 'ForceProfileFromFtFx.xls');
   CoefficientsFileName = sprintf('%s', 'CoefficientsFtFx.xls');
   case 2    % use Avg Ft and Fy
   % calibrate Ktc and Kte with power (average Ft )
   for i = 1:NumToUseForCalibration;
      iDataIndex = i + NumToStartCalibration - 1;
      M_C(i, 1) = C1(iDataIndex, 1)*fpt(iDataIndex);
      M_C(i, 2) = C2(iDataIndex, 1);
      M_C(i, 3) = 0;
      M_C(i, 4) = 0;
      M_F(i, 1) = Ft_ave(iDataIndex);
      M_F(i+NumToUseForCalibration, 1) = Fy_ave(iDataIndex);
      M_C(i+NumToUseForCalibration, 1) = -C5(iDataIndex, 1)*fpt(iDataIndex);
      M_C(i+NumToUseForCalibration, 2) = -C6(iDataIndex, 1);
      M_C(i+NumToUseForCalibration, 3) = C3(iDataIndex, 1)*fpt(iDataIndex);
      M_C(i+NumToUseForCalibration, 4) = C4(iDataIndex);
   end;
   % output file name
   ForceProfileFileName = sprintf('%s', 'ForceProfileFromFtFy.xls');
   CoefficientsFileName = sprintf('%s', 'CoefficientsFtFy.xls');

   case 3    % use Avg Fx and Fy
   for i = 1:NumToUseForCalibration;
      iDataIndex = i + NumToStartCalibration - 1;
      M_C(i, 1) = C3(iDataIndex, 1)*fpt(iDataIndex);
      M_C(i, 2) = C4(iDataIndex);
```

```
      M_C(i, 3) = C5(iDataIndex, 1)*fpt(iDataIndex);
      M_C(i, 4) = C6(iDataIndex, 1);
      M_F(i, 1) = Fx_ave(iDataIndex);
      M_F(i+NumToUseForCalibration, 1) = Fy_ave(iDataIndex);
      M_C(i+NumToUseForCalibration, 1) = -C5(iDataIndex, 1)*fpt(iDataIndex);
      M_C(i+NumToUseForCalibration, 2) = -C6(iDataIndex, 1);
      M_C(i+NumToUseForCalibration, 3) = C3(iDataIndex, 1)*fpt(iDataIndex);
      M_C(i+NumToUseForCalibration, 4) = C4(iDataIndex, 1);
    end;
    % output file name
    ForceProfileFileName = sprintf('%s', 'ForceProfileFromFxFy.xls');
    CoefficientsFileName = sprintf('%s', 'CoefficientsFxFy.xls');

    case 4    % use Avg Ft, Fx and Fy
    for i = 1:NumToUseForCalibration;
      iDataIndex = i + NumToStartCalibration - 1;
      M_C(i, 1) = C1(iDataIndex, 1)*fpt(iDataIndex);
      M_C(i, 2) = C2(iDataIndex, 1);
      M_C(i, 3) = 0;
      M_C(i, 4) = 0;
      M_F(i, 1) = Ft_ave(iDataIndex);     % average power

      M_C(i+NumToUseForCalibration, 1) = C3(iDataIndex, 1)*fpt(iDataIndex);
      M_C(i+NumToUseForCalibration, 2) = C4(iDataIndex, 1);
      M_C(i+NumToUseForCalibration, 3) = C5(iDataIndex, 1)*fpt(iDataIndex);
      M_C(i+NumToUseForCalibration, 4) = C6(iDataIndex, 1);
      M_F(i+NumToUseForCalibration, 1) = Fx_ave(iDataIndex);        % average
Fx

      M_C(i+NumToUseForCalibration*2, 1) = -C5(iDataIndex, 1)*fpt(iDataIndex);
      M_C(i+NumToUseForCalibration*2, 2) = -C6(iDataIndex, 1);
      M_C(i+NumToUseForCalibration*2, 3) = C3(iDataIndex, 1)*fpt(iDataIndex);
      M_C(i+NumToUseForCalibration*2, 4) = C4(iDataIndex, 1);
      M_F(i+NumToUseForCalibration*2, 1) = Fy_ave(iDataIndex);     % average
Fy
    end;
    % output file name
    ForceProfileFileName = sprintf('%s', 'ForceProfileFromFtFxFy.xls');
    CoefficientsFileName = sprintf('%s', 'CoefficientsFtFxFy.xls');

    case 5    % use Avg Fx
    for i = 1:NumToUseForCalibration;
      iDataIndex = i + NumToStartCalibration - 1;
      M_F(i, 1) = Fx_ave(iDataIndex);
      M_C(i, 1) = C3(iDataIndex, 1)*fpt(iDataIndex);
      M_C(i, 2) = C4(iDataIndex, 1);
```

```
    M_C(i, 3) = C5(iDataIndex, 1)*fpt(iDataIndex);
    M_C(i, 4) = C6(iDataIndex, 1);
  end;
  % output file name
  ForceProfileFileName = sprintf('%s', 'ForceProfileFromFx.xls');
  CoefficientsFileName = sprintf('%s', 'CoefficientsFx.xls');

  case 6    % use Avg Fy
  for i = 1:NumToUseForCalibration;
    iDataIndex = i + NumToStartCalibration - 1;
    M_C(i, 1) = -C5(iDataIndex, 1)*fpt(iDataIndex);
    M_C(i, 2) = -C6(iDataIndex, 1);
    M_C(i, 3) = C3(iDataIndex, 1)*fpt(iDataIndex);
    M_C(i, 4) = C4(iDataIndex, 1);
    M_F(i, 1) = Fy_ave(iDataIndex);    % average Fy
  end;
  % output file name
  ForceProfileFileName = sprintf('%s', 'ForceProfileFromFy.xls');
  CoefficientsFileName = sprintf('%s', 'CoefficientsFy.xls');

  case 7    % use Avg Ft first to get Ktc and Kte, then use Avg Fx and Fy to get
Krc and Kre
  for i = 1:NumToUseForCalibration;
    iDataIndex = i + NumToStartCalibration - 1;
    M_CFt(i, 1) = C1(iDataIndex, 1)*fpt(iDataIndex);
    M_CFt(i, 2) = C2(iDataIndex, 1);
    M_Ft(i, 1) = Ft_ave(iDataIndex, 1);
  end;
  T_CFt = M_CFt';
  Inv_CFt = inv(T_CFt*M_CFt);
  M_Kt = Inv_CFt*T_CFt*M_Ft;
  Ktc = M_Kt(1,1);
  Kte = M_Kt(2,1);
  % calibrate Krc and Kre with average Fx and Fy
  for i = 1:NumToUseForCalibration;
    iDataIndex = i + NumToStartCalibration - 1;
    M_CFxy(i, 1) = C5(iDataIndex, 1)*fpt(iDataIndex);
    M_CFxy(i, 2) = C6(iDataIndex, 1);
    M_Fxy(i, 1) = Fx_ave(iDataIndex)-C3(iDataIndex, 1)*fpt(iDataIndex)*Ktc-
C4(iDataIndex, 1)*Kte;
    M_Fxy(i+NumToUseForCalibration, 1) = Fy_ave(iDataIndex) +
C5(iDataIndex, 1)*fpt(iDataIndex)*Ktc + C6(iDataIndex, 1)*Kte;
    M_CFxy(i+NumToUseForCalibration, 1) = C3(iDataIndex,
1)*fpt(iDataIndex);
    M_CFxy(i+NumToUseForCalibration, 2) = C4(iDataIndex, 1);
  end;
```

```
    T_CFxy = M_CFxy';
    Inv_CFxy = inv(T_CFxy*M_CFxy);
    M_Kr = Inv_CFxy*T_CFxy*M_Fxy;
    Krc = M_Kr(1, 1);
    Kre = M_Kr(2, 1);
    % output file name
    ForceProfileFileName = sprintf('%s', 'ForceProfileFromFt1FxFy2.xls');
    CoefficientsFileName = sprintf('%s', 'CoefficientsFt1FxFy2.xls');
end;

% calculate cutting coefficients
if(CalibrateModel < 7 )     % for the first 6 types of model
    T_C = M_C';
    Inv_C = inv(T_C*M_C);
    M_K = Inv_C*T_C*M_F;
    % output cutting coefficients
    Ktc = M_K(1,1);
    Kte = M_K(2,1);
    Krc = M_K(3,1);
    Kre = M_K(4,1);
end;

%Ktc = 275830;
%Kte = 116.38;
%Ktc = 3.5797e+005;
%Kte = 52.479;
%Ktc = 335188.1;
%Kte = 227.02;
%Krc = 235541.4;
%Kre = 237.91;
K = [Ktc Kte Krc Kre]

%P_predict = fpt.*C1*Ktc/6600 + C2*Kte/6600;
Ft_ave_predict = fpt.*C1*Ktc + C2*Kte;
Fx_ave_predict = fpt.*C3*Ktc + C4*Kte + fpt.*C5*Krc + C6*Kre;
Fy_ave_predict = -fpt.*C5*Ktc - C6*Kte + fpt.*C3*Krc + C4*Kre;
%Dev_p = P_predict - P;
Dev_ft = Ft_ave_predict - Ft_ave;
Dev_fx = Fx_ave_predict - Fx_ave;
Dev_fy = Fy_ave_predict - Fy_ave;

Max_Dev_ft = max(max(Dev_ft), abs(min(Dev_ft)) );
Max_Dev_fx = max(max(Dev_fx), abs(min(Dev_fx)) );
Max_Dev_fy = max(max(Dev_fy), abs(min(Dev_fy)) );

%Err_p = abs(Dev_p./P)*100;
```

```
Err_ft = abs(Dev_ft./Ft_ave)*100;
Err_fx = abs(Dev_fx./Fx_ave)*100;
Err_fy = abs(Dev_fy./Fy_ave)*100;

Max_Err_ft = max(Err_ft);
Max_Err_fx = max(Err_fx);
Max_Err_fy = max(Err_fy);

%Stdev_p = std(Err_p);
Stdev_ft = std(Dev_ft);
Stdev_fx = std(Dev_fx);
Stdev_fy = std(Dev_fy);

figure(1);
sTitle = sprintf('Calibration results of %.4f inch tool, %d flutes, s=%drpm,
Ktc=%.1flbf/in^2, Kte=%.2flbf/in, Krc=%.1flbf/in^2, Kre=%.1flbf/in', D, Nt, w(1),
Ktc, Kte, Krc, Kre);
subplot(4,3,1);
plot(Ft_ave,'-*');
hold on;
plot(Ft_ave_predict, '-o');
ylabel('Ft_ave (lb)');
legend('Actual avg Ft', 'Predicted avg Ft');
title( sTitle, 'fontweight', 'bold', 'fontsize', 12);
subplot(4,3,4);
plot(Dev_ft,'-o');
%title('Deviation between actual and predicted Ft_ave');
ylabel('Dev\_ft (lb)');
string = sprintf('Std dev = %.2f lb', Stdev_ft);
text((NumToEnd-NumToStart)/2, 0, string);
%figure(2);
subplot(4,3,7);
plot(Err_ft,'-o');
axis([1,NumToEnd,0,max(Err_ft)]);
%title('Relative error percentage of Ft_ave prediction');
%xlabel('Number');
ylabel('Err\_ft(%)');
%figure(3);
subplot(4,3,10);
maxx=ceil(max(Ft_ave)/0.5)/2;
plot(Ft_ave, Ft_ave_predict,'*', Ft_ave, Ft_ave, '-');
axis([0,maxx,0,maxx]);
grid on
xlabel('Actual avg Ft (lb)');
ylabel('Predicted avg Ft (lb)');
subplot(4,3,2);
```

```
plot(Fx_ave,'-*');
hold on;
plot(Fx_ave_predict, '-o');
ylabel('Fx (lb)');
legend('Actual avg. Fx', 'Predicted avg. Fx');
subplot(4,3,5);
plot(Dev_fx,'-o');
%axis([1,Num(:,1),-30,30]);
%title('Deviation between actual and predicted average Fx');
ylabel('Dev\_fx (lb)');
string = sprintf('Std dev = %.2f lb', Stdev_fx);
text((NumToEnd-NumToStart)/2, 0, string);
subplot(4,3,8);
plot(Err_fx,'-o');
axis([1,NumToEnd,0,max(Err_fx)]);
%title('Relative error percentage of average Fx');
%xlabel('Number');
ylabel('Err\_fx(%)');
subplot(4,3,11);
maxx=ceil(max(Fx_ave)/0.5)/2;
minx=floor(min(Fx_ave)/0.5)/2;
plot(Fx_ave, Fx_ave_predict,'*', Fx_ave, Fx_ave, '-');
%axis([minx,maxx,minx,maxx]);
grid on
xlabel('Fx\_ave (lb)');
ylabel('Predicted Fx\_ave (lb)');
subplot(4,3,3);
plot(Fy_ave,'-*');
hold on;
plot(Fy_ave_predict, '-o');
ylabel('Fy (lb)');
legend('Actual avg Fy', 'Predicted avg Fy');
subplot(4,3,6);
plot(Dev_fy,'-o');
%axis([1,Num(:,1),-30,30]);
%title('Deviation between actual and predicted average Fx');
ylabel('Dev\_fy (lb)');
string = sprintf('Std dev = %.2f lb', Stdev_fy);
text((NumToEnd-NumToStart)/2, 0, string);
subplot(4,3,9);
plot(Err_fy,'-o');
axis([1,NumToEnd,0,max(Err_fy)]);
%title('Relative error percentage of average Fx');
%xlabel('Number');
ylabel('Err\_fy(%)');
subplot(4,3,12);
```

```
maxx=ceil(max(Fy_ave)/0.5)/2;
minx=floor(min(Fy_ave)/0.5)/2;
plot(Fy_ave, Fy_ave_predict,'*', Fy_ave, Fy_ave, '-');
%axis([minx,maxx,minx,maxx]);
grid on
xlabel('Fy\_ave (lb)');
ylabel('Predicted Fy\_ave (lb)');

% end of file
```